

**RAPID ROTATIONAL FOAM MOLDING OF POLYETHYLENE
INTEGRAL-SKIN FOAMED CORE MOLDINGS**

by

Kimberly Christian

A Thesis Submitted in Partial Fulfillment
of the Requirements for the Degree of

Master of Applied Science

in

The Faculty of Engineering and Applied Science

Mechanical Engineering

University of Ontario Institute of Technology

June 2009

© Copyright by Kimberly Christian (2009)

RAPID ROTATIONAL FOAM MOLDING OF POLYETHYLENE INTEGRAL-SKIN FOAMED CORE MOLDINGS

Kimberly Christian

Degree of Master of Applied Science, 2009
Faculty of Engineering and Applied Science
University of Ontario Institute of Technology

ABSTRACT

This thesis focuses on the design, development, and evolution of a novel patent-pending plastic processing technology entitled “Rapid Rotational Foam Molding” with special emphasis on the processing of polyethylene (PE) integral-skin foamed core moldings. Rapid Rotational Foam Molding is a technology deliberately designed to address the intrinsic disadvantage of conventional rotational foam molding, i.e., its very long cycle times. In this context, a physical system that exploits the positive synergistic effects of innovatively combining extrusion melt compounding and rotational foam molding was designed and built. The fundamental processing steps of this system comprise (i) rotationally molding a non-foamable PE powder in a lab-scale oven while, (ii) simultaneously melt compounding and foaming a pre-dry blended foamable PE and chemical blowing agent (CBA) formulation in an on-line lab-scale extruder, and then (iii) filling the newly created foaming material into the non-chilled hollow article thereby created in the mold through a special interface.

Two varieties of PE resins ranging from linear low density PE (LLDPE) to high density PE (HDPE) were selected for experimentation with melt flow rates (MFR) ranging from 2.0 to 3.6 g/10min. The implemented CBA was Celogen OT. The materials were characterized using thermal analysis techniques such as differential scanning calorimetry (DSC) and thermogravimetric analysis (TGA) to ensure their correct operating temperatures ranges. Scanning electron microscopy (SEM) was utilized for characterizing the quality of the foam samples and achieved skin-foam interface for the final moldings. Improvements to the achieved molding quality were accomplished through various system and process modifications described throughout this research work.

ACKNOWLEDGEMENTS

This thesis would not have been made possible without the guidance and support of my supervisor Professor Remon Pop-Iliev. His encouragement, willingness to help and patience allowed me to be successful throughout my research. I also want to extend my deepest appreciation to him in giving me every opportunity to enhance my graduate experience from introducing me to an industrial rotational molding facility, to allowing me to attend conferences across North America to present my work.

I would also like to take the time in expressing great thanks to my colleagues Emad Abdalla and Gregory Eberle for their kind collaboration and efforts. Our effective teamwork had allowed us to tackle the most unexpected tasks no matter how daunting they may have been.

Primary funding for this research was graciously acquired from an NSERC Discovery Grant with additional funding provided through the Natural Sciences and Engineering Research Council (NSERC) of Canada, General Motors Canada Limited (GMCL), and UOIT in supporting UOIT's Design Chair budget. The software support necessary for completing this work was courteously provided by PACE (Partners for the Advancement of Collaborative Engineering Education). The material samples used throughout the experimental process were generously donated by Equistar Chemical and Crompton Corporation.

Special thanks also go out to Peter Mckinnion from Durham Tool and Mr. Michael Macleod who contributed greatly in constructing and maintaining the experimental setup.

TABLE OF CONTENTS

PRELIMINARY SECTIONS

ABSTRACT	i
ACKNOWLEDGEMENTS	ii
TABLE OF CONTENTS.....	iii
LIST OF TABLES	vii
LIST OF FIGURES	viii
LIST OF SYMBOLS	xi

CHAPTER 1

INTRODUCTION	1
1.1 Preamble	1
1.2 Technical Details.....	1
1.2.1 Foamed Plastics	1
1.2.2 Production of Foamed Plastics.....	2
1.2.3 Significance of Polyethylene and its Use in Rotational Foam Molding.....	4
1.3 Thesis Purpose Statement	5
1.4 Current Technologies	5
1.5 Thesis Scope	6
1.6 Thesis Methodology and Approach	7
1.7 Intended Thesis Contribution.....	7
1.8 Thesis Format and Outline.....	7

CHAPTER 2

LITERATURE REVIEW AND THEORETICAL BACKGROUND	9
2.1 Conventional Rotational Molding.....	9
2.1.1 Conventional Rotational Molding Processing Principle.....	9
2.1.2 Advantages of Conventional Rotational Molding	11
2.1.3 Disadvantages of Conventional Rotational Molding	11
2.1.4 Rotational Molding Technology	12

2.2	Integral-Skin Rotational Foam Molding	17
2.2.1	Rotational Foam Molding Process	17
2.2.2	Material Preparation.....	21
2.2.3	Material Formulation Amounts.....	23
2.2.4	Advantages of Rotational Foam Molding.....	24
2.2.5	Disadvantages of Rotational Foam Molding	25
2.3	Introduction to Polymers.....	25
2.3.1	Polymer Production	26
2.3.2	Molecular Weight Distribution	27
2.4	Polyethylene.....	28
2.4.1	Morphology.....	30
2.4.2	Thermal Analysis	31
2.4.3	Processing Considerations	33
2.5	Successful Polyethylene Foam Formation in Rotational Foam Molding	35
2.6	Engineering Design Tools.....	36
2.6.1	Quality Function Development.....	36
2.6.2	Pugh Method.....	37
2.7	Characterization of Experimental Results	38

CHAPTER 3

	DESIGN AND DEVELOPMENT OF AN EXTRUSION-ASSISTED ROTATIONAL FOAM MOLDING EXPERIMENTAL SYSTEM	40
3.1	Introduction.....	40
3.2	Problem Statement	40
3.3	EARFM Process Variables	42
3.4	EARFM Experimental Setup Design.....	45
3.4.1	Design Requirements	45
3.4.2	Engineering Specifications	46
3.4.3	Design Opportunities	47
3.4.4	Design Constraints	48
3.5	House of Quality for EARFM.....	48
3.6	Concept Generation for EARFM Experimental Setup	48

3.7	Final Concept Selection for EARFM Experimental Setup	50
3.8	Final Component Design and Implementation	51
3.8.1	Extruder Design	51
3.8.2	Oven Design.....	54
3.8.3	Mold Rotational Mechanism Design	55
3.8.4	Mold Design.....	59
3.9	Final EARFM Experimental Setup.....	62

CHAPTER 4

	EXPERIMENTAL EVOLUTION OF THE NOVEL EXTRUSTION- ASSISTED ROTATIONAL FOAM MOLDING PROCESS	65
4.1	Introduction.....	65
4.2	Experimental Materials.....	65
4.3	PE Characterization	66
4.4	CBA Characterization.....	68
4.5	EARFM Process Control Consideration.....	71
4.5.1	EARFM Processing Steps.....	71
4.5.2	EARFM Material Preparation.....	74
4.6	Process Modifications of EARFM.....	76
4.7	Process Modifications of EADFRM.....	78
4.8	Process Modifications of RRFM	81
4.9	Final RRFM Experimental Setup.....	81
4.10	Final RRFM Processing Variables.....	83
4.11	Final RRFM Material Preparation	84
4.12	Final RRFM Processing Steps	84
4.13	Introduction of Plastic Welding (Where Necessary)	85

CHAPTER 5

	EXPERIMENTAL RESULTS AND DISCUSSION OF EARFM PROCESS AND RESULTING PROCESS ITERATIONS.....	86
5.1	Introduction.....	86
5.2	Experimental Results and Discussion of Extrusion-Assisted Rotational Foam Molding (EARFM)	86

5.2.1	Skin Formation.....	86
5.2.2	Foam Formation.....	87
5.2.3	Integral-Skin Foam Core Formation.....	89
5.3	Experimental Results and Discussion of Extrusion-Assisted Direct Foaming Rotational Molding.....	92
5.4	Experimental Results and Discussion of Rapid Rotational Foam Molding (RRFM)	95
5.5	Quality Comparison of Process Iterations	98
5.6	Experimental Optimization Results and Discussion of Rapid Rotational Foam Molding (RRFM).....	99
5.6.1	Qualitative Quality Analysis.....	100
5.6.2	Quantitative Quality Analysis.....	109
5.7	Final Process Comparison Analysis.....	115

CHAPTER 6

	CONCLUSIONS AND RECOMMENDATIONS FOR FUTURE WORK.	118
6.1	Concluding Remarks.....	118
6.2	Summary of Contributions.....	119
6.3	Recommendations for Future Work.....	119
	REFERENCES	121
	APPENDIX A.....	126
	APPENDIX B.....	130
	APPENDIX C.....	136

LIST OF TABLES

Table 3.1: Concept Feasibility Decision Matrix for the EARFM Process	50
Table 4.1: Typical Properties of Chosen PE Resins [56-57]	65
Table 4.2: Typical Properties of Celogen OT [58]	66
Table 4.3: DSC PE Characterization Results.....	66
Table 5.1: EARFM Skin Formation Parameters	89
Table 5.2: EARFM Foam Formation Parameters	90
Table 5.3: EADFRM Skin Formation Parameters	92
Table 5.4: EADFRM Foam Formation Parameters	92
Table 5.5: EADFRM Cell Analysis Results	94
Table 5.6: RRFM Skin Formation Parameters	95
Table 5.7: RRFM Foam Formation Parameters.....	95
Table 5.8: Summation of Experimental Results for all Process Iterations	98
Table 5.9: Final RRFM Skin Formation Parameters	99
Table 5.10: Final RRFM Foam Formation Parameters	99
Table 5.11: Foam Density Results for Final RRFM Experiments.....	109
Table 5.12: Average Cell Size Results for Final RRFM Experiments	111
Table 5.13: Cell Population Density Results of Final RRFM Experiments	112

LIST OF FIGURES

Figure 1.1: Conventional Rotational Molding Process.....	3
Figure 1.2: Integral-Skin Plastic Foam Morphologies.....	4
Figure 2.1: Mold Internal Air Temperature during Rotational Molding of PE	10
Figure 2.2: Rock and Roll Rotational Molding Machine [15].....	12
Figure 2.3: Clamshell Rotational Molding Arms [15].....	13
Figure 2.4: Shuttle Style Rotational Molding Machine [15]	14
Figure 2.5: Vertical Rotational Molding Machine [15]	15
Figure 2.6: Fixed-Arm Turret Rotational Molding Machine [15]	16
Figure 2.7: Simplified LDPE Branch Structure	29
Figure 2.8: Simplified LLDPE Branch Structure.....	29
Figure 2.9: Simplified HDPE Branch Structure	30
Figure 2.10: Three-Phase Structure of PE	30
Figure 2.11: Simplified Example of HofQ.....	36
Figure 3.1: Schematic Representation of the Proposed Process Solution	41
Figure 3.2: EARFM Concept 1	48
Figure 3.3: EARFM Concept 2	49
Figure 3.4: EARFM Concept 3	50
Figure 3.5: Extruder Control Panel	52
Figure 3.6: CAD Representation of Variable Height Adjustment Modification	53
Figure 3.7: Extruder Filling Modifications	53
Figure 3.8: Final Extruder Design	54
Figure 3.9: Chosen Oven Design with Process Modifications	55
Figure 3.10: Final Mold Rotational Arm Assembly	56
Figure 3.11: Final Carriage Assembly	58
Figure 3.12: Final Frame Assembly.....	59
Figure 3.13: CAD Representation of the Cylindrical Mold Design	60
Figure 3.14: CAD Representation of Flat-Plate Mold Design.....	61
Figure 3.15: Specialized Gate Design.....	62

Figure 3.16: Extruder and Accompanying Melt Injection Equipment of the EARFM Experimental Setup.....	62
Figure 3.17: Modified Oven of the EARFM Experimental Setup.....	63
Figure 3.18: Carriage Assembly with Cylindrical Mold Mounted to Translational Mechanism of the EARFM Experimental Setup	63
Figure 3.19: Final EARFM Experimental Setup	64
Figure 4.1: DSC Thermogram of the LLDPE resin (MP643662).....	67
Figure 4.2: DSC Thermogram of the HDPE resin (MP652762)	67
Figure 4.3: TGA Thermogram of Celogen OT at Various Heating Rates	68
Figure 4.4: TGA Thermogram of Celogen OT at 50 °C/min	69
Figure 4.5: TGA Thermogram of Celogen OT at 75 °C/min	69
Figure 4.6: TGA Thermogram of Celogen OT at 100 °C/min	69
Figure 4.7: Step 1 – Mold Preparation.....	71
Figure 4.8: Step 2 – Mold Translation	72
Figure 4.9: Step 3 – Charging Extruder with Pre-Dry Blended Foamable Formulation	72
Figure 4.10: Step 4 – Translation and Alignment of the Mold with the Extruder	73
Figure 4.11: Step 5 – Extrudate Filling of Uni-Axially Rotating Mold.....	73
Figure 4.12: Step 7 – Fan Cooling of Bi-Axially Rotating Mold	74
Figure 4.13: Extruder with Modified Nozzle Assembly.....	77
Figure 4.14: Modified "Pizza Valve"	78
Figure 4.15: Insulated Mold Interface Assembly.....	79
Figure 4.16: Second Extruder Nozzle Modification	80
Figure 4.17: Final Cylindrical and Flat-Plate Mold Designs	82
Figure 4.18: Final RRFM Experimental Setup	82
Figure 5.1: Typical “Pizza Valve” Functionality Result	87
Figure 5.2: Typical "Pizza Valve" Puncture Test Result	87
Figure 5.3: Typical Cross-Sections of Foam-Only Molding	88
Figure 5.4: Micrograph of Typical EARFM Foam-Only Sample (50x Magnification) .	88
Figure 5.5: Typical Integral-Skin Foam Core Result of EARFM.....	90
Figure 5.6: Micrographs of Typical EARFM Sample (50x Magnification).....	91
Figure 5.7: Typical Result of the EADFRM Process (VER = 6).....	93

Figure 5.8: Micrographs of LLDPE EADFRM Sample (50x Magnification).....	94
Figure 5.9: Micrographs of HDPE EADFRM Sample with (50x Magnification).....	94
Figure 5.10: Typical Result of RRFM for the Cylindrical Mold.....	96
Figure 5.11: Typical Result of RRFM for the Flat-Plate Mold	96
Figure 5.12: Micrographs of RRFM Skin/Foam Interface (50x Magnification)	98
Figure 5.13: Scanned Foam and Micrograph (50x Magnification) Results of Varying Melt Temperature with LLDPE using the Cylindrical Mold	100
Figure 5.14: Scanned Foam and Micrograph (50x Magnification) Results of Varying Melt Temperature with HDPE using the Cylindrical Mold	101
Figure 5.15: Scanned Foam and Micrograph (50x Magnification) Results of Varying Melt Temperature with LLDPE using the Flat-Plate Mold.....	103
Figure 5.16: Scanned Foam and Micrograph (50x Magnification) Results of Varying Melt Temperature with HDPE using the Flat-Plate Mold.....	104
Figure 5.17: VER Comparison for Cylindrical Mold	105
Figure 5.18: VER Comparison for Flat-Plate Mold.....	106
Figure 5.19: Typical Mold Filling Result of Both Molds.....	106
Figure 5.20: Typical Mold Interface Result.....	108
Figure 5.21: Sample PE Weld to Fill Mold Interface Channel.....	108
Figure 5.22: Scanned Picture of Sample PE Weld in Mold Interface Channel (50x Magnification).....	108
Figure 5.23: Foam Density Comparison Varying Resins and Mold Shapes @ 130°C ..	110
Figure 5.24: Foam Density Comparison Volume Expansion Ratios @ 130°C	110
Figure 5.25: Average Cell Size Comparison Varying Resins and Mold Shapes @ 130°C	112
Figure 5.26: Cell Population Density Comparison Varying Resins and Mold Shapes @ 130°C	113
Figure 5.27: Average Cell Size Comparison Varying Volume Expansion Ratios @ 130°C	114
Figure 5.28: Cell Population Density Varying Volume Expansion Ratios @ 130°C.....	114
Figure 5.29: Processing Cycle Timeline Comparisons [64]	116

LIST OF SYMBOLS

n_i	= Number of molecules of i
M_i	= Molecular weight of i^{th} molecule (g/mol)
\bar{M}_n	= Number average molecular weight (g/mol)
\bar{M}_w	= Weight average molecular weight (g/mol)
ϕ_{STP}	= Volume of gas generated per unit mass of CBA at standard temperature and pressure (cc/g)
T_m	= Melt temperature ($^{\circ}\text{C}$)
T_c	= Crystallization temperature ($^{\circ}\text{C}$)
V_{SKIN}	= Volume of non-foamable resin to create skin of desired thickness (cm^3)
m_{SKIN}	= Mass of non-foamable resin to create skin of desired thickness (g)
ρ_{PE}	= Density of PE resin (g/cm^3)
V_{FOAM}	= Volume of expanded foam (cm^3)
VER	= Volume Expansion Ratio
V_i	= Volume of resin before expansion (cm^3)
m_{FOAM}	= Mass of resin required to create foam of desired VER (g)
$\phi_{\text{corrected}}$	= Volume of gas generated per unit mass of CBA at experiment conditions (cc/g)
T_{room}	= Lab room temperature ($^{\circ}\text{C}$)
m_{CBA}	= Mass of CBA required to create foam of desired VER (g)
$\% \text{CBA}$	= Percentage by weight of CBA
ρ_{FOAM}	= Final expanded foam density of a 1 cm^3 sample (g/cm^3)
W_s	= Final expanded foam weight of a 1 cm^3 sample (g)
V_s	= Final expanded foam volume of a 1 cm^3 sample (cm^3)
N	= Cell population density (g/cm^3)
n_{cells}	= Number of cells contained in a 1 cm^2 area of foam
D_{average}	= Average cell size (μm)

CHAPTER 1

INTRODUCTION

1.1 Preamble

Foamed plastics, a subset of polymeric foams feature enhanced insulation, energy absorption, improved strength to weight ratios, and buoyancy capabilities compared to un-foamed plastics [1,2].

1.2 Technical Details

1.2.1 Foamed Plastics

Foamed plastics normally consist of two phases, a solid polymer matrix and a gaseous phase encapsulated within the matrix. Additional phases can also exist within this cellular structure if a polymer blend or filler material is used to improve the properties achieved by using a single polymer [2].

The cellular structure is commonly created via gas dispersion within a molten polymer that can create two varieties of cell geometries: closed-celled and open-celled foams.

Closed-celled foams consist of distinct and independent cells throughout the foam structure, where open-celled foams consist of interconnected cells. These differing cell geometries aid in determining the type of applications for these materials. For example, open-celled foams cannot achieve high mechanical or insulative properties making it suitable for furniture, bedding, and other cushioning related applications. This is due to the interconnected structure of the cells that offer little resistance to mechanical forces and allow gases to easily pass through it. Conversely, a closed-celled foam is more appropriate for thermal insulation, damping, and applications requiring high rigidity [2,3].

This is due to the enclosed cell structure as it is generally seen as a rigid structure that offers little to no gas or liquids to pass through it. Additional potential applications for various foamed polymers include such products as toys, automobile parts, aerospace parts, sports equipment, packaging, and harbour buoys [1, 2].

The mechanical properties of plastic foams are proportionally related to the density of the foamed material. Therefore low density foams, typically starting at 1.6 kg/m^3 , are used for packaging and insulation applications, where high density foams with densities up to 960 kg/m^3 are used for load-bearing applications. In regards to thermal properties, it is seen that lower density foams feature greater insulating capabilities [2].

However, given the same foam density, different cell sizes can alter the mechanical properties and insulative capabilities of plastic foams for both open and closed-celled structures. For example, with smaller cells, foam will likely withstand greater forces in load-bearing applications as it features better load distribution than foam with larger cells. Smaller cells can also contribute to greater insulative properties as there is more limited movement of gases trapped within the cells, for closed-celled foams in particular.

It is anticipated that the popularity of polymeric foams may rise over the next few years with the advancement of such applications as plastic lumber, molding and trim, windows, and doors. There may also be an increase in use of polymeric foams in the transportation industry for automotive parts as the automotive industry moves towards lighter more compact vehicles [4].

1.2.2 Production of Foamed Plastics

Current processing methods of polymer foam production include compression foam molding, reaction injection foam molding, foam extrusion, injection foam molding, and rotational foam molding [2]. However, two of the most utilized and well known processes for foaming polyolefins are injection foam molding and foam extrusion [1].

Rotational foam molding, in particular, is a process derived from conventional rotational molding that is well suited for the production of single and multi-layered hollow moldings [5]. The conventional rotational molding process begins with charging a

mold with a designated amount of rotational molding grade plastic resin in powder form that will create a hollow molding of a desired thickness as illustrated in Figure 1.1 (a). The mold is then bi-axially rotated to distribute the resin powder throughout the internal structure of the mold (Figure 1 (b)). With the addition of heat, this melts the powder particles causing them to adhere to the inside of the mold as illustrated in Figure 1 (c) creating a hollow plastic molding. The process is completed by cooling the mold using water or air cooling systems with continued bi-axial rotation, after which the completely cooled molding can be removed from the mold.

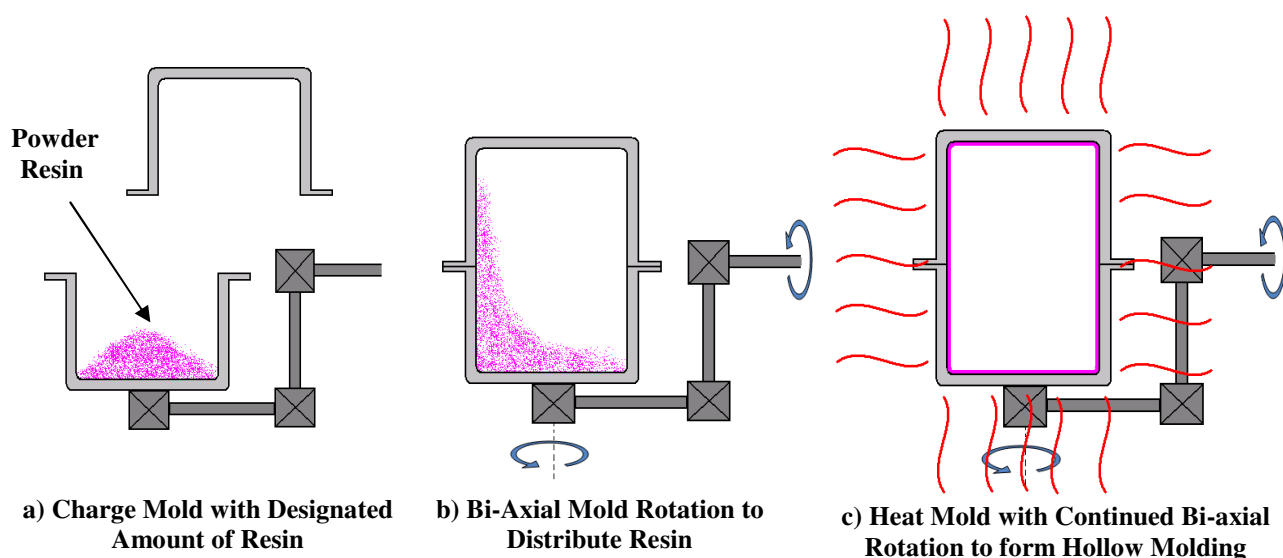


Figure 1.1: Conventional Rotational Molding Process

It wasn't until the early 1970's that the conventional rotational molding process was modified for production of foamed moldings to become rotational foam molding that was later followed by research in the creation of integral-skin foam moldings [2]. As presented in Figure 1.2, an integral-skin foam molding consists of a solid non-foamed outer skin layer that encapsulates, either a plastic foamed layer (Figure 1.2 (a)), or foamed core (Figure 1.2 (b)).

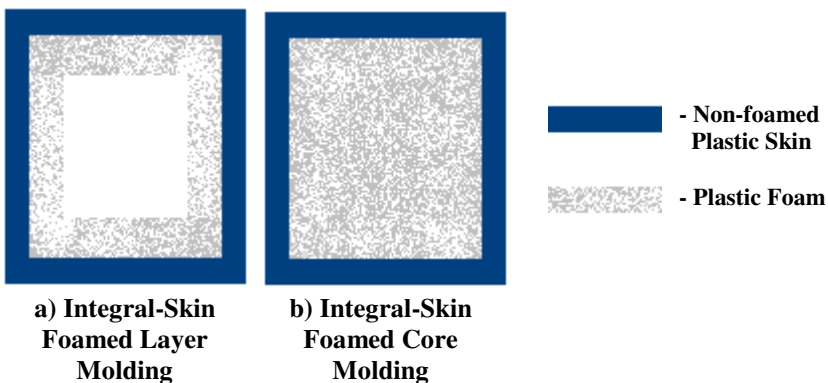


Figure 1.2: Integral-Skin Plastic Foam Morphologies

1.2.3 Significance of Polyethylene and its Use in Rotational Foam Molding

Polyethylene (PE) was initially created in the 1930's by chemists working for the British company Imperial Chemical Industries studying organic compounds of ethylene. During a failed experiment chemists discovered a waxy textured solid material that had been produced as a by-product, which was the first reported evidence of PE. At that time, PE was quickly recognized for its potential for electrical insulation and chemical inertness [1]. The next great innovation of this material came in the late 1950's with the advent of a PE material with improved stiffness and strength known as high-density PE (HDPE). This caused the previously discovered types to be renamed to low (LDPE) and medium density PE (MDPE) due to their lower degree of crystallinity and density compared to the new material [2].

A number of common physical properties of PE include being light-weight, with good impact strength, UV and weather resistance, and excellent environmental stress crack resistance. In addition, since different density grades are available for PE, the higher the density, the more the material features increased hardness, heat deflection, tensile strength, chemical resistance, stiffness, and permeation [6].

The flexibility of this material has helped to promote its rise in popularity over the last 5 years to where its current industry use accounts for a total of 30 % of the worldwide plastics consumption. It is also projected that with the versatility of the material to meet current industry needs of balancing cost with performance, the increase in demand will continue through 2012 by approximately 7 % per year [4].

For rotational molding, PE has dominated as the most utilized material since the 1960's when first introduced in powder form. Currently, PE accounts for approximately 80 % of all rotomolding materials used [7] due to its early availability and advantageous physical properties.

For use in rotational foam molding, PE has a wider operational melt temperature range making it easier to process compared to its main competitor polypropylene [8].

1.3 Thesis Purpose Statement

Over the past two decades, the advantages of plastic foam have become overshadowed by its negative environmental impacts in terms of processing and recycling [9]. Current industry trends of increasing efficiency, reducing processing costs, and reducing environmental impacts have created a drive to discover a way to produce advantageous moldings such as integral-skin foam moldings in a way superior to any that are currently available. Rotational foam molding is a process that needs immediate improvement because of its inefficiency. This inefficiency is caused by the fact that the mold and plastic need to be heated from room temperature to required processing temperatures and then cooled back to room temperature, which is slowed even further down due to the insulative effect of the foam [10].

1.4 Current Technologies

Although there have been significant findings published regarding rotational foam molding, only recently research has begun creating significant modifications to the process to reduce the effects of its intrinsic disadvantages. This can be attributed to the lack of advancement and industry attractiveness of the process because of its low production volumes and slow processing cycles. Advantageously, rotational foam molding does feature the same low tooling costs as its conventional counterpart for which there have been more technological advances. Such advances that can have a direct correlation to the foaming process have been heavily focused on control by improvement of temperature sensing devices, simulation software, mold automation, and more sophisticated venting devices. Other advances include focus on various ways of heating

and cooling the mold more efficiently using direct heating and cooling methods that do not require, for example, the use of an oven.

One such innovation created by Persico SpA is the first fully automated oven-less rotational molding machine named “Leonardo” that can be called one of the most significant advances in rotational molding technology. Processing with this machine begins with automatic charging of the mold for single or multi-layer moldings accomplished with a retractable filling nozzle. Heating and cooling is accomplished with a high-tech fluid transmission system that cycles heated oil and chilled water simultaneously over the outer surface of the mold for precise control of the mold’s internal temperature. Another unique feature of this machine is that this temperature controlling system is not affected by the bi-axial rotation of the mold. Mold venting is also automatically controlled and triggered by changes within the mold monitored by internal temperature measurements. Once completed, the final part can be removed and translated away from the mold without any operator assistance by a conveyor belt and displayed conveniently to be taken for storage or secondary processing [7, 11].

This machine offers many technological advances such as increased processing control and a novel heating and cooling system to help overcome many of the disadvantages associated with rotational molding. However, despite its outstanding advantages and superb engineering solutions, it is most economically suited for relatively large production runs as each machine must be custom engineered to meet customer requirements. Additionally, with all of the improved features of this machine, it potentially may still experience similar lengthy heating cycle times associated with conventional rotational molding and rotational foam molding.

Such process enhancements have been adopted throughout Europe and North America, but there is still more that could be gained with further advancement of this valuable technology with respect to foaming [7, 12].

1.5 Thesis Scope

The work of developing an improved rotational foam molding process for the fabrication of PE integral-skin foam moldings, specifically integral-skin fine-celled foam core

moldings, is proposed in this thesis. In developing this process, the first step was to determine the most effective way to improve its efficiency compared to the current rotational foam molding process. As it is well documented the heating cycle is the most predominant cause of the fundamental disadvantage of the process creating a great opportunity to utilize the most efficient method for continuously melting plastics: i.e., extrusion. Ultimately, if successful this could ensure the sustainable and improved economical production of integral-skin PE foam moldings with rotational foam molding technology and could potentially make it more desirable by industry and warrant a future industrial scale-up.

1.6 Thesis Methodology and Approach

The methodology of the design process implemented into this work include: Quality Function Development (QFD) tools such as a House of Quality and the Pugh method involving decision matrices. These methods were utilized to derive feasible concepts and determine the most effective one, which was implemented into the final design. Upon completion of the final process design, experimental analysis was performed based on previous findings and theoretical knowledge to determine the feasibility of the process to produce high quality moldings.

1.7 Intended Thesis Contribution

It is intended that this work will result in the successful creation of a lab-scale rotational foam molding experimental setup that can most effectively utilize extrusion melt compounding. In addition, processing steps and appropriate material formulations intended for the production of acceptable quality PE integral-skin foam core moldings will also be created.

1.8 Thesis Format and Outline

Throughout the remainder of this thesis it will be demonstrated how to accomplish the above stated tasks, ultimately resulting in a conclusive experimentally validated design.

Chapter 2 presents current research, scholarly literature, and theoretical background relating to conventional rotational molding and rotational foam molding. This chapter also includes detailed descriptions of PE and foaming mechanisms for their applicable use within these technologies. Applicable engineering design tools used throughout the design of the experimental setup, and molding quality characterization methods are also described in detail.

Chapter 3 outlines the design process in creating a lab-scale experimental setup of a novel process that produces integral-skin foamed core moldings beginning with concept generation. This process ends with a final selection of the most feasible concepts with the use of a decision matrix to assist in creating the final experimental setup of the proposed process.

A detailed description of the experimental process and accompanying processing steps has been outlined in Chapter 4. This chapter includes experimental material characterization, and investigates the capability of the process to produce better quality moldings through process and experimental setup modifications.

Chapter 5 presents the experimental validation of the feasibility of all process iterations to produce acceptable quality integral-skin foamed core moldings. Experimental analysis has been performed and compared to results of previous process iterations to determine the final capabilities of this process.

All concluding remarks are presented in Chapter 6 in addition to a discussion of recommendations for potential future work.

CHAPTER 2

LITERATURE REVIEW AND THEORETICAL BACKGROUND

2.1 Conventional Rotational Molding

Conventional rotational molding or rotomolding is a cyclic semi-continuous process used to create hollow single-piece parts. Since its introduction in the 1940's, this process has been capable of producing extremely large parts, for example, a 100,000 liter storage tank, in addition to being able to create parts with very complex shapes [5]. Yet despite this variety of processing capabilities, the process saw little positive attention due to its lengthy processing cycle and limited initial material availability compared to other plastic processing methods. Ten years later, with the introduction of powdered plastics, the outlook on utilizing this process began to improve and various rotational molding machines became commercially available [13-15]. Further evidence of this positive change came in the 1960's when the toy industry became the main user of rotationally molded parts [15]. Since then, there have been many improvements as well as an increase in the number of materials available for use. This ultimately contributed to an increase in popularity throughout various industries.

2.1.1 Conventional Rotational Molding Processing Principle

The process of conventional rotational molding begins with charging a vented mold with a specified predetermined amount of plastic resin. The particular type of plastic used is called rotational grade that usually comes in powdered form but a pre-melted liquid polymer can also be used. The specified amount of this plastic resin to be charged into the mold is dictated by the desired thickness of the final part. For example, to achieve greater wall thickness for a hollow part, more plastic resin should be initially charged into the mold, proportional to how much thicker it is desired the part to be.

Once charged, the mold consisting of two or more segments is closed then rotated simultaneously on one or two perpendicular axes and heated to above the melting point of the plastic resin. The processing cycle involves six steps: initial temperature rise (1), melting/sintering (2), bubble removal and densification (3), pre-cooling (4), crystallization (5), and final cooling (6) as illustrated in Figure 2.1.

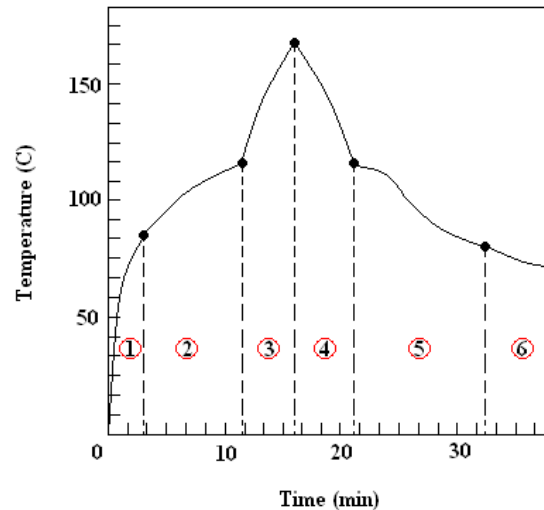


Figure 2.1: Mold Internal Air Temperature during Rotational Molding of PE

The initial temperature rise essentially heats the mold from room temperature up to the point before melting of the polymer occurs [16]. The melt/sintering stage involves a continual rise in temperature causing the polymer's particles to melt and fuse together forming a polymer melt. Simultaneously the particles closest to the mold's internal wall surface begin to adhere to the mold until all of the powder has melted and can flow around the cavity of the mold by its own weight, in a so called zero shear viscosity fashion, during the rotation of the mold. This rotational flow creates a uniform wall thickness of the final part assuming there are no interruptions in the process and a constant rotational speed is used [2]. The bubble removal and densification stage involves a further increase in temperature at a higher heating rate to dissolve bubbles created during rotation of the molten material as any bubbles remaining can reduce the quality of the part. The next stage involves pre-cooling the mold by initializing a large temperature drop. As the material begins to crystallize during this stage, the temperature drop slows and begins to even out before the final cooling stage is reached. Once cooled,

the material has become fully solidified and the molded part can then be removed from the mold and the cycle is repeated [16].

2.1.2 Advantages of Conventional Rotational Molding

Several advantages of rotational molding include the ability to create rather complex large parts with the potential for molded inserts at a low cost. The low cost of production is associated with relatively simple mold designs, which is beneficial if part details change frequently. Molds are relatively inexpensive because the process is atmospheric and does not require heavy duty molds as, for example, in injection molding where pressures can reach anywhere around 5.51×10^4 kPa within the mold [13]. It is also possible for different molds of various sizes and shapes to be used simultaneously in multiple mold machines allowing for additional flexibility. Changing of the molds is also quite fast allowing for production of small quantities most justified for just-in-time applications [15].

When compared to other processing technologies rotational molding is one that can achieve a uniform wall thickness that is virtually stress-free [15]. Having no residual stresses is important for the quality of the finished product as it will have improved impact strength and chemical resistance with reduced part warpage during cooling. This process also has the capability of producing hollow parts with extremely thin wall thickness allowing for reduced required material amounts and cycle times. Once molding is complete little to no secondary operations are required as minimal scrap is produced due to the parts being free of flash or scars such as weld-lines, gates, or seams [6].

2.1.3 Disadvantages of Conventional Rotational Molding

As with any process there are inherent disadvantages that must be considered with the use of rotational molding relating to different areas of the process cycle. Even before the process begins despite significant improvements in the area of material availability the current amount of materials available are less than that for any other process. There is also an increased cost for the production of rotational grade plastics, as common plastics come in the form of pellets instead of the powder form that is required. The need for

grinding the material prior to use is what increases costs where the quality of the grind further raises the financial burden [15]. During the process only a hollow shell can be created void of any internal features. All dimensions and details of the part are controlled only by the internal surface of the mold, where dimensional accuracy can be a problem due to part shrinkage and warpage. This and other factors, such as the typical lengthy cycle time prove that this process is not well suited for high production rates. Additionally, since rotational molding requires high heating temperatures in addition to long cycle times, there is a high-energy cost associated with its use as well as a higher risk of thermal degradation of the material [6]. Once molding is complete, the more complex a part is also dictates how labour intensive it can be to remove it from the mold [15].

2.1.4 Rotational Molding Technology

Essentially all rotational molding machines perform the same task to heat then cool a rotating mold, but the way in which this process occurs can differ from the various machines available today. Common types of rotational molding machines will be briefly described in the following sub-sections with their various advantages and disadvantages.

Single Mold Technology: The least complex and most economical of all single mold rotational molding machines for the production of very large parts is the rock and roll machine, as presented in Figure 2.2 [15].

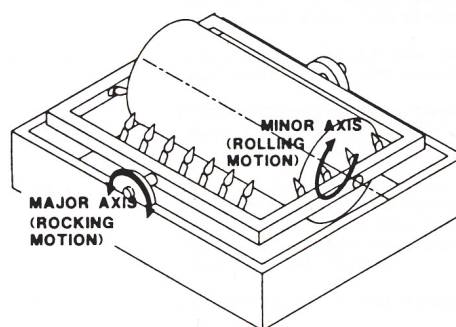


Figure 2.2: Rock and Roll Rotational Molding Machine [15]

Its process begins with rotating the mold about its major axis, and tipping from left to right along its minor axis, with the speed of rotation being much faster than the tipping action. Heating is achieved using an open flame around the outside perimeter of the

mold. Cooling is accomplished by blowing high-pressure cooled air on the outer surface of the mold, while it rotates only on its major axis. The tipping motion is not required at this point since the polymer has already evenly distributed and adhered to the inner surface of the mold. To improve the cooling process, water can be sprayed or misted over the mold near the end of the cooling cycle to speed up the final cooling rate [15].

Another single mold machine called a box oven machine is well suited for creating such rounded parts as certain automotive components and children toys. This machine consists of a mold with the capability of bi-axial rotation housed inside an oven that effectively heats by either a gas or oil fired burner with a re-circulating air system. The cooling system involves the mold to be manually placed on a roller mechanism powered by an air cylinder used to plunge the mold into a bath of cold water until an optimal cooling temperature is reached. Once complete, the roller mechanism brings the mold out of the bath to be moved to the loading/unloading station for part removal [15].

A more popular single mold design, the clamshell rotational molding machine offers reduced floor space usage, reduced labour, and low initial cost. This machine consists of a hot-air oven that controls heating and allows cooling by circulating outside air around the mold after the heating element has been disabled. Two variable speed gear motors rotate the mold on its major and minor axes accomplishing the bi-axial rotation that can be performed by two different arm variations: a straight arm design for smaller molds and an offset arm design for larger molds, as presented in Figure 2.3 [15].

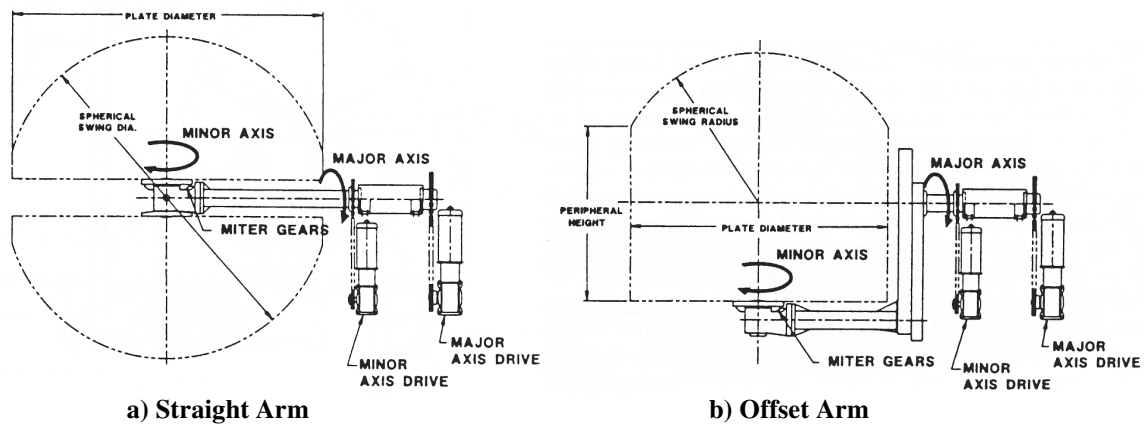


Figure 2.3: Clamshell Rotational Molding Arms [15]

In comparison these single mold rotational molding machines are quite different and that makes them attractive for use in different capacities. As previously stated, the rock and roll machine is economical for creating very large parts, but at the same time its process is slow and bulky. There is also little advantage for automation of this process, making it only usable for very small production volumes. With the box oven machine, there is considerable labour involved in transferring the mold between stations. For this reason, this process is viewed as being primitive and is not widely used throughout industry. The clamshell machine, on the other hand has a major advantage of having its entire process housed within the oven allowing improved control and requiring less space on the plant floor. A disadvantage, however, is the fact that more energy is required during processing as cooling is controlled by the oven rather than controlled externally using air or water [15].

Multiple Mold Technology: A multiple mold machine design known as a shuttle-style machine has the ability to mold one part directly after another by utilizing a two shuttle system that essentially acts as two separate rotational molds. When the first shuttle enters the oven, similar to a box oven, it rotates bi-axially throughout the heating process. Concurrently, the second shuttle is charged with material and waits to be moved into the oven as presented in Figure 2.4 [15].

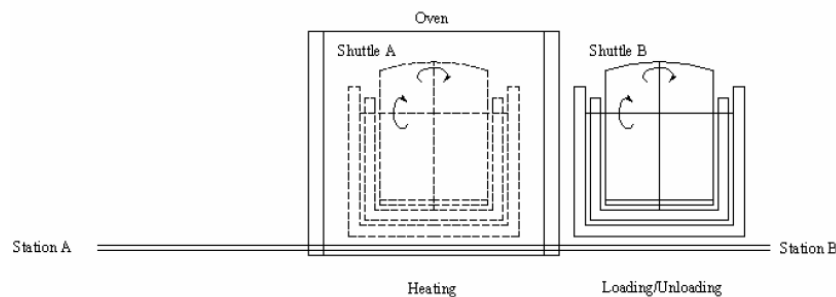


Figure 2.4: Shuttle Style Rotational Molding Machine [15]

Once the heating cycle is complete for the first shuttle, it is pushed out of the oven to begin the cooling process, while the second shuttle is simultaneously pushed into the oven. Upon cooling and eventual part removal of the first shuttle the heating process of the second shuttle is well underway [15].

Additional multiple mold machine designs such as the vertical, fixed-arm turret and independent-arm machines are similar in operation but feature different configurations. For example, the vertical machine has the option of having either a three or six mold configuration and is oriented similar to a carnival Ferris wheel where each mold is indexed vertically to different molding stations of heating, cooling and loading/unloading. Each station is encapsulated within the machine similar to the three mold configuration as presented in Figure 2.5 [15].

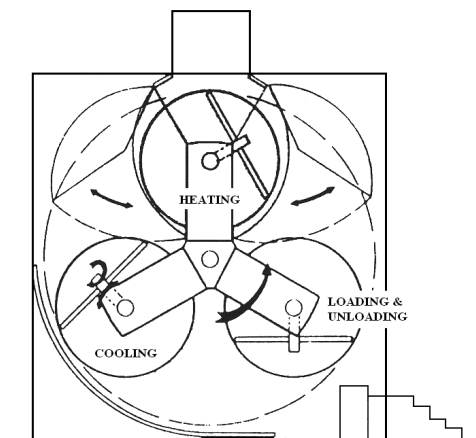


Figure 2.5: Vertical Rotational Molding Machine [15]

Rotation of the molds is controlled with two variable gear motors, and heating and cooling are accomplished via a gas-fired element and utilization of both air and water cooling [15].

Fixed-arm turret rotational molding machines can feature three or four mold arms mounted to a horizontally oriented rotating turret assembly. The assembly consists of combinations of heating, cooling and unloading/loading stations depending on the longest of the three cycle times of the parts to be produced as presented in Figure 2.6 [15].

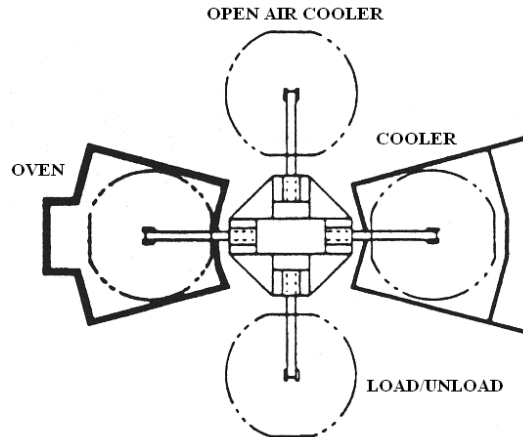


Figure 2.6: Fixed-Arm Turret Rotational Molding Machine [15]

The heating station within this machine consists of a forced air convection oven with automated entrance and exit doors. The cooling station also features a similar entrance and exit system and uses a cooled forced air and/or water mixture to be sprayed onto the mold [15].

Independent-arm rotational molding machines are similar in orientation but more automated than fixed-arm style machines as they feature individual arm movement divided into five different stations. Having the process divided into five sections allows modification to be possible. For example, if a longer heating cycle time is required an additional station to accommodate that cycle can be added into the fifth section that is normally used for holding. Heating stations consist of forced-air re-circulating ovens with cooling stations consisting of forced air and water-cooling compartments [15].

After comparing the capabilities of multiple mold machines, it is reasonable to say that they all feature reduced cycle times due to the ability to create numerous parts simultaneously. Shuttle-style machines introduce reduced labour in addition to a reduced consumption of floor space that gives this type of rotational molding machine advantages over the rest. Vertical machines also utilize a minimum amount of floor space as the machine is oriented vertically, yet when the number of arms increases, the size of the machine also increases. There is however, a physical limitation to this machine since the size of the parts produced is limited to the size of the machine. Independent-arm machines have an added advantage of the independent movement of the molds as they may encompass different cycle times [15].

2.2 Integral-Skin Rotational Foam Molding

Integral-skin rotational foam molding can create composite rotational moldings featuring a distinct non-foamed solid skin encapsulating a foam core or layer. The first published methods of creating such moldings have been available since the 1960's and are inherently similar to the conventional rotational molding technology but with additional complexities. Over the years, due to research in the area of rotational foam molding, several other continuous and interrupted processing methods have been established known as single and two-step methods. Additional research has also been performed in material production since the first material specific for this process was made commercially available in the 1990's by Equistar and Wedtech [6].

2.2.1 Rotational Foam Molding Process

The process of creating skinless foam core (or layer) parts using rotational foam molding begins with charging the mold with a pre-prepared amount of foamable material, preparation of which is described in Section 2.2.2. Once charged the material is heated from room temperature to above the melting temperature of the resin and rotated bi-axially. The temperature is then increased further to activate the decomposition of the chemical blowing agent (CBA) that initiates foaming of the plastic by releasing a gas into the resin melt creating bubbles in the resin structure [15]. Upon completion of the decomposition of the CBA, the mold is cooled to solidify this newly created structure and to complete the foaming process. It is important to note that only CBAs can be utilized as the foaming mechanism for rotational foam molding as its process is pressure-less, where other types of foaming agents require a pressurized environment.

Single-Step Foam Molding: In order to produce integral-skin foams using rotational foam molding, such as a non-foamed skin layer encapsulating a foamed inner core or layer additional processing steps are required. Since two different materials (non-foamable and foamable) are required to create this more complex structure, these materials must be charged in to the mold either together or separately. If all of the materials are charged together this is known as the single-step continuous process as it does not have any interruptions in the processing cycle. Several variations of this process

have been proposed but an important consideration for all involves the necessity of the non-foamable resin to adhere to the inner surface of the mold before the foamable compound begins foaming, in such a way that the two layers are separated from one another [17].

Hoppe et al. [18] invented a rotational foam molding process that takes advantage of different material densities in conjunction with the centrifugal forces created during rotation of the mold. With this process, the polymer resin with the greatest density will be drawn to the outer edge of the mold surface where the peripheral speed of the mold is greatest, thereby creating the distinct skin layer. For the foam layer to be produced within this skin, the foamable material must have a lesser density so as not to be affected as much by the centrifugal pull towards the mold walls. However, this option normally is not utilized as there are not many resins available with such a required difference in density [1].

Rielly et al. [19] proposed a rotational molding process of multi-layered thermoplastic parts utilizing different melting points to be able to achieve distinct layers. It was disclosed that a difference in melt temperature of at least 10 °F for each material is required for the successful creation of these layers. Therefore, as each melt temperature is achieved during the heating process the materials will adhere to the mold then to subsequent layers in order of their increasing melt temperatures. For example, the non-foamable resin with the lowest melt temperature will adhere to the mold first creating the outer skin layer where the foamable resin with a higher melt temperature will form a cellular core or layer within this layer. This process is limited to usually dissimilar polymer materials where the lower melting point outer layer causes its parts not to be suitable for heat resistant applications [20].

Hosoda et al. [20] and Lammers [21] similarly determined that a difference in particle size can achieve the same layer distinction while not limiting the materials available for use. Specifically with the combined use of powdered plastics and a foamable compound in pellet form or other large particles, the powdered plastic has a larger contact surface area and the ability to move throughout the voids amongst the large particles and spread over a larger surface area causing it to melt first. This allows the powdered plastic to first adhere to the inner mold surface to form the molten skin layer

while the foamable pellets are still in the process of melting to form the inner layer. It is also described that the degree of difference in particle size required for this process is from three to ten times.

Similarly, Mori et al. [22] proposed creating distinct layers such as integral-skin foam moldings with rotational foam molding using various thermoplastic materials featuring different heat capacities. In particular, the non-foamable material would be chosen such that it would feature a lower heat capacity than that of the foamable material by a factor of no less than 50 (preferably 100). If this factor is increased by up to 1000 successful layer formation can still be achieved but with greatly increased foam processing temperatures. If this factor is less than 50, the materials will not be able to achieve distinct layers as they will be intermixed. Varying the heat capacity of a material to attain these factors depends proportionally on its specific heat, density, and volume. Therefore, what makes this process similar to the last is that assuming the densities of the layer materials are the same, the heat capacities are altered by the varying sizes of the materials particles. For example the material with a lower heat capacity will have smaller particle sizes and will melt and adhere to the mold before the one with a higher heat capacity (larger particles) creating the inner layer [22].

Park et al. [23] disclosed a process of producing only polypropylene (PP) foams by utilizing single-step rotational foam molding with different methods of material preparation. These methods include either dry-blending, or melt compounding a dry-blended mixture of a suitable CBA with a resin under conditions allowing for proper mixing without CBA decomposition both to create foamable compositions. The dry-blended only composition is directly charged into the mold, while the melt compounded composition is processed into pellets to be charged into the mold to begin the rotational foam molding process. Both compositions were able to produce PP foams of desired expansion ratios where it was discovered in comparison of the two that a much finer foam structure was obtained using the melt compounding process [23].

Two-Step Foam Molding: The process of charging the mold separately with two or more materials is called a two-step or multi-step operation that can either be continuous or interrupted. The continuous two-step operation involves the physical separation of the non-foamable and foamable materials via different mechanisms.

Slapnik [24] first disclosed such a process for the manufacture of non-foamed thermoplastic skin foam core moldings. The key of this process was that the foamable material was contained within a thermoplastic air-tight bag that is charged into the mold. Upon activation of the CBA within the foamable material, the expanding foam causes the heat-softened thermoplastic bag to conform to the mold creating the outer skin layer successfully encapsulating the foam.

Duffy [25] more recently created a more controlled process of separating the non-foamable and foamable materials. Within his proposed mold design, a bar extending across the mold that holds one or multiple containers charged with the foamable compound contained by means of removable lids either at one or both ends secured with a heat-resistant filament-reinforced tape. Upon reaching an appropriate temperature and after the non-foamable resin has melted and adhered to the mold surface, the foamable material begins to expand and break this tape releasing the foaming material into the mold. Alternatively, plastic bags were also proposed as a possible container for this process, but unlike the invention of Slapnik, this bag ruptures only to release the foaming material at an appropriate time and not contribute to the outer skin layer. Modern interpretations of the use of a “drop-box” or bag idea are performed via containers with electronically activated doors for precise control of the release of the foamable/foaming compound [1].

Interrupted Foam Molding: Another variation of two-step foam molding is an interrupted process that involves first charging the mold with the non-foamable resin only. After the molten skin has adhered to the surface of the mold through heating and bi-axial rotation, the foamable compound is filled into the mold in some way through a specially designed gate. Such a process was proposed by Carrow et al. [26] along with specific considerations regarding when the process should be interrupted. Specifically, it is said that the process should be interrupted in the time between just before the skin resin has become fully melted and densified to when its surface becomes smooth and glossy. This process has more disadvantages when compared to single-step or two-step continuous methods as it is more complex and has longer processing cycles due to the interruptions [27].

2.2.2 Material Preparation

Essentially the first step before any rotational foam molding operation can begin is to prepare the materials to be charged into the mold. Depending on the type of part to be produced, different materials will need to be used, for example, for a rotational grade resin in powder form should be used. For a foam core or layer, a plastic resin usually in the form of foamable pellets should be introduced into the mold. These pellets are normally obtained by mixing a foaming agent such as a chemical blowing agent (CBA) with the plastic resin by melt compounding. There are two different ways to mix and prepare a foamable formulation before compounding: the dry-blending method and the melt-compounding method.

Dry-Blending Method: The dry-blending method of mixing foamable formulations with CBAs in industrial settings involves the materials being physically blended together in dry powder form using a high speed mixer. It is common practice to use a polymer resin and CBA in powder form, but when the raw materials come in the form of pellets this requires the need for grinding. If any other materials such as additives or fillers are to be used, they can also be added and mixed in powder form using this process. Once mixing is complete the material can directly be charged into the mold to begin rotational foam molding.

This method has the advantage of being low in cost but suffers in the reduced dispersion or mixing capability achieved between the powdered materials [15]. The amount of dispersion achieved is greatly affected by the quality of the powder particles that are being blended together. These particles could vary in size, shape, and size distribution depending on the quality of grinding [28], which could potentially increase the cost of this blending process if a good dispersion is required.

Melt-Compounding Method: The melt-compounding method involves mixing the CBA, polymer resin, and any additional fillers or additives in a molten state using an extruder [28]. Once in the extruder, the materials are melted and blended together as the screw rotates within the extruder barrel where overall heating (both frictional and external) must occur below the onset of the CBAs decomposition temperature [29]. CBAs by decomposing nature may be endothermic or exothermic. Endothermic CBAs absorb heat once activated and releases carbon dioxide (CO₂) gas during decomposition.

Conversely, exothermic CBAs generate heat, and generally release nitrogen (N₂) gas during decomposition [30].

When selecting a CBA for use with a particular polymer such as PE there are several important factors that need to be considered. The first being whether the decomposition temperature of the CBA is close to the melting temperature of the polymer. This is important because if decomposition occurs before melting of the polymer successful foaming cannot be accomplished. The details involving gas generated by a CBA such as its rate of generation, type, ability to disperse within the polymer and how it may react with the polymer are also crucial to the success of the CBA. Some of these details are used to characterize CBAs and others are determined through various testing and analysis practices. The main characteristics that are typically used for all CBAs include gas number, initial decomposition temperature, temperature range at which the maximum rate of decomposition occurs, the rate and kinetics of gas generation and the pressure developed by the gas. The gas number of a CBA is the volume of gas in cm³ that is released by 1 g of the CBA during 1 minute at the temperature of maximum gas generation [2].

Depending on the type of plastic resin this can also have an effect on how easily the two materials blend. For example, if there are different additives within the plastic resin such as pigments, flame-retardants, or anti-oxidants, this can change the surface tension of the resin. It is the surface tension of the plastic resin that determines whether it and the CBA can mix properly, or if they will remain separated coming out of the extruder. If successful mixing is accomplished, this creates an emulsion that is suitable for foam molding that exits the extruder in its molten state. Solid pellets of this mixture are then created by cooling the molten material upon exit of the extruder and cutting it into small pellets [30]. This leaves the material ready to be charged into the mold for rotational foam molding.

This mixing method has the advantage of not being affected by any inconsistencies in quality of powdered materials and can achieve a more uniform dispersion of the different particles. However, in addition to being a more costly method this process is more complex as the decomposition of the CBA must be retarded during mixing. This is a

crucial step where if the decomposition was activated, gas could be lost at the exit of the extruder that later would not be available for foaming [28].

2.2.3 Material Formulation Amounts

Non-foamed Skin Layer Formulation Amounts: To obtain the amount of resin required to create a solid non-foamed layer of a desired thickness, the exact volume taken up by a chosen skin thicknesses of the mold is determined. This volume is used to determine the mass in grams of resin (m_{SKIN}) required to create the chosen skin thickness using:

$$m_{SKIN} = V_{SKIN} \rho_{PE} \quad (2.1)$$

Foamable Formulation Amounts: To determine required amounts of resin and CBA to fill the volume of a mold, the total mold volume must be determined. The required non-foamed skin volume (V_{SKIN}) is subtracted from this total mold volume to determine required expanded foam volume (V_{FOAM}) for the resin used. To successfully fill this volume, a volume expansion ratio (VER) is chosen. VER is defined as the ratio between the volume of the expanded foam and volume of the initial un-foamed resin (V_i) further illustrated using [27]:

$$VER = \frac{V_{FOAM}}{V_i} \quad (2.2)$$

Using the initial un-foamed resin volume, the mass amount of resin in grams (m_{FOAM}) for each desired VER is determined [27] using:

$$m_{FOAM} = V_i \rho_{PE} \quad (2.3)$$

To determine the appropriate amount of CBA to achieve the chosen VER the gas yield needs to be corrected using [27]:

$$\varphi_{corrected} = \varphi_{STP} \cdot \frac{T_c}{T_{room}} \quad (2.4)$$

where $\varphi_{corrected}$ and φ_{STP} represent the corrected and given manufacturer's gas yield respectively, and T_c and T_{room} represent the resin crystallization temperature and room temperature during foaming, respectively. Once the correct gas yield was established, the following is used to determine the amount of CBA required in grams (m_{CBA}) for the given VER [27]:

$$m_{CBA} = \frac{V_{FOAM} - V_i}{\varphi_{corrected}} \quad (2.5)$$

Typically, the amount of CBA within a foamable compound is expressed in terms of its percentage by weight ($\%CBA$) calculated using [27]:

$$\%CBA = \frac{m_{CBA}}{m_{FOAM}} \cdot 100 \quad (2.6)$$

2.2.4 Advantages of Rotational Foam Molding

The advantages of rotational foam molding, when compared to conventional rotational molding are essentially the same as described in Section 2.1.2. This is due to the fact that neither requires high pressures reducing the operation and high tooling costs [31] and that the same equipment can be used requiring only slight modifications. For example, a standard rotational mold cannot be used as gases are released during the foaming process requiring the mold to have appropriate ventilation modifications. It is also known that foam expanding within the mold makes shrinkage of the final part less likely depending on the material composition [21]. For this reason it is required that the mold have greater draft angles than what may be required for conventional rotational molding for part removal [32].

The main difference in advantages between these two processes is related to their finished parts. As first described in Chapter 1 the rotational foam molding process

creates a cellular structure where much of the material is filled with a gas that make foamed products good thermal insulators as gases have a low thermal conductivity. The voids of gas that create the expanded structure also make the material relatively lightweight when compared to the same volume of solid material. This results in a reduced cost to produce a foamed part rather than a solid part of the same size as densities reductions of up to 70% can be achieved [1]. When compared to solid skin hollow parts, the foamed equivalent could have greater physical properties where depending on the strength of the cell walls, the foamed material can act as an energy absorber. This is accomplished by the flexibility of the cells and how much they can collapse or absorb energy upon impact. Stronger foams that exhibit much less flexibility can have the advantage of having a high strength to weight ratio where instead of flexing, the cell walls remain rigid and can bear loads [31].

2.2.5 Disadvantages of Rotational Foam Molding

In addition to the disadvantages of conventional rotational molding as described in Section 2.1.3, the major disadvantage to rotational foam molding is that the total cycle time is greatly extended [32]. This overall cycle time increase is partly due to the additional heating required for foam processing in addition to an increase in cooling times from the insulating affect of the resulting foam structure. As well, during processing a uniform foam density cannot always be controlled which could contribute to a loss in mechanical properties within certain areas of the finished part [31].

2.3 Introduction to Polymers

The word polymer is derived from two Greek words “poly” meaning many and “mer” from “meros”, meaning part as polymers are large chain-like molecules built by hundreds of small repeating units. These repeating units are called monomers and consist of such atoms as carbon, hydrogen, oxygen, or nitrogen in different orientations depending on the specific polymer type [31].

One of the many forms of polymers known as plastic can be further classified as either thermoplastics or thermosets. Thermoplastic materials consist of randomly

distributed long chain molecules held together by relatively weak Van der Waals forces. When heated these forces are weakened making the material soft and flexible turning it into a viscous melt that solidifies upon cooling. This heating and cooling process can be repeated as much as required without experiencing a quality reduction if processed at proper temperatures. Thermosets consist of long chain molecules that are interlinked by strong bonds created during a process termed cross-linking. These strong bonds allow the material to become a viscous melt when heated, but upon cooling and solidification, the material cannot be heated again as it will degrade. Unlike thermoplastics, due to their stronger bonds thermoset materials are typically more rigid and are not heat sensitive [14].

2.3.1 Polymer Production

Polymers are produced by a method known as polymerization and characterized by the type of polymerization used either chain-growth or step-reaction polymerization. Chain-growth polymerization, once known as addition polymerization, is the sequential addition of monomers rapidly to a polymer chain without the loss of monomer molecules [33]. To begin this process requires the use of an initiator such as a free radical, anion, or cation. A free radical is a molecule with an unpaired electron where anions and cations are negatively and positively charged ions. Reactions caused by these initiators cause double bonds of a vinyl monomer to open allowing the initiator to attach to one side of the opened bond leaving the other open to continue the process known as propagation. Termination of this reaction is caused when two radicals meet and satisfy their unpaired electrons. When one radical existing at an active chain end meets with another radical existing at another active chain end this is known as combination termination. Another form of termination known as disproportionation involves a chain radical giving up one of its electrons to another rendering both chains inactive [34]. Impure molecules can also terminate the polymerization reaction unnecessarily [3].

Step-reaction polymerization, also referred to as condensation polymerization, involves the addition of monomer molecules in a step like-sequence to a polymer chain while creating a condensation byproduct such as water or acid. This process occurs when chemicals added to a polymer chain consisting of at least two functional groups react

together creating a low molecular weight polymer. As the reaction progresses the molecular weight of the substance increases allowing for various molecular weight materials to be synthesized typically without carbon as a crucial element in the chain structure due to the nature of the reactions [34].

Ziegler-Natta catalyzed polymerization is a form of polymerization occurring at relatively low temperature and pressure conditions. A Zeigler-Natta catalyst consists of a base metal alkyl or halide with a transition metal salt. There are numerous varieties of these catalysts that can be produced in a soluble homogeneous variety for solution polymerization or a heterogeneous variety such as silica for use in gas-phase reactors that create varied reactions ultimately producing different polymers. This is accomplished by a mixture of active sites within the catalyst, that vary with the type used, reacting with added molecules such as ethylene, for example, in a repetitive action that creates a polymer chain. The type of catalyst that tends to produce longer chains is less likely to have alkyl comonomers, where shorter chains are created with catalysts containing more comonomer. To counteract the repetitive chain reaction polar comonomers are added to deactivate the catalysts [3].

Similarly, metallocene catalyzed polymerization involves use of metallocene catalysts under similar reaction conditions as those used for Zeigler-Natta polymerization. This type of catalyst, available in hundreds of variations, however, features only one type of active site that reacts with the available monomers in an identical way [3]. The advantage of this type of reaction is that all polymer molecules created will tend to be identical offering superior properties compared to the multi-site reaction of Zeigler-Natta catalysts that produce polymers with varying chain lengths [14].

2.3.2 Molecular Weight Distribution

Depending on the way in which they were synthesized during polymerization all polymers feature molecular weight distributions. This is known as the degree of polymerization. Molecular weights are determined by two variables, the number average molecular weight (\overline{M}_n) and the weight average molecular weight (\overline{M}_w) calculated using the following equations:

$$\bar{M}_n = \sum_{i=1}^{\infty} \frac{n_i M_i}{n_i} \quad (2.7)$$

$$\bar{M}_w = \sum_{i=1}^{\infty} \frac{n_i M_i^2}{n_i M_i} \quad (2.8)$$

where n represents the number of molecules of i and M_i represents the molecular weight of i [33].

The properties of a polymer are greatly affected by its molecular weight where, for example, stiffness and strength increase with increasing molecular weights. In relation to temperature, the flow temperature increases and degradation temperature decreases with increasing molecular weight [16].

2.4 Polyethylene

Polyethylene (PE) is a thermoplastic polymer known as a polyolefin. This is a class of polymer derived from petroleum and natural gases that consist of carbon atoms covalently linked with two hydrogen atoms with methyl groups terminating the polymer chains. The chemical formula for PE is $C_{2n}H_{4n+2}$ where n represents the degree of polymerization. The degree of polymerization can typically be from approximately 100 to 250,000 resulting in varying molecular weights of up to 3,500,000 [3].

PE has a number of material varieties relating to the level of branching within the polymer chains. With increased levels of branching the polymer experiences more variations or defects from the pure PE structure limiting the crystallinity of the material. As the degree of crystallinity increases the density of the material will increase. Therefore the more branching existing in a polymer results in a lower density material, which best describes the first type of PE known as low density PE (LDPE). LDPE is a highly branched material consisting of ethyl and butyl groups in combination with long chain branches in an orientation as presented in Figure 2.7 [3].

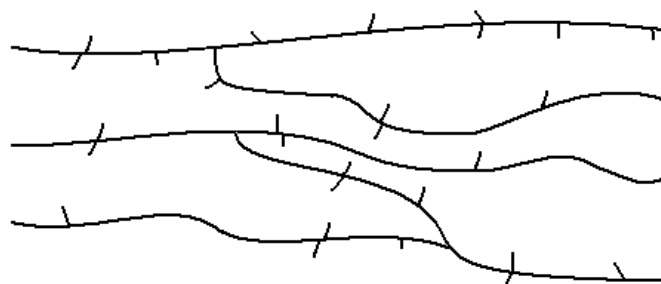


Figure 2.7: Simplified LDPE Branch Structure

The many side branches of this material prevent individual molecules from being packed tightly together resulting in a low density. The typical density range for this material is from 0.910 g/cm^3 to 0.925 g/cm^3 [3-6].

Linear low density PE (LLDPE) is similar to LDPE as it shares the same fundamental structure apart from having short alkyl groups attached at random intervals to the base polymer chains. A simplified representation of the LLDPE branch structure is presented in Figure 2.8.

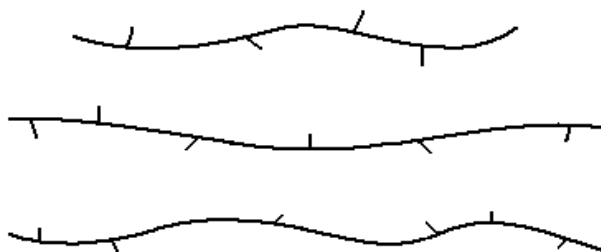


Figure 2.8: Simplified LLDPE Branch Structure

As it is apparent from the above representation the side branches are shorter and more uniformly distributed along the length of the chains when compared to a LDPE structure. This branch structure allows the material to retain its low density with the added ability of being able to pack molecules closer together improving the physical properties of the material. The typical density range for this material is from 0.926 g/cm^3 to 0.940 g/cm^3 [6].

Another of the most common varieties of PE is high density PE (HDPE) which is the closest to pure PE and sometimes known as linear PE (LPE) due to its almost complete lack of branches as presented in Figure 2.9.

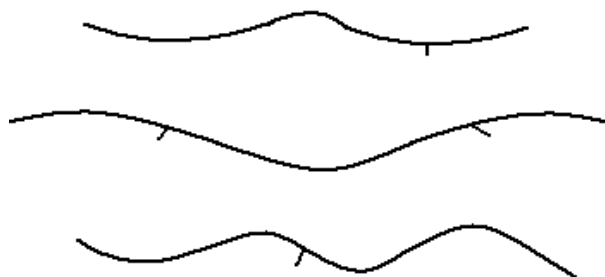


Figure 2.9: Simplified HDPE Branch Structure

The lack of branches allows for the molecules to be packed tightly together. As the molecules are held together by Van der Waals forces, the closer together they are the stronger the bond between them. This allows for a high degree of crystallinity and rigidity of the material in addition to higher densities. The typical density range for HDPE is from 0.941 g/cm^3 to 0.959 g/cm^3 [3-6].

2.4.1 Morphology

As with most polyolefins, PE has a three-phase semicrystalline morphology closely derived by its molecular characteristics and method of preparation. A representation of this morphology is presented in Figure 2.10 [3].

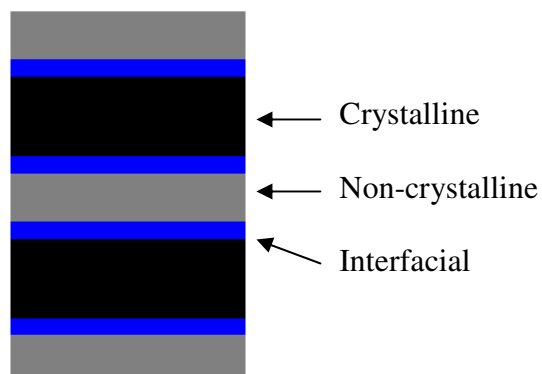


Figure 2.10: Three-Phase Structure of PE

Within this structure the crystalline phase consists of submicroscopic crystals surrounded by a non-crystalline phase comprised of a somewhat ordered layer and disordered interfacial layer. The physical properties of the resulting PE material are directly related to the proportions of these phases in addition to their physical relations with respect to each other known as the degree of crystallinity [3].

Knowing the degree of crystallinity of PE is important in determining its mechanical behavior during processing. For example, semicrystalline polymers such as PE exhibit a range of melting rather than a single melting temperature due to the existence of the various phases. Furthermore, the specific morphology of PE also allows it to melt at lower temperatures when compared to other semicrystalline materials [3].

2.4.2 Thermal Analysis

Thermal analysis involves measurement of different physical or chemical changes of a material as a function of temperature by isolating the material and subjecting it to a certain thermal treatment. This characterizes thermal analysis as destructive testing where the material generally melts/degrades when heated [35]. There are many techniques of thermal analysis, including but not limited to, differential scanning calorimetry (DSC) and thermogravimetric analysis (TGA) which are popular in the plastics industry for characterizing resins and other related materials such as CBAs and additives.

Differential Scanning Calorimetry: Characterizing a resin means determining its important transition temperatures such as where melting and crystallization occur to establish its best suited processing temperatures. Melt temperature (T_m) is the temperature at which a material begins to transform from a solid to a molten state, while crystallization temperature (T_c) is the temperature where a material begins to experience a crystalline or solid structure upon cooling [36]. Both of these characterization parameters can be determined by performing DSC experiments.

DSC is a technique of thermal analysis that involves measuring the amount of energy required to maintain a close to zero temperature difference between a sample and an inert reference sample. This is determined by acquiring the difference in heat flow rate between the samples when both are subjected to the same temperature treatment.

There are two varieties of DSC systems: power-compensated and heat-flux. Power compensated DSC involves heating and/or cooling of the samples with separate identical furnaces. The temperatures of these furnaces are kept constant through a variation of their power input. The resulting energy required to maintain a constant

temperature between the furnaces is the enthalpy or heat capacity of the sample with respect to the inert reference sample.

A heat-flux DSC, such as TA Instruments' Q20 that will be used for characterization of the chosen PE resins, involves heating and/or cooling of both samples within the same environment by a single furnace. The change in enthalpy or heat capacity of the sample material causes a temperature difference compared with the inert reference sample that is used to determine the heat flow of the sample [37].

The respective heat flows of the sample and reference sample are determined through constant monitoring of the temperature measured from a constantan disc base between the samples, the temperatures of the samples measured with chromel disc thermocouples, as well as the thermal resistance and thermal capacitance. It should also be noted that each determined heat flow measurement includes heat flow to the sample pans so final heat flow of the sample is determined by subtracting the heat flow of the sample and reference sample [38]. This final value is determined over time and plotted versus temperature.

Thermogravimetric Analysis: TGA involves heating and/or cooling a material sample in a controlled atmosphere while recording any resulting weight change. Weighing of the material can be accomplished in two ways: a null-point or deflection balance. For a null-point balance system, a balance beam attached to the sample holder detects any weight change occurring in the sample and attempts to restore itself back to its original position. The force required to bring the beam to its original position is seen as proportional to the weight change of the sample. A deflection balance system, seen as a more reliable method of weight measurement, is based on the idea of conventional analytical balances. Temperature measurements during a TGA experiment can be recorded with either a direct contact or a non-contact thermocouple [37].

A TGA experiment measures the absolute weight change of a material subjected to a temperature change in the presence of a purge gas, e.g., nitrogen which is used in the Q50 TGA. Other measurements that can be determined using TGA experiments including thermal stability, decomposition, degradation, moisture content, morphology, and reactivity [37].

2.4.3 Processing Considerations

Viscosity: Before utilizing a material like PE in a plastics process it is important to understand the rheological characteristics of the material such as its viscosity. In its molten form PE does not behave as a liquid but rather as a non-Newtonian fluid. A non-Newtonian fluid is one that experiences a change in its viscosity or resistance to flow depending on the temperature and shear forces it experiences. For example, with increasing the shear rate experienced by a polymer melt the viscosity will increase. In contrast, Newtonian fluids such as water always maintain a constant viscosity no matter the temperature or shear conditions they experience. Typically, as the temperature and amount of shear experienced by the molten polymer increases its viscosity decreases, a phenomenon that is not experienced by all polymers. By nature molten PE is very viscous and exhibits elastic properties as it can be deformed and recover its shape in this state making it a viscoelastic material. The exact viscosity of the material and its level of elasticity are determined by the molecular structure [3]. For example, given a typical shear rate of a process it is known that a greater viscosity will be experienced by a material with a narrow molecular weight distribution (NMWD), i.e., the polymerization process created little variation in the molecular weights [29].

In terms of processing, higher viscosity materials are favored for processes involving extrusion such as blow molding where the ease of flow is not required as higher pressures and shear stresses are utilized. Lower viscosity materials are more suited for processes such as injection molding due to their greater ability to flow [39].

Viscosity can also have an affect on foamability of PE, where to ensure an acceptable foam structure in rotational foam molding, it is important to use a higher viscosity resin. For example, if using a low viscosity resin, the lack of resistance to flow of the material would make it more difficult for the cells to maintain an acceptable smaller size. This is due to the melt having reduced melt strength allowing cell drainage to occur leading to cell coalescence [40].

Melt Flow Properties: The melt flow rate (MFR) or melt flow index (MFI) is a measured value relating to the viscosity of a polymer but does not take into account changes in viscosity with changing shear rates. This value represents the rate at which a molten polymer extrudes through a capillary die under standard conditions measured in

grams extruded over a 10 min period (g/10min) as per ASTM D1238. It generally reflects how a polymer may act not given any shear forces that may exist during processing, and given that MFR is widely used by industry for characterization it is helpful in determining the available processing methods for a material. Typical MFR values can range from 0.05 g/10min to up to 120 g/10min and are inversely related to viscosity and molecular weight allowing for MFR ranges to be matched with plastic processing technologies [3, 39]. For use in rotational molding and rotational foam molding, the typical MFR range for PE and other polymers is from 3 to 10 g/10min with values of 5 and 6 being the most common. This range is lower on the available MFR scale as the material is required to melt and adhere to the mold walls to create the hollow or outer layer structure, where a higher MFR material would not be able to experience the same adhesion. However, the part geometry can be a factor in which MFR should be chosen as large parts are best created using higher MFR materials with higher density [3].

Degradation: Degradation of PE is any detrimental change to the polymer in terms of physical appearance, mechanical properties, or chemical structure caused by a chemical reaction. Examples of degradation include loss of clarity, change in colour, increase in viscosity, and/or increase in brittleness that could be caused by thermal, mechanical, chemical, or other influences. However, the main factor causing degradation is the gradual introduction of oxygen into the polymer molecules, which is also known as oxidation or chain scission. Degradation can occur in many environments (e.g., outdoors due to the presence of UV light or weathering). In terms of processing degradation, this most commonly occurs in the presence of high temperature environments in the absence of light for prolonged periods of time. Given that in rotational foam molding the polymer is in a hot oven for long periods of time to accommodate foam formation, it is possible for this degradation to be experienced. Once degradation has begun within a material there is no way to stop or reverse its effects. The way to prevent degradation, however, is to add stabilizers to the material before processing or to ensure proper processing parameters are utilized [3].

Stabilization: Stabilizers are capable of preventing degradation by inhibiting its reaction from occurring. A common form of stabilizer is an antioxidant that comes in different varieties depending on which step in the oxidation reaction is needed to be

retarded. Other chemical substances can be utilized to shield specific causes of oxidation reactions such as titanium dioxide and carbon black for ultraviolet light stabilization. These stabilizing materials can be added at various stages of material processing but it is best to add them using an extruder as the level of dispersion is critical to the success of the stabilizer [3].

2.5 Successful Polyethylene Foam Formation in Rotational Foam Molding

If rotational foam molding is utilized for chemical polymer foaming there are three things to consider in the creation of better quality fine-celled foams: cell nuclei density, cell coarsening, and cell coalescence. For cell nuclei density, it is important to note that in the beginning of foam processing a large number of the cells must be nucleated to be able to achieve a fine-celled structure. To ensure that cell nucleation will occur for large number of cells, excellent dispersion of the CBA in the polymer resin matrix is required [8].

With cell growth it is known that for a given volume, a system favours having fewer large cells than having a large number of smaller cells as the system will be more stable. This occurs if neighboring cells have different diameters where larger cells will try to grow at the expense of adjacent smaller cells, to lower the overall surface energy of the system [41]. This can occur if a smaller cell diffuses gases into an adjacent larger cell due to a pressure difference between them causing shrinking and the eventual collapse of the smaller cell. Cell wall collapse can also cause the same affect between adjacent cells. This phenomenon is known as cell coarsening [2, 8, 42]. Similarly, cell coalescence occurs due to thinning of cell walls as the density of the foam decreases causing gas diffusion between two neighboring cells which results in them joining. The occurrence of cell coalescence also creates a stable system as it is thermodynamically favored due to the surface energy of a coalesced cell being lower than the sum of the surface energy of the two adjacent cells [42].

Cell coarsening and cell coalescence during cell growth are undesirable because they both deteriorate the initial cell density and lower the cell population density reducing the quality of the foam. To prevent this, the melt strength of the polymer can be increased thus increasing the resistance of the material to change the size of its cells. This is possible since the melt strength of a polymer is the degree of resistance to extensional

flow of the cell walls. If this is low, the cell walls will be weak and more vulnerable to change. Therefore, by increasing melt strength of the polymer, the chance of cell coarsening and coalescence occurring will be reduced [43]. This can be accomplished by utilizing lower temperatures. This means that there is a need to keep the heating temperature during foam processing as low as possible [44]. It is also known that the final cell size of the foam is dependent on the cooling cycle at which time the polymer can reach its crystallization temperature and solidify [28].

2.6 Engineering Design Tools

2.6.1 Quality Function Development

A House of Quality (HofQ) is a Quality Function Development (QFD) tool used for a means of “customer focused thoughtful engineering” to translate design requirements into engineering specifications [45]. The HofQ is completed by filling information into various tables called rooms as illustrated in Figure 2.11.

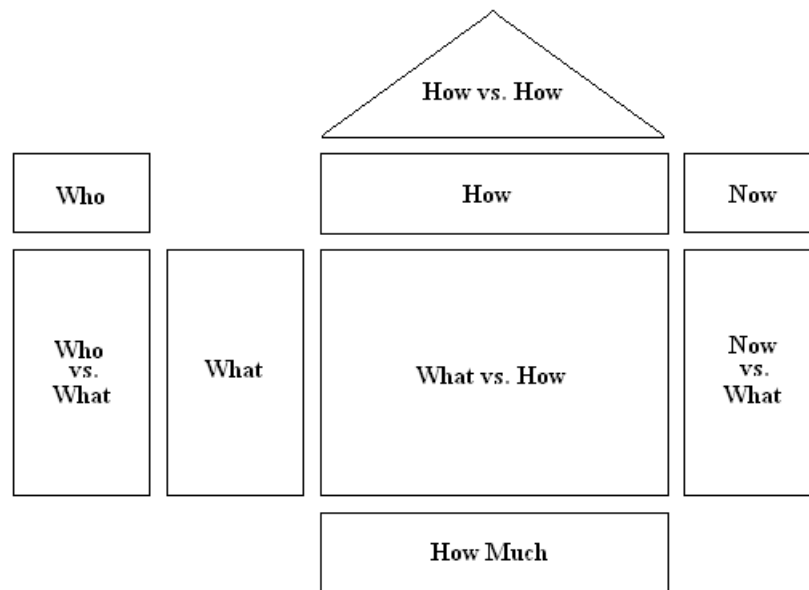


Figure 2.11: Simplified Example of HofQ

The first step to complete a HofQ is to input the design requirements and technical requirements into the “What” and “How” rooms respectively and rate them for their importance and direction of improvement. Each element of these two categories is correlated in the roof of the HofQ as either a synergy (positive relationship) or a

compromise (negative relationship). The “What” and “How” rooms are then compared together in a relationship matrix with either a strong, medium, or weak relationship. If a prior design exists a customer competitive assessment room (“Now vs. What” room) can be completed by rating how well the potential new design will compare to existing designs in accomplishing requirements. The final areas of the HofQ involve determining the final importance and relative weightings of each item from the “What” and “How” rooms and use them to qualify the most important items for the new design [45].

2.6.2 Pugh Method

Design concepts can be evaluated in terms of set important factors using the Pugh Method [46]. This method involves inputting data relating to the ability of the different concepts to meet set criteria into a table called a decision matrix.

To complete a decision matrix, certain criteria that the concepts can be compared with are generated and rated for their importance. The next step is to list the various concepts in their respected columns, where a concept that initially appeared to be preferred or better than the rest is called the datum and is used for comparison. The comparison involves how each concept meets the criteria compared to the datum with use of the following symbols: -, + or S. The - sign means the concept has failed to meet the criterion or cannot meet it as well as the datum. Conversely a + sign means the criterion has not only been met but also exceeded the ability of the datum. The S symbol, however, means the datum and the concept met the criterion equally and is ignored for final calculations [46].

Once the initial evaluation is complete each concept is given a score calculated by the summation of symbols and the weighting total that is determined by the summation of multiplying each importance rating by its given symbol. The summation of symbols is used to determine which concept best meets the criteria by interpreting the resulting sign and value for each concept. If the value is negative the concept is not as good as the datum and conversely, a positive value means the concept is a better choice than the datum. The value of the weighted total, however, is used when there are multiple positive concepts and only one can be chosen. In this situation the higher positive weighted total will be taken as the best choice as it will have met the criteria better than the others [46].

2.7 Characterization of Experimental Results

The experimentally obtained foam morphologies will be characterized as a combination of: achieved foam density; average cell density; and average cell size. The evaluation method for determining polymer foam density is described in ASTM D1622-08 where a foam sample not less than 1 in³ is obtained and weighed on a scale to a precision of $\pm 0.1\%$. All dimensions of the sample are measured with digital calipers to a precision of $\pm 0.1\%$ where the final foam density (ρ_{FOAM}) to three significant figures is calculated using Equation 2.9.

$$\rho_{FOAM} = W_s / V_s \quad (2.9)$$

where W_s is the weight and V_s is the calculated volume of the sample respectively [47].

Equation 2.10 is used to evaluate cell population density (N) [48]:

$$N = (n_{cells})^{3/2} \cdot VER \quad (2.10)$$

where VER , as mentioned previously, represents the volume expansion ratio of the created foam structure and n_{cells} represents the number of cells contained in a 1 cm² area of foam. Due to the small size of the cells, n_{cells} is determined from counting the number of cells contained in a scanned micrograph taken using a Scanning Electron Microscope (SEM). As the area within the micrograph is much smaller than 1 cm², the number of cells is adjusted proportionally to represent how many cells would be present in the required area (1 cm²). The resulting cell population density can then be used to determine average cell size ($D_{average}$) using Equation 2.11 [48].

$$D_{average} = \sqrt[3]{(VER - 1) \cdot \frac{6}{\pi \cdot N}} \quad (2.11)$$

Visual Presentation of Foam Structures: To illustrate the level of cell coalescence and degree of foam filling in the developed foam structures, the naturally white foam was coloured black and scanned using a conventional document scanner. The

resulting scanned image effectively shows larger bubble sections within the foam that can represent the level of cell coalescence and cell non-uniformity. These images also show the presence of trapped air pockets between the foam and skin layer that represent the degree of filling of the moldings. A fully filled foam core is defined as one that does not experience any trapped air pockets between the skin and foam, and one that is void of any large bubbles within its centre.

Similarly, scanned micrographs are used to illustrate the foam structure on a cellular level in order to further evaluate the quality of the foam both qualitatively, and quantitatively. All of these images are used to assist in the comparative analysis in determining how to achieve the best quality molding.

Visual Presentation of Skin/Foam Interface Quality: An acceptable quality skin/foam interface of an integral-skin foamed core molding occurs if there is no visible partition between the two structures. On a cellular level, an acceptable level of quality is achieved if the cells of the foam appear to protrude into the non-foamed skin layer with no gaps. Scanned micrographs taken at various areas along the skin/foam interface will be used to qualitatively illustrate the achieved quality of this area of the moldings of the experimental results.

CHAPTER 3

DESIGN AND DEVELOPMENT OF AN EXTRUSION-ASSISTED ROTATIONAL FOAM MOLDING EXPERIMENTAL SYSTEM

3.1 Introduction

It is the goal of this chapter to generate and evaluate concepts that attempt to solve the problem of how to significantly reduce the overall cycle time of rotational foam molding PE integral-skin foam core moldings. The first step was to outline the problem at hand and generate a potential solution. It is crucial to define all design requirements and technical specifications relating to this proposed solution to determine various feasible concepts that will attempt to meet these requirements. To better understand each concept, they were evaluated for their feasibility.

3.2 Problem Statement

As stated previously, the principle intrinsic disadvantage of rotational foam molding for the production of integral-skin foam core moldings is the long cycle time. This lengthy cycle time results because the materials within the mold must be heated from room temperature to above the melting temperature of the polymer and decomposition temperature of the CBA, and subsequently cooled. This provides an opportunity to create a novel processing technology that attempts to overcome this principle disadvantage. Research has been performed in this area, in that a process was proposed that decouples the typical heating cycle associated with the creation of integral-skin foamed core moldings. This was accomplished with the proposed process by conjoining rotational molding practices with the most efficient form of melting plastics, extrusion [49]. A schematic representation of this process is presented in Figure 3.1.

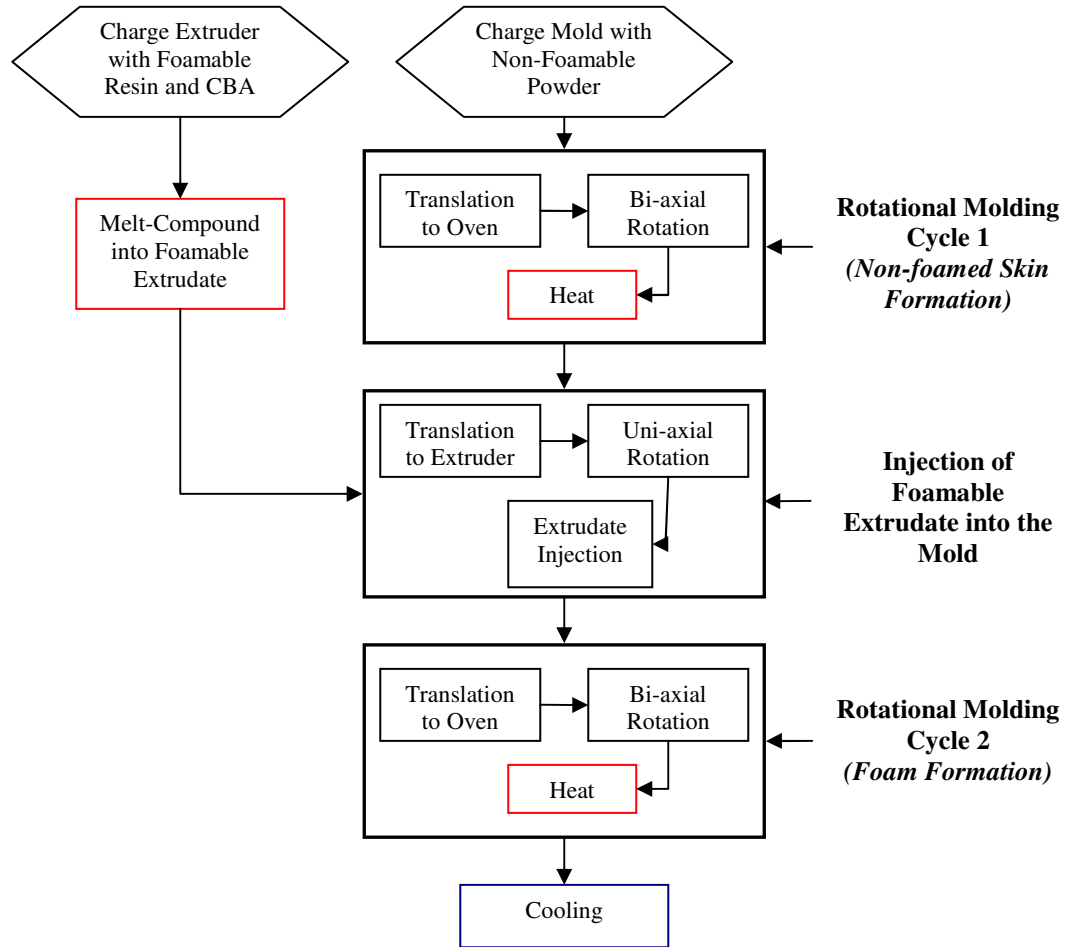


Figure 3.1: Schematic Representation of the Proposed Process Solution

The first step in this proposed process requires melt-compounding a foamable resin with a chemical blowing agent (CBA), while simultaneously rotationally molding a non-foamable material creating an skin layer within the mold. The melt-compounded foamable melt is directly filled into the mold, containing a still molten non-foamed skin layer, via a specially designed port for foam formation and final shaping to commence with continued heating and bi-axial rotation [49].

This novel process is referred to as Extrusion-Assisted Rotational Foam Molding (EARFM). It has the potential of drastically reducing the overall cycle times normally associated with rotational foam molding by allowing the foamable compound to only be heated once in an interrupted cycle. Reducing the need to heat the foamable compound multiple times allows for a potential energy savings and improved control of cell growth [49]. Consequently, there was a need to experimentally verify these claims with the

creation of a lab-scale experimental setup dedicated to this process, which was the focus of this research.

With the successful creation of this process that may have the potential to produce high quality moldings with notable time and energy savings it was hoped that it will be attractive for industrial implementation. More specifically, the achieved moldings could be used in such applications including but not limited to water buoys, floating docks, large fish collection bins, and sound insulation panels. All of these potential applications involve the creation of large moldings most of which require being air-tight, but are generally created as hollow parts or secondary foam-filled moldings with a dissimilar resin protective outer skin. With EARFM, these normally hollow large parts could be filled with foam, and the secondary foam-filled moldings could feature an enhanced skin/foam interface with use of like resin layers. Both of these suggested modifications with use of the successful creation of EARFM could potentially improve mechanical and insulative properties while potentially increasing the useful product life of these parts.

3.3 EARFM Process Variables

As the EARFM process represents a departure from both conventional rotational and rotational foam molding, it features additional process variables due to the addition of the simultaneous extrusion melt compounding process that will be discussed next.

Phase 1: Rotational Molding Variables. The most important consideration for producing a hollow rotomolded part is to create a uniform solid skin thickness and good surface quality. The quality of the skin is typically dependant on the type, grinding quality, and amount of resin used, the oven heating temperatures, the mold material, the mold thickness, the mold RPMs and the cycle times [5]. As stated previously, when heated and rotated bi-axially at controlled speeds the resin melts and adheres to the internal surface of the mold creating a solid skin structure that replicates its shape. This means that the rotational speed and rotation ratio can also have a significant effect on the quality of this layer. The heating cycle time and oven temperature set, however, are dependent on the required skin thickness and the thermal degradation limit of the resin. For example, for a longer heating cycle a thicker skin can be produced, but for a higher

processing temperature there is more of a chance that degradation can occur. Yet, higher processing temperatures and long heating cycles can help dissolve bubbles that form in the skin faster than during shorter, lower temperature heating cycles [50].

Phase 2: Extrusion Variables. To ensure that high quality foam morphologies can be achieved during the subsequent (second) rotational molding heating cycle, it is important to disperse the CBA and preserve it un-foamed in the melt within the extruder. A well mixed foamable melt that has not reached its CBA onset decomposition temperature has the potential to produce fine-celled foam as no large bubbles will be produced due to agglomerated CBA particles, and the gas loss during rotational molding will be minimized. Variables related to such conditions include the extruder processing barrel temperatures, the temperature of the melt, the screw RPMs, the melt pressure, the residence time of the melt in the barrel, and the achieved degree of dispersion of the pre-dry blended powder polymer-CBA mixture. The most important of these variables relating to preserving the un-decomposed state of the CBA are the extruder barrel set processing temperatures. Thus, careful consideration must be taken when setting the band heaters because the barrel temperature must be at the same time kept above the melting temperature of the resin to achieve a flow capable of CBA dispersion, but below the onset decomposition temperature of the CBA.

In addition, affecting the processing temperatures, more specifically the melt temperature, is the screw rotation RPM as it produces a shear flow of the resin that creates friction between the resin and the extruder barrel. This occurs due to the resin becoming trapped in the gap between the screw flights and the walls of the extruder barrel. This friction generates heat that actually melts the resin and increases the melt temperature [29] potentially reducing the achievable quality of the final foam structure by causing a premature CBA decomposition. The shear flow also causes dispersive mixing of the solid particles of the CBA within the melt. Dispersive mixing is created when the foamable compound melt is rotated by the screw creating the same shear forces of the flow that break up agglomerated particles of the CBA [16]. Therefore, the shear forces created are proportional to screw rotational speed and the RPMs should be kept at an appropriate rate in order to reduce friction and maximize the dispersion.

The rate at which the resin and CBA are heated within the extruder as dictated by the processing temperatures and screw rotation can cause premature decomposition of the CBA. Similarly, with lower heating rates if the un-decomposed CBA remains in the extruder for a long time, known as a long residence time, this could also cause an unwanted premature decomposition.

Phase 3: Mold Filling Variables. Once the solid skin layer has been formed, the amount of time the mold is out of the oven and the speed of uni-axial rotation while the foamable compound filling takes place can further influence the final skin uniformity and quality. For instance, if the mold is out of the oven too long, the skin can begin to solidify potentially altering its initial adhesion affection intensity to the foamable compound, and a slower uni-axial filling rotation can cause the skin layer to sag. This sagging effect is greatly dependant on the MFR of the resin. A higher MFR resin will feature lower viscosities and sag more as a result of a lower uni-axial rotation.

Phase 4: Rotational Foam Molding Variables. Upon the completion of filling a lot of identical previously mentioned variables involving rotational molding still apply as the mold returns to the oven for a second rotational molding heating cycle for foam production and final foam shaping. However, mold venting now becomes a more crucial variable due to the temperature-triggered CBA gas generation. If a proper venting system is implemented, it will have the ability to allow the creation of a good quality foam structure given all other variables are optimized. Also, the heating cycle for foam formation should be slightly different than for skin production in that in order to prevent cell coalescence the lowest possible heating rates must be implemented. After foam formation completion the cooling cycle, that is dependant on the cooling apparatus and cooling time, also greatly affected by insulative properties of the resulting foam, can affect part warpage and the final cell density of the foam [5]. For example, for short cooling cycles is it possible the final part will experience more warpage which is less apparent when a foam core is introduced into the molding [51]. In terms of cell density, it is believed that the cooling rate will determine the rate at which the cell's structure will freeze and maintain their shape [40]. Thus if the cooling and heating rates are not properly optimized together, excellent quality foam may not be achieved.

Therefore, these and all abovementioned variables must be investigated carefully in order to ensure an excellent quality PE integral-skin foamed core can be achieved.

3.4 EARFM Experimental Setup Design

To assess the design requirements and technical specifications for the creation of an EARFM process the major components were investigated individually.

3.4.1 Design Requirements

Extruder: The extruder required for this process must be capable of melt compounding and dispersing a CBA within the polymer matrix to produce an un-foamed compound in molten form. The extruder must also be capable of filling this molten mixture into the mold, requiring alignment abilities to ensure it can successfully interface with the mold. Control of the extruder parameters, such as screw rotation speed and temperatures of various barrel zones must be simple to use for ease of operation. In terms of safety, the extruder barrel must withstand pressures created if the CBA decomposition is activated and foaming occurs within the extruder. If this or any other emergency situation occurs, the extruder must feature a simple emergency shutdown procedure and a standard rupture disk.

Oven: An oven, chosen to be the desired heating method for the initial proposed process as it is one of the most common heating methods for rotational molding and rotational foam molding, should be capable of melting thermoplastic materials within a mold. It should feature a simple to use control interface. It must be large enough to contain the mold and mold rotational mechanism during bi-axial rotation and possibly require alignment capabilities. To be well implemented into the proposed process the oven must include manual and/or automatic operation. If any emergency situation were to occur, the oven must feature a simple emergency shutdown procedure.

Mold Rotational Mechanism: The mold rotational mechanism must allow for both uni-axial and bi-axial rotation of the mold, with individual control of each to ensure different rotation ratios can be achieved. There must also be an adaptable mold attachment method to allow the capability of various mold designs to be utilized.

Translational capabilities may have to be implemented in conjunction with the mold rotational mechanism to accommodate mold translation during processing. All components of this system must be able to withstand operating temperatures and weights of different molds in addition to any vibrations created due to mold rotation. As with other components an easily activated emergency shutdown procedure would also be necessary.

Mold: The mold must accommodate easy part removal. For foamable compound filling, connection to the extruder should be accomplished via a specialized port that can maintain the surface integrity of the non-foamed skin layer after filling. Venting must also be included in the mold design to permit gases generated during foam formation to escape. As heat transfer is an important condition in rotational molding, the mold material must allow for efficient heat transfer.

3.4.2 Engineering Specifications

Extruder: The extruder must feature sufficient horsepower to allow for efficient filling of the foamable melt into the mold. During filling, the mold will be interfaced with the extruder nozzle resulting in the need for possible vertical position adjustment of the extruder up to at least ± 10 cm to permit exact positioning for interfacing with the mold. Filling may also be accomplished with the use of a heated nozzle with an accuracy of no more than ± 5 °C that may allow for sealing when not in use to prevent unwanted material leakage. The number of screws within the extruder barrel determines the degree of dispersion of a mixture, in which two screws would be preferred. Emergency control of the extruder could be accomplished using emergency stop controls that disable all functions once activated.

Oven: The oven must provide heat evenly of up to at least 300 °C and at a rate of approximately 5 °C/s maintaining an accuracy of ± 5 °C, potentially by use of convection technology. Temperature control can be accomplished via a programmable controller such as a proportional-integral-derivative feedback control (PID) to allow for programming of temperature profiles. Permanent or variable height adjustment can be required for oven alignment and a controlled door operation possibly via pneumatics may

allow for the option of manual or automatic operation. Emergency control of the oven could be accomplished using emergency stop controls or simple on/off controls that disable all functions easily. The oven must also allow the mold and mold rotational mechanism to be encapsulated within it and allow for full mold rotation.

Mold Rotational Mechanism: All components of this design could be fabricated from high strength materials and feature high temperature coatings to be able to withstand mold weights, rotational vibration, and oven temperatures up to 300 °C during processing. Adding modularity to the mold attachment design would allow for multiple shape designs to be used. Having individual motor control would accomplish the need for individual control of the uni- and bi-axial mold rotations. The size of this mechanism must fit within the chosen oven and accommodate mold alignment with the chosen extruder. A variable height position mechanism may assist in accommodating alignment between these components and must be capable of ± 5 cm. Emergency control of this assembly could be accomplished using emergency stop buttons that disable all motors.

Mold: The mold can be designed for ease of part removal by requiring a draft angle of no less than 1°. The mold/extruder interface, due to the required uni-axial rotation during extrudate filling, must be no less than 1 cm away from the axis of rotation in an attempt to prevent damage of the extruder nozzle or the mold. Metal tubes can be implemented into the mold design to allow for venting and a high heat transfer material can be used for the mold to allow for efficient heat transfer.

3.4.3 Design Opportunities

Both extruders and ovens are commercially available in numerous sizes with various functionalities, therefore locating and sourcing a suitable extruder and oven requiring little to no modifications is possible. As injection molding requires the rapid injection of molten polymers it is probable that an appropriate nozzle and/or filling equipment can be found to meet some or all requirements associated with material filling within the proposed process. Also, currently available rotational molding equipment features the capability for bi-axial rotation where it may be beneficial to model the mold rotational mechanism after these designs.

3.4.4 Design Constraints

One constraint associated with the design of this EARFM processing technology was the size of the laboratory for which it was located. The laboratory measures approximately 3.7x3.7 m and was a factor in the selection and design of all components. The available power sources in the laboratory room also had a determining factor on equipment selection. Due to the complexity of the technology implemented into this process, a complex maintenance schedule could result constraining the available experimentation time. Therefore, selecting and designing the equipment and components was done in such a way that the overall complexity of the system was minimized so that it would require little to no maintenance.

3.5 House of Quality for EARFM

A House of Quality (HofQ) was completed for each major component (as presented in Appendix A, Figures A1-A4) where importance ratings and their relative overall weighting were determined for each design requirement and technical specification. These values were important in selecting final design components, and to aid in the concept generation and selection process.

3.6 Concept Generation for EARFM Experimental Setup

In order to conceptualize plausible design ideas the process was simplified in terms of the required movement of the major components. The first concept is illustrated in Figure 3.2.

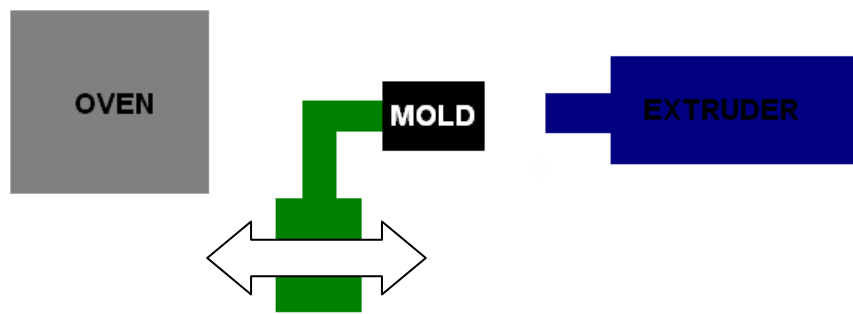


Figure 3.2: EARFM Concept 1

This concept involves translation of only the mold rotational mechanism between the oven and extruder allowing the heaviest equipment to remain stationary. The design of the mold rotational mechanism then must be created to accommodate for the translation and successful connection with the extruder and encapsulation within the oven. Alignment of the mold with the extruder will rely only on the translation and rotational position of the mold as the extruder is fixed in place, while alignment of the mold with the oven is also dependant on the translation and rotational position of the mold.

Concept 2 is presented in Figure 3.3. It involves translation of the mold rotational mechanism between the oven and extruder, and translation of the extruder to interface with the mold. This concept is more complex in movement as translation of the extruder will need to be controlled and coordinated with the movement of the mold. Thus alignment of the mold with the extruder will rely on the translation of the mold and the extruder with the rotational position of the mold. Alignment of the mold with the oven will remain the same as the previous concept as the motions of these two components remains the same.

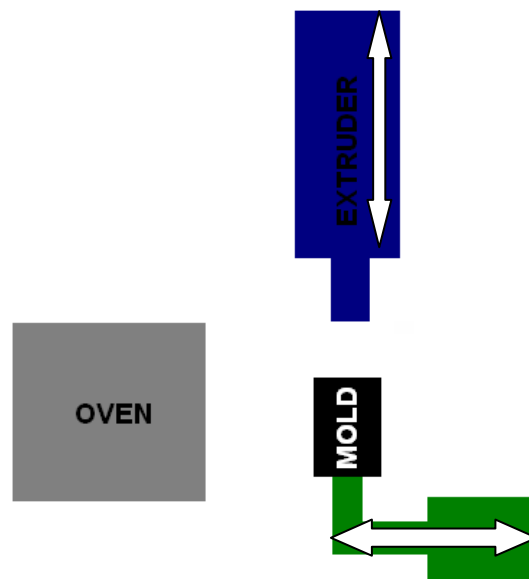


Figure 3.3: EARFM Concept 2

Concept 3, as depicted in Figure 3.4, involves translation of the oven and the extruder to individually interface with the mold. As this concept involves the translation of the two heaviest components that are not normally designed for translation this may require a great deal of physical and control modifications to these components.

Alignment of the mold with the extruder and oven now rely on the translations of the extruder and oven in addition to the rotational position of the mold.

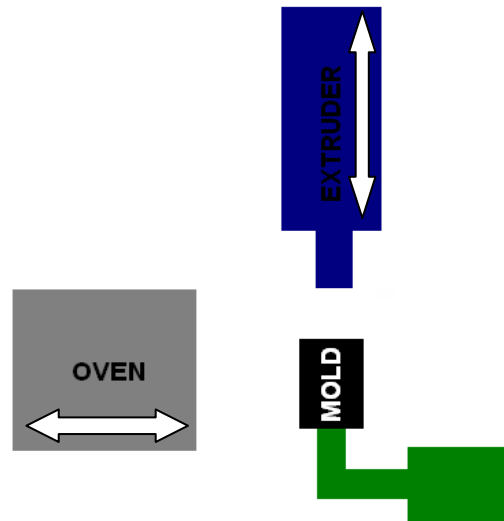


Figure 3.4: EARFM Concept 3

3.7 Final Concept Selection for EARFM Experimental Setup

A completed decision matrix for the EARFM process is presented in Table 3.1.

Table 3.1: Concept Feasibility Decision Matrix for the EARFM Process

	Criteria	Importance	Alternatives		
			Concept 1	Concept 2	Concept 3
1	Control complexity	9		-	-
2	Design complexity	8		-	-
3	Ease of alignment of components	10	Datum	-	-
4	Space required for operation	8		-	-
5	Access to components in confined lab space	6		+	+
6	Operator safety	9		-	-
7	Ease of fabrication	5		-	-
	Total +		0	1	1
	Total -		0	6	6
	Overall Total		0	-6	-6
	Weighted Total		0	-43	-43

The criteria to which the concepts were compared are related to the overall operation of the process rather than individual component operation. The importance ratings for each criterion were listed out of 10 with 10 being the most important and relating to the successful operation and implementation of the system. The criterion rated as most important was the ease of alignment of the components as this was one of the most important tasks for the success of the process. The next important criteria involved the control complexity and operator safety followed closely by design complexity, space considerations and ease of fabrication. Each concept was then compared on whether it met each criterion better (using a + symbol) or worse (using a – symbol) than Concept 1, which was set as the datum. The summation of these symbols multiplied with the importance rating of each criterion resulted in the weighted total that was found to be the same for Concepts 2 and 3 with a value of -43. Since these values were both negative, Concepts 2 and 3 failed to measure up to Concept 1. The similarity between the two failed concepts was potentially due to the fact that they both featured translation of more than one component, thus increasing the complexity of the system. Therefore in completing this decision matrix, Concept 1 was chosen to be used for the experimental setup design.

3.8 Final Component Design and Implementation

Now that the overall process design has been determined, further design and selection of the individual components was completed. As some components were commercially available some only required customization to allow implementation into the process.

3.8.1 Extruder Design

Custom extruder design is quite complex and requires a lengthy process, therefore since a wide variety of extruders are commercially available, an extruder was chosen and purchased by Zak Denis [52] for the purpose of this research. The extruder chosen to be most feasible due mostly to its small size was a refurbished extruder by Wayne Machine and Die Company. This extruder featured a single 32 mm diameter screw with a compression ratio (a ratio of length and diameter of the extruder screw) of 24:1. The

screw drive system featured a 7.5 HP motor capable of producing a rotation speed of 100 RPM with a torque accuracy of $\pm 1\%$. The barrel of the extruder was bi-metallic lined and featured three temperature zones with precise control through a nearby control panel [52] as pictured in Figure 3.5.

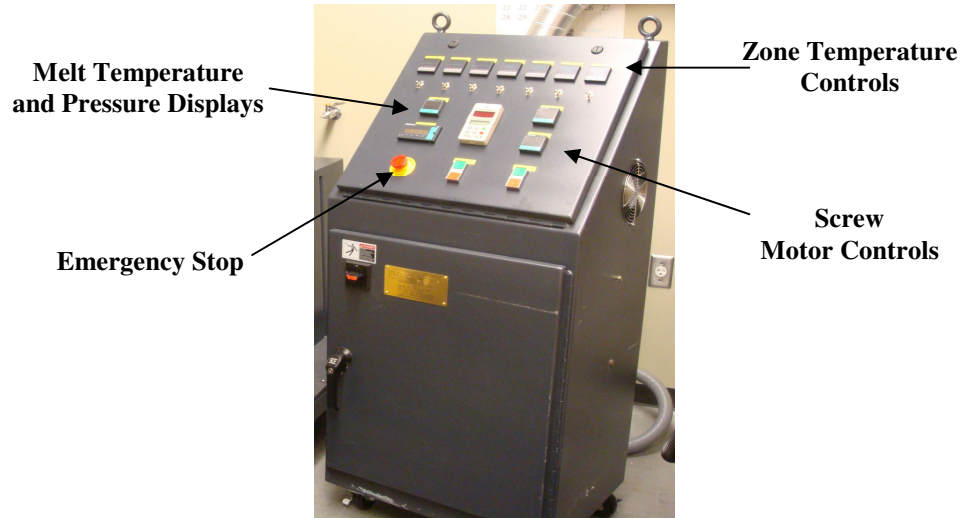


Figure 3.5: Extruder Control Panel

As displayed, the extruder control panel featured easy to use zone temperature and screw motor controls as well as real-time melt temperature and pressure displays with an emergency stop button.

Modifications: As the extruder came with fixed wheels allowing for only lateral motion, a collaborative effort with colleagues Emad Abdalla and Greg Eberle resulted in the design and creation of a variable height adjustment assembly consisting of long threaded bars held in place by a nut assemblies welded to a steel frame and ball joint feet. This modification is illustrated with the CAD representation depicted in Figure 3.6.

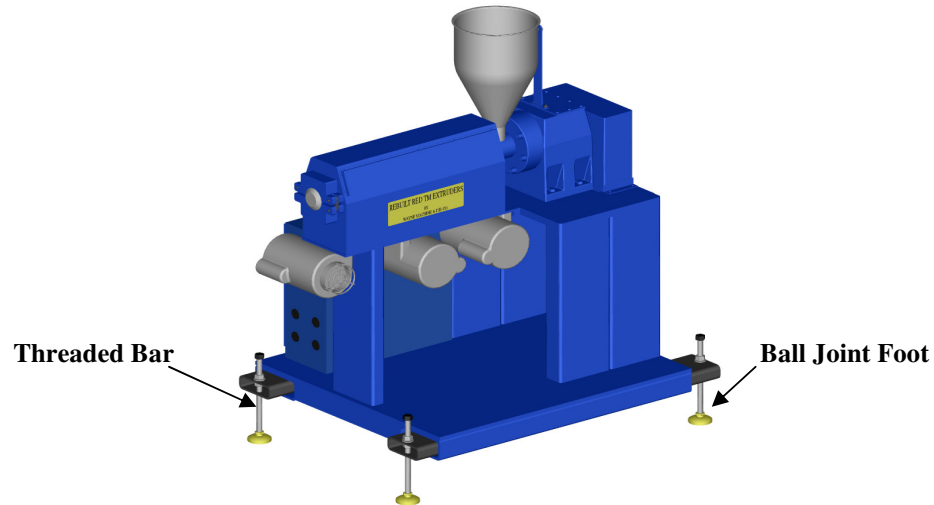


Figure 3.6: CAD Representation of Variable Height Adjustment Modification

The extruder also did not come with a means of filling so a hot-runner assembly was purchased. The hot-runner system chosen was a typical form of injection device for injection molding systems that featured a pneumatically controlled sealable tip [52] and specially designed conical nozzle. As the extruder only had a single screw the dispersion quality was reduced. Therefore to counteract this, a static melt blender was purchased to aid in the dispersion the CBA particles within the foamable melt. These additions were retrofit to the exit of the extruder barrel with the design of a simple connection adaptor [52]. An additional support frame for this equipment was also created as the only point of support was the connection with the extruder as displayed in Figure 3.7.

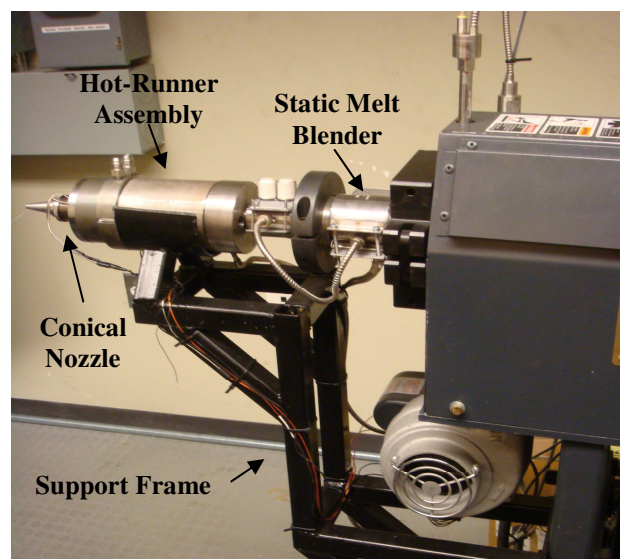


Figure 3.7: Extruder Filling Modifications

The final modified extruder design is presented in Figure 3.8.

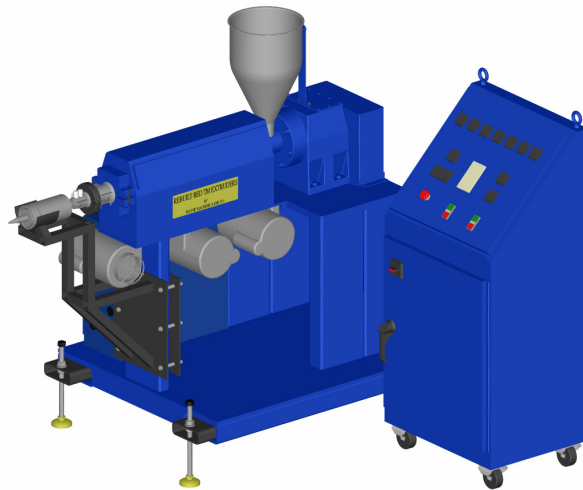


Figure 3.8: Final Extruder Design

3.8.2 Oven Design

As ovens are widely commercially available, an oven was purchased and modified by Ben Fagan [53] to meet the requirements of the EARFM process. The oven chosen to be most feasible was a forced convection oven capable of an operating temperature of 300 °C at a rate of 15 °C/min with an accuracy of ± 0.5 °C. To accommodate for mold rotation within the oven the internal oven dimensions were 0.609x0.609x0.609 m [53].

Modifications: Since typical ovens are not designed to accommodate bi-axially rotating molds the chosen oven had to be modified by cutting its side leaving a tight tolerance slot for the mold rotational mechanism to pass. To prevent losing heat, an equivalent section to the one cut out of the oven was attached to the oven door to surround the mold rotational mechanism when the door was closed. The next major modification was implementing a pneumatic powered linear actuator to the operation of the oven door with a simple physical control mechanism for optional manual and automatic door operation. Variable height adjustment was achieved by creating a steel frame with adjustable feet that are similar in design to the extruder feet. The fixed height of this frame was chosen so that the slot in the side of the oven would be higher than the extruder nozzle as the adjustable feet in this design only allow for slight flexibility for mold alignment [53]. Therefore, there was more of a reliance on the extruder and design

of the mold rotational mechanism to ensure proper alignment of all components. A CAD representation of the chosen oven with its modifications is presented in Figure 3.9.

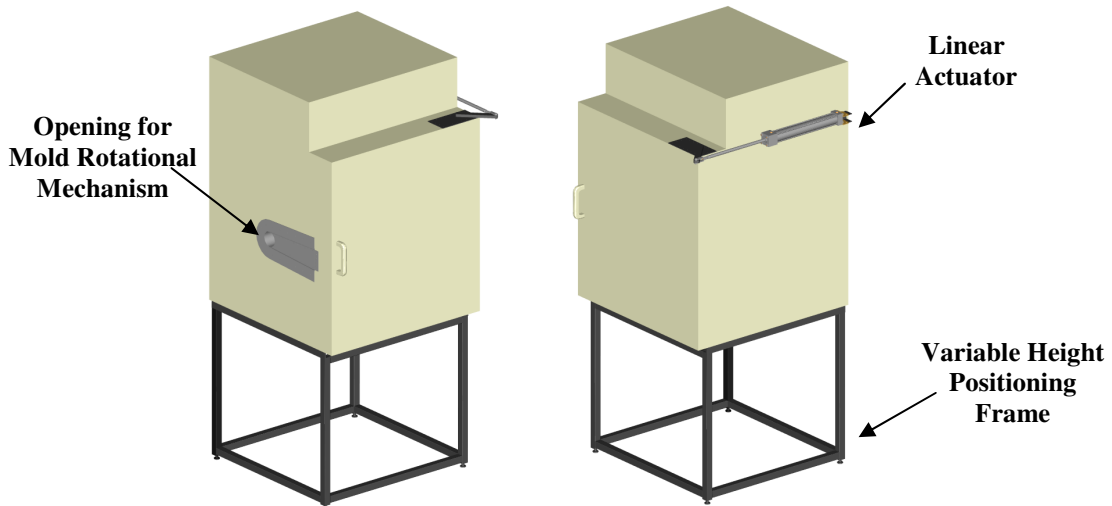


Figure 3.9: Chosen Oven Design with Process Modifications

3.8.3 Mold Rotational Mechanism Design

Rotational Arm Design: Given that numerous mold rotational mechanisms are currently used in different rotational molding machines (as presented in Section 2.1.4) it was found beneficial to model this component for the EARFM process after such designs, as determined by Michael Macleod in creating the final rotational arm design [54].

As bi-axial rotation and the use of various mold shapes were required, it was decided an offset rotational arm design as presented in Figure 2.3 (b) would be used. This design gave the required rotational ability and allowed the opportunity to use larger and different shaped molds compared to the use of a straight rotational arm. To achieve bi-axial rotation, each rotation had to be fit within the single offset shaft. This was accomplished by utilizing a shaft within a shaft design where the outer shaft enables rotation of the entire arm (along the x-axis), and coupled internal shafts driven by bevel gears enables rotation of the mold (along the y-axis) [54].

Since the rotational arm will rotate within the enclosed oven, it was essential that its position be in the middle of the corresponding oven slot and allow for sufficient

clearance between the oven walls. Taking this into account the final dimensions were determined with a maximum usable mold space [54].

As it was required that the mold rotational mechanism withstand the weight of the mold, and be unaffected by its rotations it was decided that with the completion of an extensive material evaluation process as described in [54] it was produced out of AISI Steel 1018.

The next part of the rotational arm design was mold attachment where a permanent mounting plate was fixed to the end of the arm that rotates along its central axis by the inner shafts. Mount holes were added to this plate in a circular configuration that can be integrated into any mold design so that standard bolts can be used to attach each mold. As this plate was also be made of steel for its required strength, it would not have good heat transfer abilities resulting in the use of Teflon tubes as spacers between the mold mounting plate and the mold to allow heat to flow more effectively to the bottom of the mold [54]. The final rotational arm design is presented in Figure 3.10.

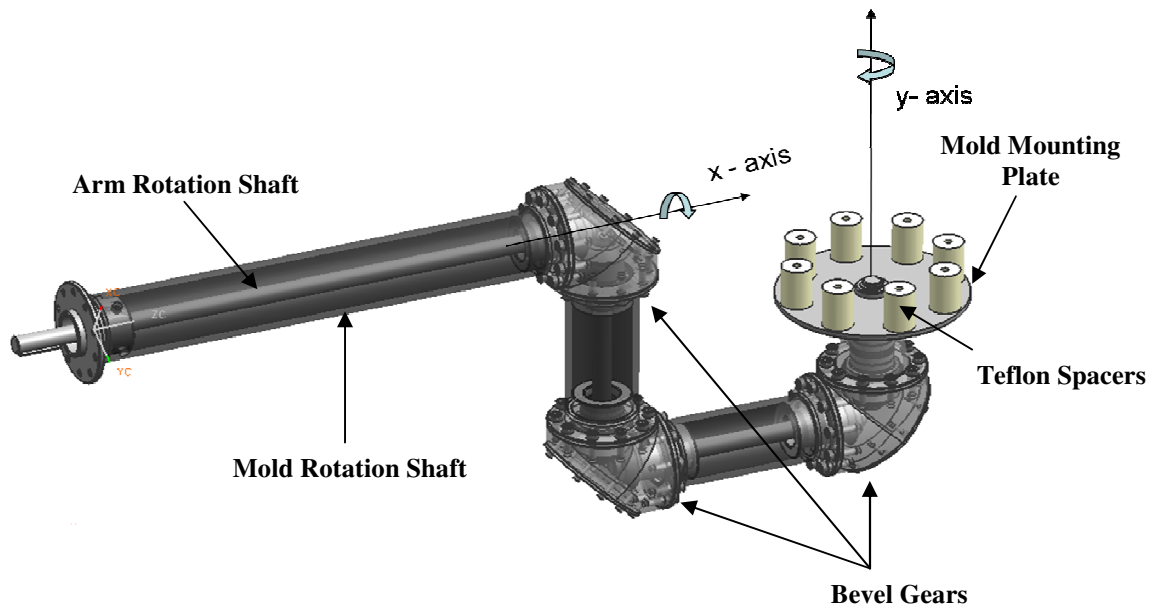


Figure 3.10: Final Mold Rotational Arm Assembly

Carriage and Frame Design: The next major component that linked the process together was the frame that allowed for translation of the arm between the oven and extruder and that held the rotational motor equipment. Given the required motion of the mold, and to reduce the complexity of the design, a simple box frame was chosen to be made of square

steel tubing for ease of fabrication. However, as the frame supports translation of the carriage holding the rotational arm and accompanying equipment, this had to be designed first as it would affect the final dimensions of the frame. To accomplish this, the required rotational components were determined.

As two independent rotational motions were required that must be run by separate motor systems, two 2 HP motors were selected, by Michael Macleod [54], that were capable of operating up to 1725 RPM and are powered by 220 V [54]. When these motors are not in use, the rotational arm must be locked in place to not damage the motors resulting in the need for implementing gearboxes. The gearboxes chosen were industrial-grade featuring a worm and spur gear locking mechanism that act as speed reducers. The speed reduction for the arm and mold rotations were chosen to be 60:1 and 40:1, respectively, as it was required that the mold rotates faster than the arm. This was determined as a higher mold rotation results in more uniform outer skin thicknesses for processing integral-skin PE foam moldings [55]. To counteract these speed reductions and achieve specific rotations for the mold and arm, sprockets with different gearing ratios were utilized. Knowing that the maximum RPM of the motor was 1725 and the minimum recommended RPM was 900 an operational RPM was chosen to be 1600. Different sprocket combinations were investigated with this speed to achieve a desired 4:1 (mold to arm) rotation ratio. The results of this investigation yielded appropriate sprocket combinations to create a 3.94:1 rotation ratio. The method of driving the rotational equipment with the motors was chosen to involve sprocket chain systems. The chosen sprocket gage was 50 because of its strength as the system deals with high RPMs and operator safety was a high priority.

With the rotational motion system components determined, a collaborative effort with Emad Abdalla and Greg Eberle was utilized to design and build the carriage to house these components using a simple box design made of square steel tubing and ¼ in thick steel plates. To attach the rotational arm to this carriage, two large bearings with two bolt attachment housings were selected to ensure the arm was held straight and only be allowed to rotate along its central axis. Safety guards were also added to this assembly to contain the exposed sprocket assemblies in crucial areas that a user may need to approach during operation. To permit movement of this carriage on the frame two metal wheel

assemblies were attached to the underside of the top plate of the carriage that can move easily on an L-shaped track system that can be added to the frame. To control this movement, several forms of linear translation were investigated and it was decided that a ball screw assembly would be used resulting in the purchase of a 0.75 in ball screw and ball nut. The ball nut was connected to an attachment assembly and welded to the carriage creating translation of the carriage with a rotation of the ball screw. The base carriage with all components and the resulting final carriage design can be seen in Figure 3.11.

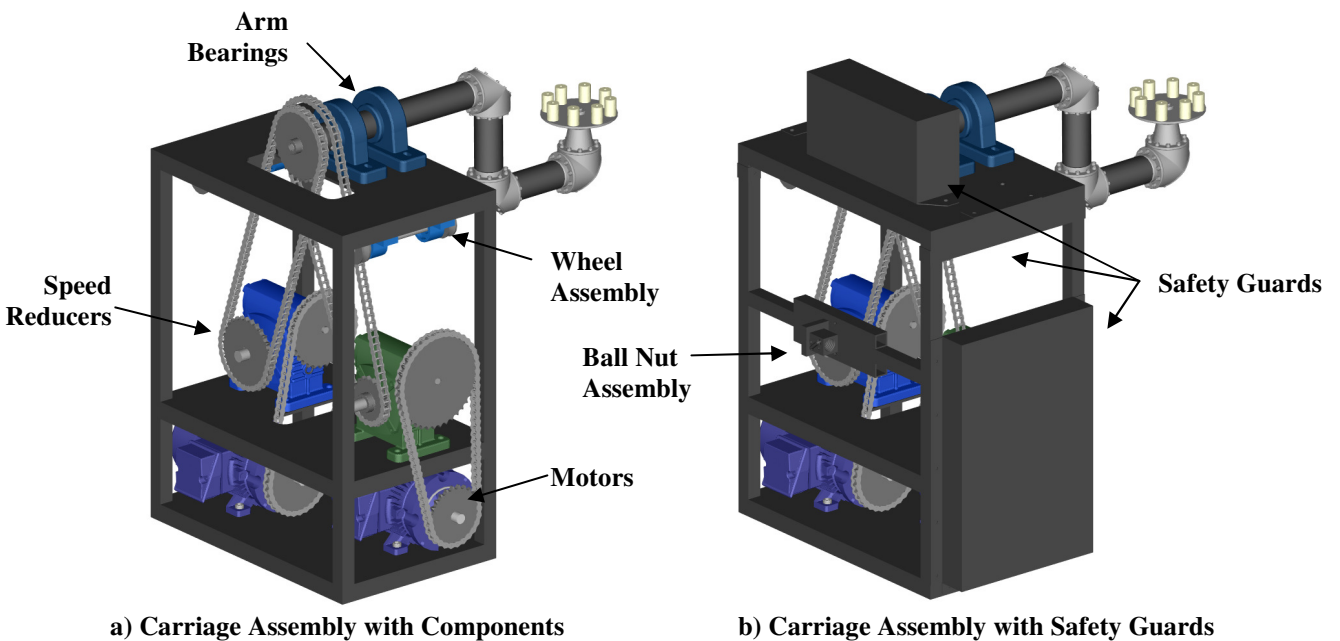


Figure 3.11: Final Carriage Assembly

The final frame dimensions were determined from the final carriage dimensions. An L-shaped track was added to the top of the frame that dimensionally corresponds with the metal wheel assemblies of the carriage to allow its weight to be supported as it moves. The ball screw was implemented into the frame design via two mountable bearing assemblies. To power the rotations of the ball screw a manual direct drive option was implemented with the potential for an automatic sprocket motor system. It is important to note that with the potential for automated motor control of the ball screw, safety guards were not initially added to the frame assembly. However, to ensure safety of even a non-experienced user proper additional safety guards should be added to this frame. To allow

leveling and minor height adjustment of the frame, small feet, similar in design to the ones used for the extruder, were used in various locations on the bottom of the frame. Given the weight of the rotational arm that will overhang off of the frame, an extra support section was added outside of the defined usable space area along the floor to not interfere with other operations. Finally since the various electrical components on the carriage need to be powered and controlled, an electrical box was mounted to the side of the frame to house these electrical components. Push button controls were added to the door of the electrical box including: individual on/off control of the arm and mold rotations, slowed interval movement control of the arm, emergency stop, and a master on/off button. To prevent damage of the wires from the electrical box to the carriage due to the carriage movement, a modular plastic wire carrier was purchased and mounted between the carriage and frame. The final frame design as it would be set up for automatic operation without the wire carrier is presented in Figure 3.12.

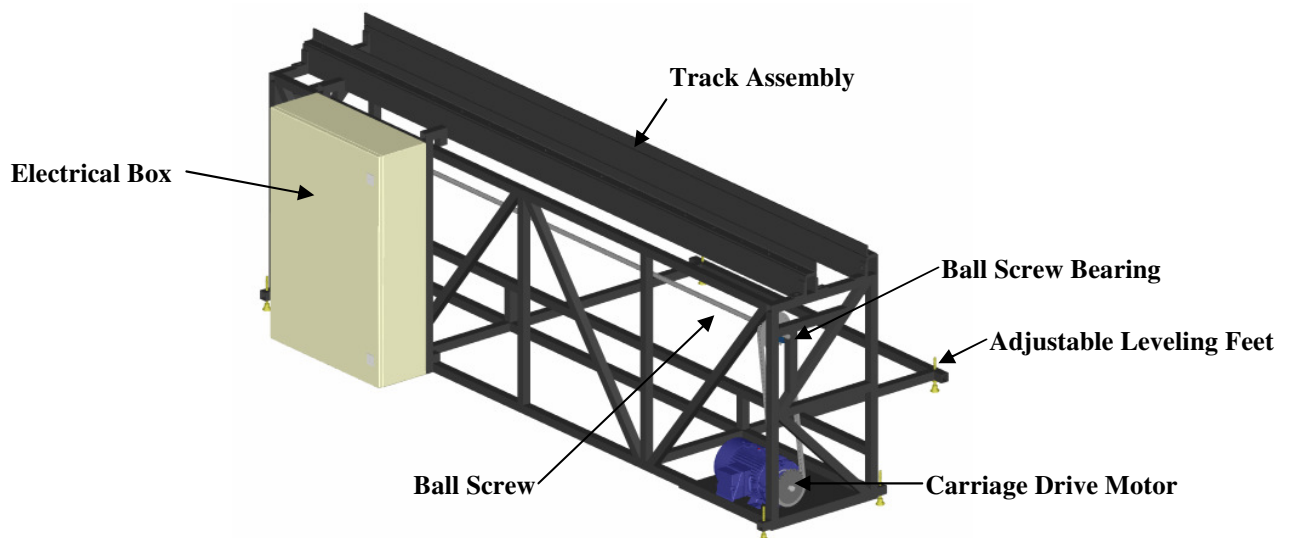


Figure 3.12: Final Frame Assembly

3.8.4 Mold Design

It was essential that a mold design chosen for the EARFM process be adequate in size, shape and complexity to best represent potential problems that may occur if this process were scaled up for industry. This was why two mold shapes were considered: cylindrical and flat-plate. The cylindrical mold, designed by Michael Macleod [54], was designed with its central axis aligned to the axis of mold rotation. Its assembly was made up of a

main cylindrical section with a 2° draft angle for easy part removal. Welded to either end of this section are two flanges with mounting holes to accommodate attachment to the rotational arm and to the specialized gate for extruder interface. Opposite to the end of filling, the mold contains a metal venting tube held in place by a set screw to avoid pressure buildup during foam formation. The selected material for the mold was Aluminum 2014, which has a thermal conductivity value of $192 \text{ W/m}\cdot\text{K}$ to ensure excellent heat transfer throughout the mold surface. To maintain the consistency of the heat transfer ability of the mold, the main cylindrical section of the mold features a constant wall thickness [54]. The final cylindrical mold design is presented in Figure 3.13.

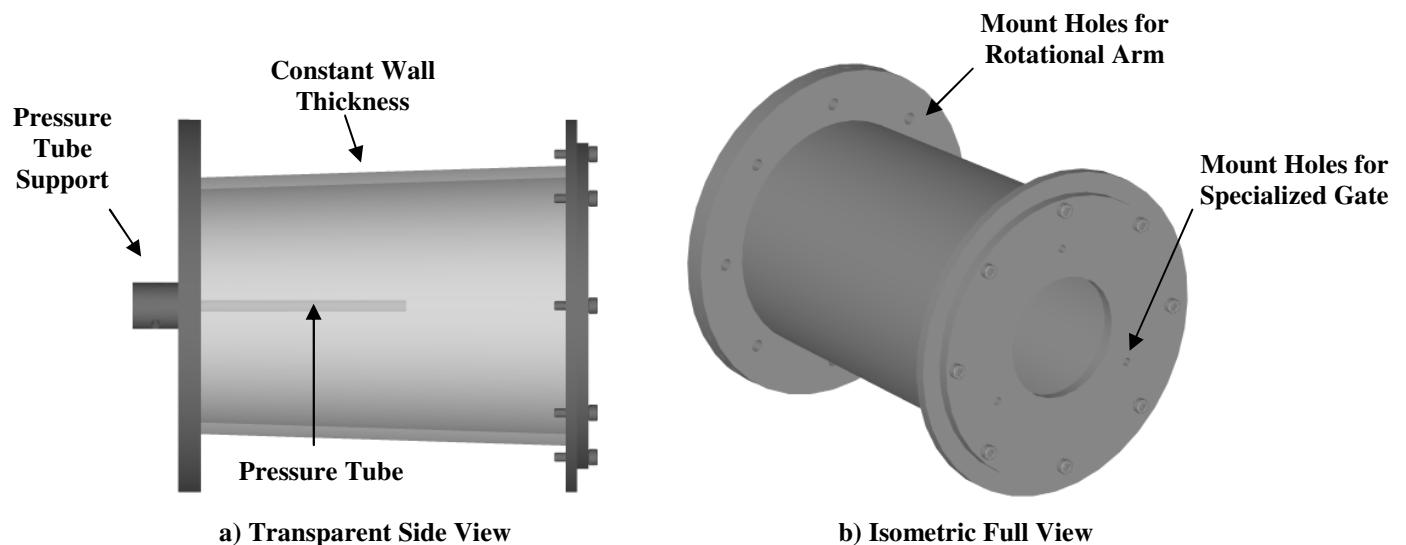


Figure 3.13: CAD Representation of the Cylindrical Mold Design

The flat-plate mold, on the other hand, was designed to share features with the cylindrical mold, such as it was also made of Aluminum 2014 with a 2° draft angle, and constant wall thickness. This mold, however, was made of two sections, the mold cavity and a flat plate, which were attached together by a circular bolt pattern. The mold was oriented in such a way that it is filled by the top through the same specialized gate. Venting was accomplished through two offset metal venting tubes held in place by set screws at either end of the mold furthest from the filling location. This mold was attached to the rotational arm via an additional mounting plate that has a matching bolt

pattern to the mold mounting plate. The final flat-plate mold design is presented in Figure 3.14.

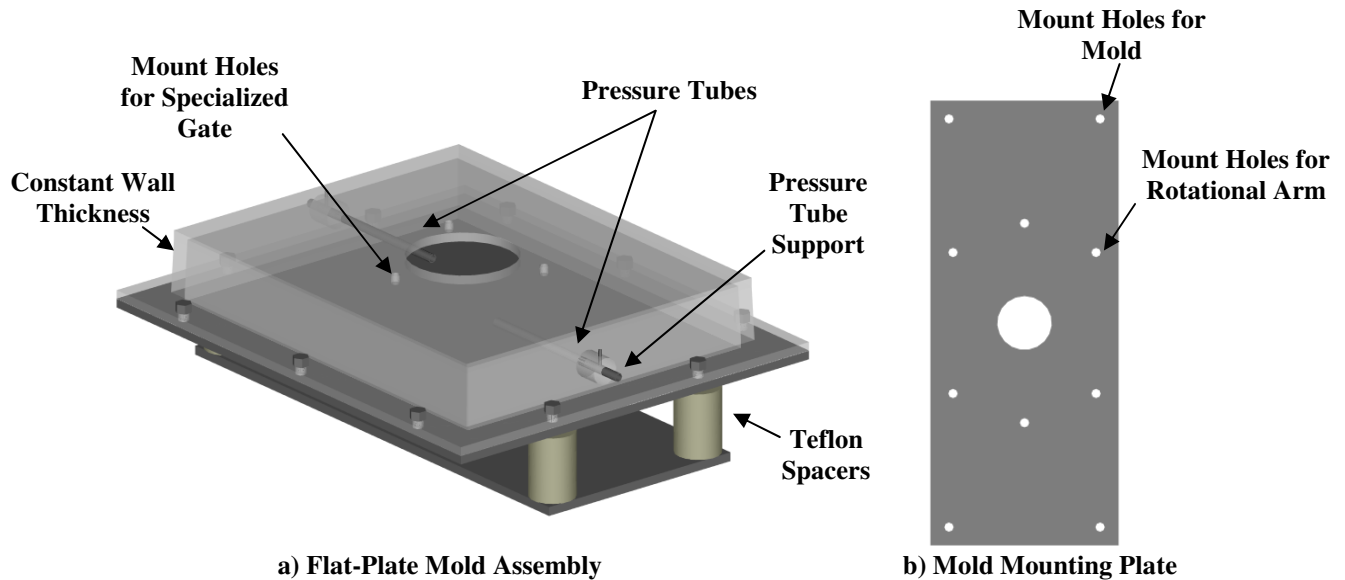


Figure 3.14: CAD Representation of Flat-Plate Mold Design

Specialized Gate: The specialized gate had to accomplish many tasks, the first of which was to contain the non-foamable powder within the mold during the first rotational molding cycle, and allow the powder to adhere to it. Next it needed to allow the conical extruder nozzle to puncture through it in a way that minimally disrupted the molten skin adhered to it. Finally, once the extruder nozzle was retracted, the molten skin needed to re-heal itself from where it was punctured and contain the expanding foam within it. Given these requirements, a gate known as a “pizza valve” (Figure 3.15) was designed and created by Ben Fagan [53] with precise triangular shaped laser cuts in 2 mm thick spring steel to allow it to be punctured after which it could regain its original shape. As laser precision was used, the slits in the spring steel should be small enough to contain powder within it. Since this component was made out of a dissimilar material to the mold, its thickness was kept to a minimum to permit excellent heat transfer and to ensure its elastic spring back behaviour. This spring back behaviour was crucial to allow the conical extruder nozzle to protrude through it into the mold and through the molten skin for foamable melt filling. The “pizza valve” design was created to be modular in that it

can be mounted to any mold with a cap plate that is held in place with three screws that can be easily removed for maintenance, part removal, or “pizza valve” replacement [53].

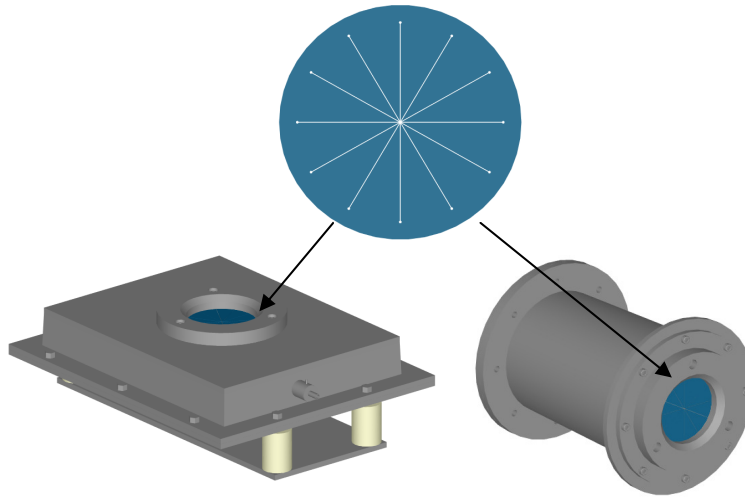


Figure 3.15: Specialized Gate Design

3.9 Final EARFM Experimental Setup

Overall, a collaborative effort was utilized to achieve the final creation of an industrial-grade, heavy-duty, lab-scale, custom-made experimental setup dedicated for verifying the feasibility of the EARFM process to produce integral-skin foam core moldings. The final designed and built components of the EARFM process can be seen in Figures 3.16-3.18.



Figure 3.16: Extruder and Accompanying Melt Injection Equipment of the EARFM Experimental Setup



Figure 3.17: Modified Oven of the EARFM Experimental Setup

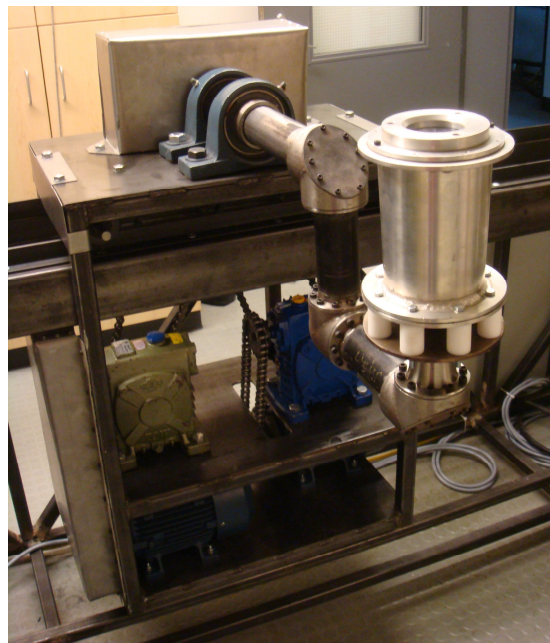


Figure 3.18: Carriage Assembly with Cylindrical Mold Mounted to Translational Mechanism of the EARFM Experimental Setup

A CAD representation to better illustrate the entire setup in its entirety is presented in Figure 3.19.

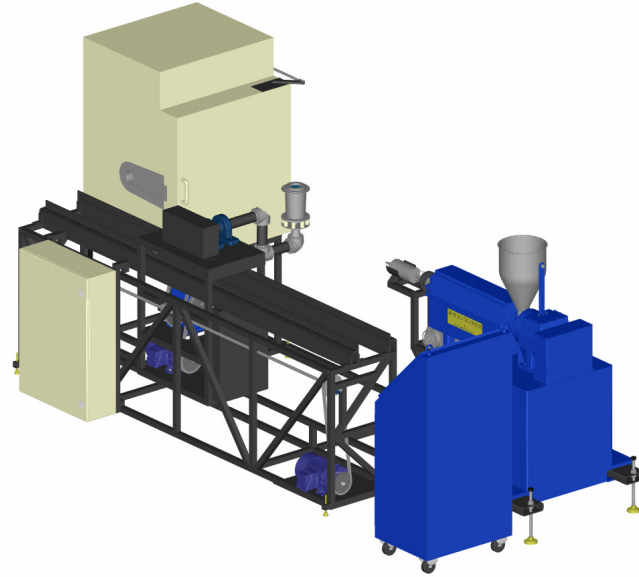


Figure 3.19: Final EARFM Experimental Setup

CHAPTER 4

EXPERIMENTAL EVOLUTION OF THE NOVEL EXTRUSION-ASSISTED ROTATIONAL FOAM MOLDING PROCESS

4.1 Introduction

The experimental process presented in this chapter was focused on determining the feasibility of the Extrusion-Assisted Rotational Foam Molding (EARFM) process to produce polyethylene (PE) integral-skin foam core moldings. Through experimentation, it was found that process enhancements and modifications were required to achieve an acceptable quality molding which will be described in detail.

4.2 Experimental Materials

Two rotational molding grade PE resins in a 35-mesh powder were selected for experimentation with EARFM. The materials are commercially known as Microthene® from LyondellBasell and include a linear low density PE (LLDPE, MP643662) and a high density PE (HDPE, MP652762) resin with melt flow rates (MFR) of 3.6 and 2.0 g/10min, respectively [56-57]. A summary of properties of these materials, as listed by the manufacturer, are listed in Table 4.1 with material data sheets available in Appendix B.

Table 4.1: Typical Properties of Chosen PE Resins [56-57]

Typical Resin Properties	ASTM Test Method	LLDPE	HDPE
MFR (g/10min)	D 1238	3.6	2.0
ρ (g/cc)	D1505	0.9395	0.942
Flexure Modulus (kPa)	D 790	7.58×10^5	8.96×10^5
Tensile Strength @ Yield 2"/min (kPa)	D 638	1.79×10^4	2.22×10^4

The chemical blowing agent (CBA) chosen for the experimental purpose of foaming the previously stated PE resins was Celogen OT in powder form provided by Crompton Chemicals. This material was chosen for its recommended use with PE and its suitable operating temperature range as listed by the manufacturer of 149 °C to 177 °C [58]. Table 4.2 presents the typical properties of this material as listed by the manufacturer.

Table 4.2: Typical Properties of Celogen OT [58]

Typical CBA Properties	Celogen OT
Chemical Composition	p,p'-oxybis(benzenesulfonylhydrazide)
Gas Composition	Nitrogen (91%), steam (9%)
ϕ_{STP} (cc/g)	125
Onset Decomposition Temperature (°C)	160
Appearance	White to off-white powder
Specific Gravity	1.55
Bulk Density (kg/m ³)	496

4.3 PE Characterization

To determine melting and crystallization temperatures of the chosen PE resins, DSC experiments using TA Instruments' Q20 DSC were set up to first erase the thermal history of the material. This was accomplished by heating the resins to above their potential melting point, which at the same time determined their actual melt temperature, kept at that temperature, and then cooled to determine the crystallization temperature. This process was performed to ensure that a known thermal history was imposed upon each resin so their crystallization temperatures could be compared [59-60].

The results of these experiments are presented in Figures 4.1 and 4.2 with the results summarized in Table 4.3.

Table 4.3: DSC PE Characterization Results

Characterization Temperatures	LLDPE	HDPE
T_m (°C)	127.23	128.31
T_c (°C)	115.11	117.14

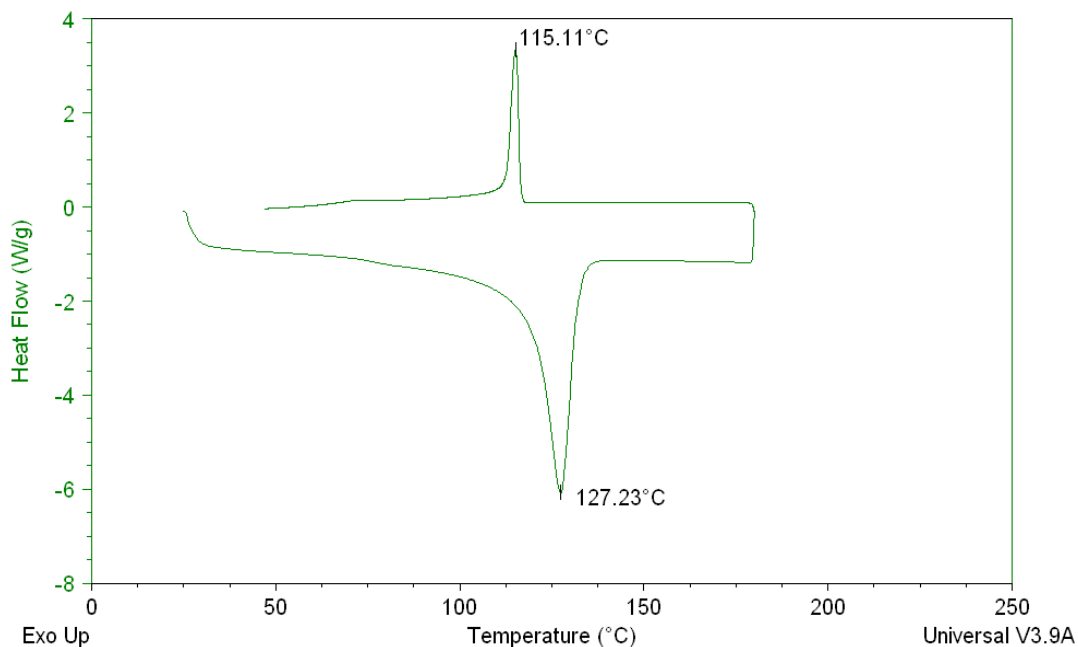


Figure 4.1: DSC Thermogram of the LLDPE resin (MP643662)

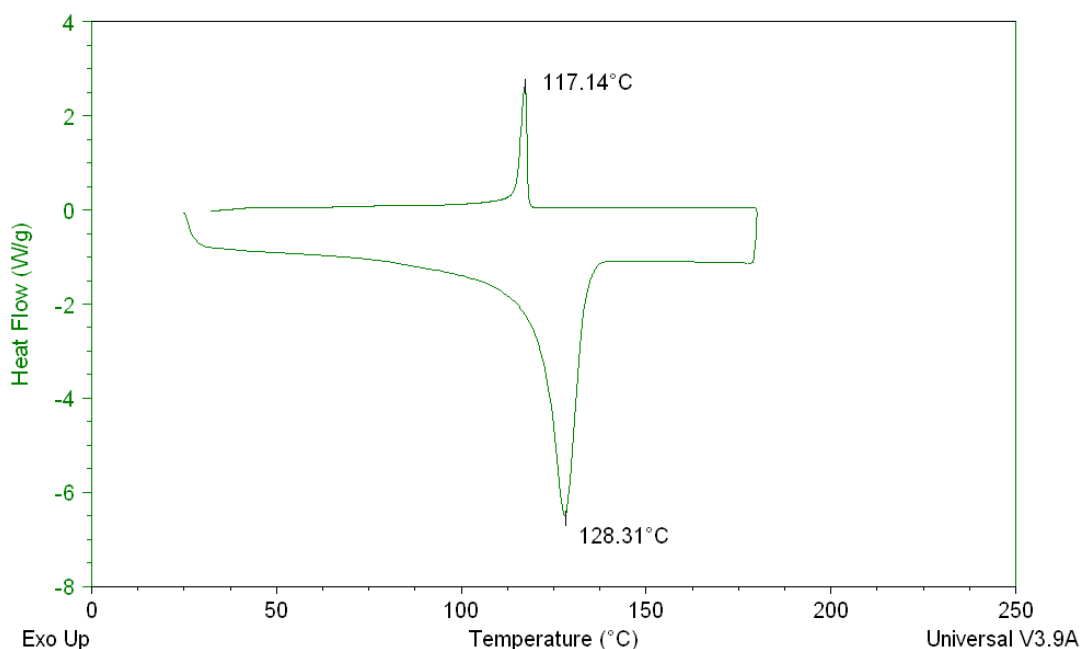


Figure 4.2: DSC Thermogram of the HDPE resin (MP652762)

From these results, the LLDPE resin with its lower crystallization temperature could potentially create finer-celled foams. This is due to the fact that this material would require less time to crystallize given identical cooling rates ultimately freezing the bubbles sooner than the HDPE resin. In terms of their MFR values, even though they are very similar, it should be noted that previous research suggested that lower MFR resins,

or ones with high viscosities, also have the potential to create better quality foams. This is caused by their increased melt strength at higher elevated temperatures, which reduces cell drainage ultimately suppressing cell coalescence [40].

4.4 CBA Characterization

Characterization of CBAs is important in determining the optimal conditions to expose them to during processing. One of the most important characterization parameters for CBAs is their onset decomposition temperatures, which vary when experiencing different heat treatments. Typically when purchasing a CBA, a range for its onset decomposition temperature is given. Without knowledge of how this temperature changes under different heating conditions, errors could be made during processing. This is why it was important to test their reaction under different heating rates similar to those that would be experienced during processing. This was accomplished by performing TGA experiments with TA Instruments Q50 TGA.

Under processing conditions during melt compounding, the resin and CBA will experience high heating rates. For this reason, the CBA was tested up to 100 °C/min to determine the effect of high heating rates on the onset decomposition temperature of the CBA. The results of these experiments are presented in Figures 4.3 to 4.6.

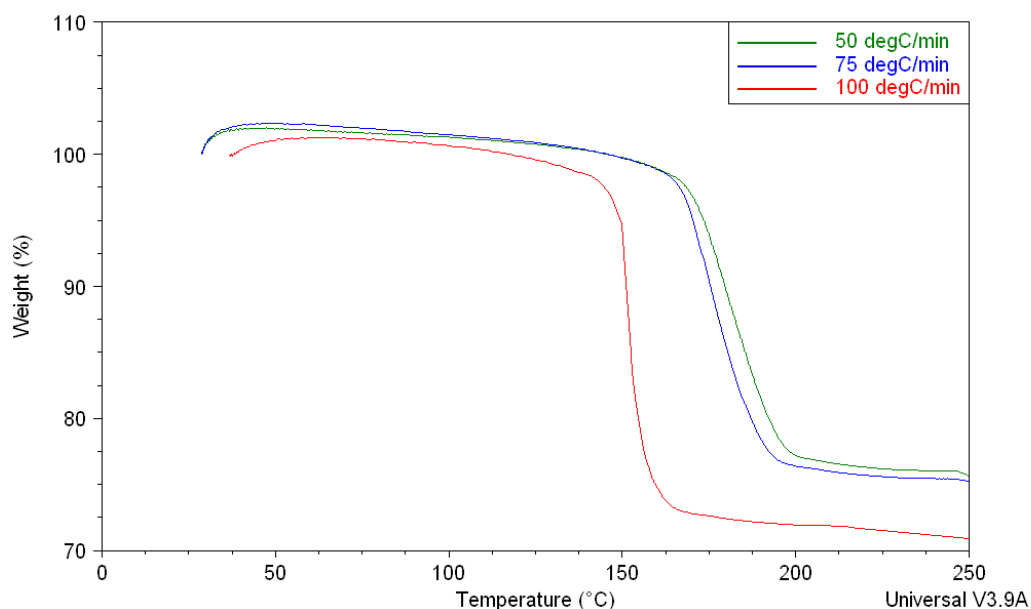


Figure 4.3: TGA Thermogram of Celogen OT at Various Heating Rates

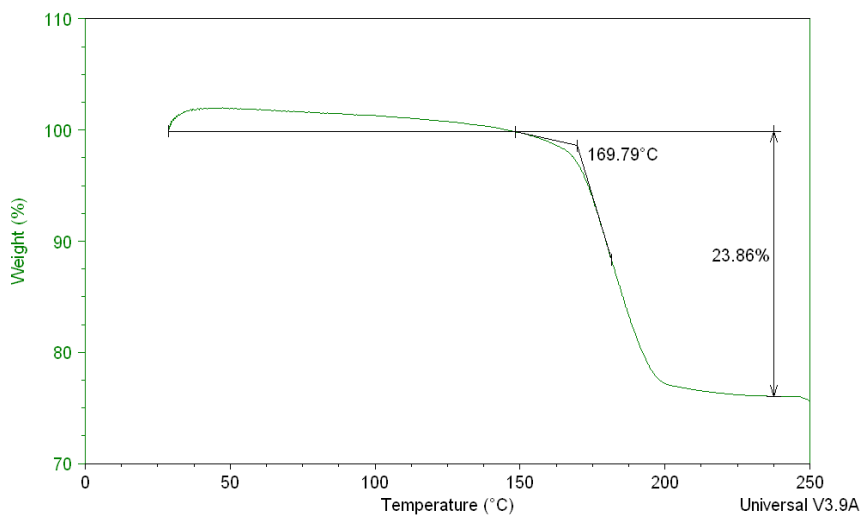


Figure 4.4: TGA Thermogram of Celogen OT at 50 °C/min

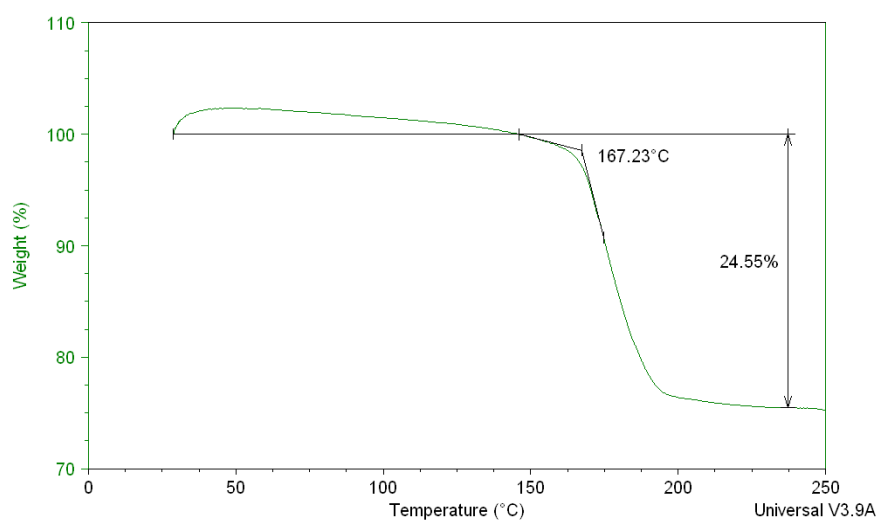


Figure 4.5: TGA Thermogram of Celogen OT at 75 °C/min

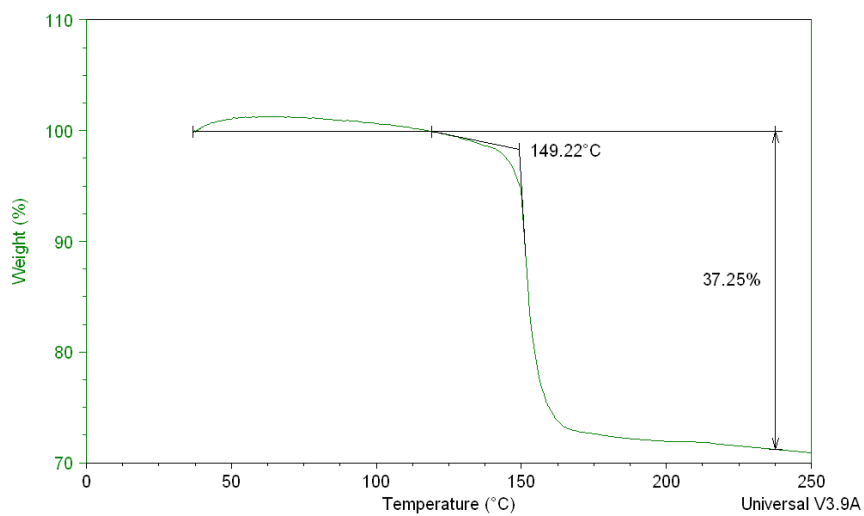


Figure 4.6: TGA Thermogram of Celogen OT at 100 °C/min

The heating rates used for these experiments ranged from 50 to 100 °C/min, and were heated up to a maximum temperature of 250 °C. From the obtained results, it was observed that as the heating rates increase the onset decomposition temperatures drops from 169.79 °C to 167.23 °C to 149.22 °C respectively (Figures 4.4 to 4.6). This was due to the fact that this material is exothermic, where higher heating rates cause the CBA to expel more heat resulting in a decrease of the onset decomposition temperature.

When comparing percent weight change of the CBA during the various heating rates, it appeared that for the higher heating rates the amount of weight lost increased as the self-heating effects became more evident. In terms of the amount of gas liberated by Celogen OT, an average of 28% of weight was lost nearing the end of decomposition.

During the TGA experiments, many factors could have altered the accuracy of the measurements. The size of the sample, for example, depending on the heating rate, could have negatively affected the resulting measurements. As with most instruments, the accuracy and resolution also depend on the speed at which experiments are performed. In terms of the TGA machine that was used, the accuracy and resolution of the results are inversely related to the heating rate, where the higher the heating rate, less accurate and lower resolution results will be achieved [61]. However, since the CBA experiences higher heating rates, accuracy and resolution had to be sacrificed to determine how these materials behaved under simulated processing conditions.

An example of loss of accuracy can be observed in each of the results where there was a large spike in the percent weight signal at the beginning of the experiment. As there was no known physical influence on the sample within the furnace that would cause this, the response was likely due to the operation of the machine as small inductive effects could possibly occur inside the furnace [62].

What can be concluded from these results was that extreme care should be taken during melt compounding not to pre-decompose the CBA as high heating rates were experienced. For example, if using a heating rate of 100 °C/min or more, the material must exit the extruder slower than if a lower heating rate was used as faster screw rotations cause less frictional heating within the extruder barrel [29].

4.5 EARFM Process Control Consideration

4.5.1 EARFM Processing Steps

The required processing steps to create an integral-skin foamed core molding with Extrusion-Assisted Rotational Foam Molding (EARFM) are presented as follows:

Step 1: Charge the mold with the predetermined amount of suitable PE resin in powder form (designated for making the desired thickness) dry-blended with an appropriate amount of pigment for better visibility as depicted in Figure 4.7 (a). Once complete, the so-called “pizza valve” and accompanying assembly was attached to the mold as depicted in Figure 4.7 (b).

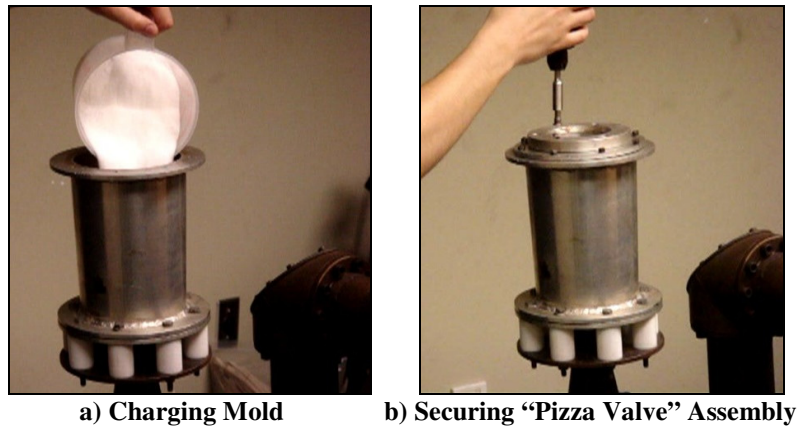
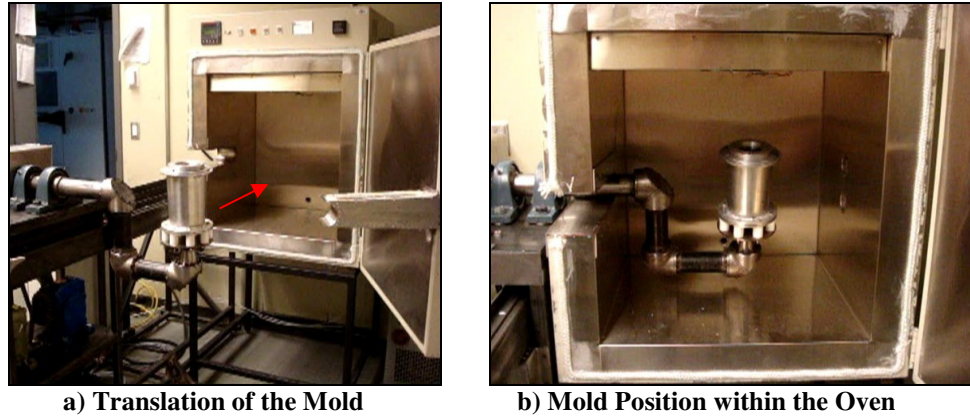


Figure 4.7: Step 1 – Mold Preparation

Step 2: The oven was preheated to the desired processing temperature, at which time the mold was moved on the carriage system into the oven (Figure 4.8) with the oven door closing behind it with the pneumatic door control. Once in the oven, the bi-axial rotation of the mold was activated to evenly distribute the resin over the inner surface of the mold.



a) Translation of the Mold

b) Mold Position within the Oven

Figure 4.8: Step 2 – Mold Translation

Step 3: The extruder was charged with the pre-dry blended foamable formulation in powder form (consisting of a non-foamable resin and a prescribed amount of CBA for achieving a desired VER) as pictured in Figure 4.9. As a result, a foamable melt was produced utilizing the process of extrusion melt compounding. Melt compounding and initial skin formation within the mold occurred simultaneously to reduce the duration of the heating segment of the traditional rotational foam molding cycle time.



Figure 4.9: Step 3 – Charging Extruder with Pre-Dry Blended Foamable Formulation

Step 4: Once the non-foamable resin had a chance to melt and adhere to the walls of the mold, the oven door was opened and the mold was translated towards the extruder while rotating uni-axially to be aligned with the extruder nozzle. See Figure 4.10.

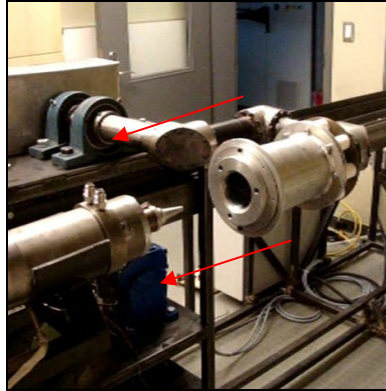


Figure 4.10: Step 4 – Translation and Alignment of the Mold with the Extruder

Step 5: The extruder nozzle then punctured through the so-called “pizza valve” into the uni-axially rotating mold to fill the molten foamable compound completely on top of the still soft solid skin layer previously formed inside the mold. See Figure 4.11.

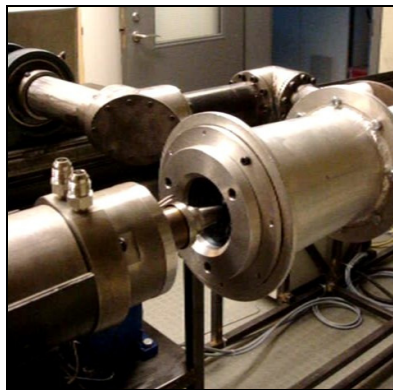


Figure 4.11: Step 5 – Extrudate Filling of Uni-Axially Rotating Mold

Step 6: The mold was translated back to the oven for a second rotational molding heating cycle. This second oven cycle was required to allow the skin to re-heal from the extruder nozzle puncture, and trigger the molten foamable compound to reach the CBA decomposition temperature to start creating the foamed core.

Step 7: Once foaming was completed, the mold moved out from the oven to the cooling location between the oven and extruder where it was cooled using an industrial sized fan while continually bi-axially rotating. See Figure 4.12.



Figure 4.12: Step 7 – Fan Cooling of Bi-Axially Rotating Mold

Step 8: The molding was then be taken out of the mold once it had solidified, where the EARFM processing cycle can then be restarted again.

4.5.2 EARFM Material Preparation

The EARFM process required a careful preparation of the melt-extruded foamable compound. As stated in Section 2.2.2, compared to dry blending, melt compounding foamable compositions is superior in terms of eventually producing higher quality rotationally molded fine-celled foams [28]. As melt compounding was utilized, it is common practice that the resulting molten foamable extrudate is cooled and formed into pellets to later be charged into a rotational mold simultaneously with the non-foamable resin based on single-shot RFM [55].

In contrast, creation of the foamable compound in EARFM involved melt compounding a pre-dry blended resin and CBA powder blend that took place in real-time to create a foamable melt that would not be pelletized or cooled before being filled into the mold.

The formulation to create the non-foamable skin layer was produced by dry-blending a non-foamable powder resin with an appropriate amount of pigment used to better visually distinguish between the integral-skin and foamed core. Exact amounts of the required formulations of both the foamable and non-foamable compounds will now be discussed.

Non-Foamed Skin Layer Formulation: To obtain the amount of PE resin required to create a solid non-foamed layer, exact volumes taken up by a chosen 3 mm skin thicknesses of each mold and each PE resin were determined. The resulting skin

volumes for the cylindrical and flat-plate mold were (V_{SKIN}) of 221.13 cm³ and 256.06 cm³, respectively. These volumes were used to determine the mass in grams of PE (m_{SKIN}) required to create the chosen skin thickness using Equation 2.1. The resulting required amounts of PE for each mold are listed in Appendix C (Table C1).

The pigment chosen to be added to the non-foamable compound was a red powder pigment named Graphfol Red 2BN (material data sheet located in Appendix B) suitable for use at PE processing temperatures. As this pigment was very strong in colour, only a small amount of approximately 0.1 g was required for each experiment to ensure acceptable colouration.

Foamable Formulation: To determine required amounts of resin and CBA to fill the remaining volume of the molds, the total mold volumes were determined using a space analysis function in a CAD software package. The resulting mold volumes of the cylindrical and flat-plate molds were 1483.72 cm³ and 1460.42 cm³, respectively. The skin volumes were subtracted from these total mold volumes to determine required expanded foam volumes (V_{FOAM}) for each resin. To successfully fill this volume, volume expansion ratios (VER) of 3 and 6 were chosen, which allowed for approximate values of V_i to be tabulated using Equation 2.2. Using these required volumes, the mass amount of PE resin in grams (m_{FOAM}) for each desired VER was determined using Equation 2.3.

To determine the appropriate amount of CBA to achieve the chosen VERs, the gas yield was also corrected using Equation 2.4. To maintain consistency between the PE resins that feature different crystallization temperatures, an average of 116.13 °C was used for this calculation. Once the correct gas yield was established, Equation 2.5 was used to determine the amount of CBA required in grams (m_{CBA}) for the given VER. The amount of CBA was also determined in terms of its percentage by weight (%CBA) calculated using Equation 2.6. The resulting foamable formulations for both molds are presented in Appendix C (Table C2).

During experimentation, there was no control of the exact amount of material that exited the extruder. Once in the extruder, the foamable material was pushed forward towards the nozzle exit via the extruder screw. However, once the material exited the extruder into the nozzle apparatus, the material was only driven forward towards the nozzle exit by material behind it still within the extruder. To counteract the lack of drive

within the nozzle equipment, additional resin and CBA amounts to maintain a proper formulation were added to accommodate for the volume from the extruder exit to the nozzle exit. This allowed for the correct amount of foamable melt to be filled into the mold.

Final preparation of the foamable compound in powder form involved dry-blending the PE resin with the CBA to promote a more uniform dispersion of CBA particles within the polymer. As the CBA had no colour there was no visual cue as to the degree of dispersion, so care needed to be taken to break up any visible clumps of CBA before melt compounding.

4.6 Process Modifications of EARFM

After performing experiments with this process using only the cylindrical mold, there was potential to create excellent quality fine-celled moldings using the experimental setup, while achieving significant processing time and energy savings. However, to produce acceptable quality fully filled moldings, modifications and further experimentation were required. This led to the modifications listed below that resulted in the second process iteration, known as Extrusion-Assisted Direct Foaming Rotational Molding (EADFRM).

Major Process Modifications: The fundamental modification with the potential to improve the achieved foam quality was to no longer accomplish foam formation within the oven for a second rotational molding heating cycle.

(1) Direct Foaming: Through experimentation, it was found difficult to create a completely un-foamed foamable melt with the extruder and accompanying equipment. From this, it appeared beneficial to allow foaming to occur within the extruder to reduce the need for a second oven heating cycle. Therefore, foam formation and final shaping occurred within the heated environment of the mold that would remain out of the oven.

An important thing to note is that for this new process, unlike prior practice, actual creation of the foam was now totally decoupled from the subsequent shaping step. In addition, the overall heating cycle and total energy consumption of this process was further reduced by eliminating the second oven heating cycle.

(2) **CBA Amount:** Consequently, the gas correction of the CBA for foamable formulations was no longer used due to the nature of the process where gas was unavoidably lost before mold filling that could not be properly accounted for. The resulting material formulations for both molds are presented in Appendix C (Tables C1 and C3).

Minor Process Modifications: To further improve the EARFM process, several additional modifications were implemented to attempt the creation of better quality integral-skin foamed core moldings, one of which was the discontinued use of the static melt blender. In addition to this, the use of the hot-runner and accompanying equipment were also discontinued from further experimentation as filling of the foaming compound proved to be difficult with these components.

(1) **New Nozzle Design:** By using a new simplified heated nozzle system closer to the exit of the extruder, less material was wasted and there was a potential increase in achieved cell density with a reduced nozzle length. Additionally, with a larger diameter, the nozzle was capable of an increased foam filling rate without increasing the extruder screw rotational speed to reduce frictional heat during filling. This modified nozzle system is depicted in Figure 4.13.

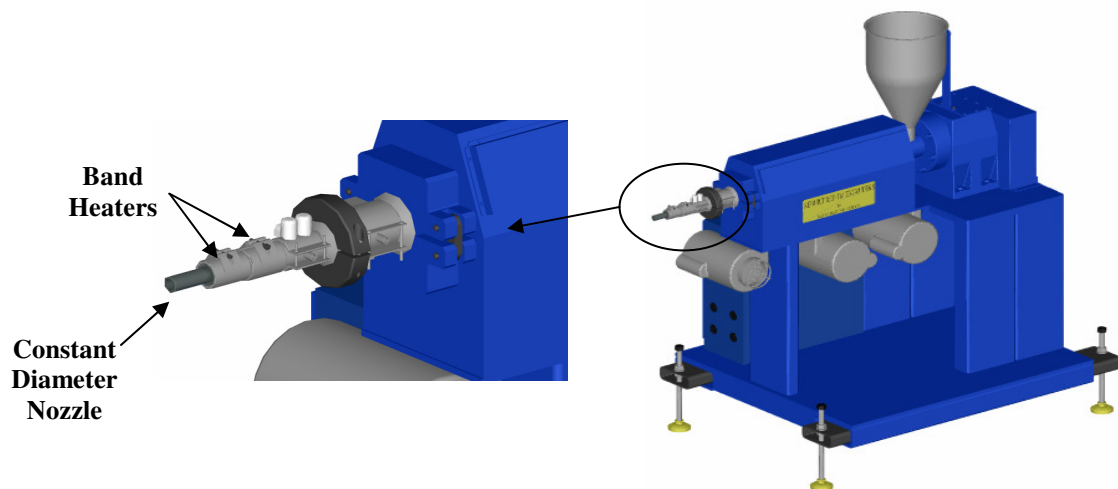


Figure 4.13: Extruder with Modified Nozzle Assembly

This nozzle was made out of steel to ensure it could withstand the harm caused by rotation of the “pizza valve” that was observed with the previous aluminum nozzle. With use of band heaters along most of the nozzle length, an appropriate temperature was maintained within the nozzle despite it not being made of aluminum.

(2) *New “Pizza Valve” Design:* To improve the interface quality, a new “pizza valve” was designed with radial cuts as pictured in Figure 4.14.



Figure 4.14: Modified "Pizza Valve"

During experimentation, it was observed that the triangular cut pieces of the “pizza valve” were fragile and broke during filling due to the rotation of the mold and contact with the extruder nozzle. Therefore, to lengthen the useful life of the “pizza valve” during filling, and to better contain the expanding foam, smaller radial cuts as seen in the above design were implemented.

(3) *New Venting System Design:* The final modification involved a re-design of the mold venting system. Since it was found that the previous system was not capable of expelling the air displaced by the foaming material, additional pressure tubes were added adjacent to the “pizza valve”. Also instead of using steel vent tubes, Teflon tubes were chosen to be used as they have excellent non-stick properties to prevent clogging.

4.7 Process Modifications of EADFRM

After performing experiments using the previously stated process modifications, there was a significant improvement in foam quality, in addition to still achieving an excellent skin/foam interface. However, the filling capability and quality of the achieved foam morphologies had not yet reached an acceptable level. This resulted in a third process iteration being created, known as Rapid Rotational Foam Molding (RRFM) with the resulting modifications listed below:

(1) *New Mold/Extruder Interface System:* The first and most significant modification of EADFRM involved improving the “pizza valve” area skin quality. This was accomplished by abandoning the idea of the “pizza valve” and implementing a new

interface system. It was important for this new system to be designed to be more robust to better withstand the filling process, be strong enough to contain the foam within the skin, and allow the skin to re-heal itself after filling. The resulting design, known as the insulated mold interface assembly, as presented in Figure 4.15, was made up of three components: the insulation cap, the mold interface and the mold connection adaptor.

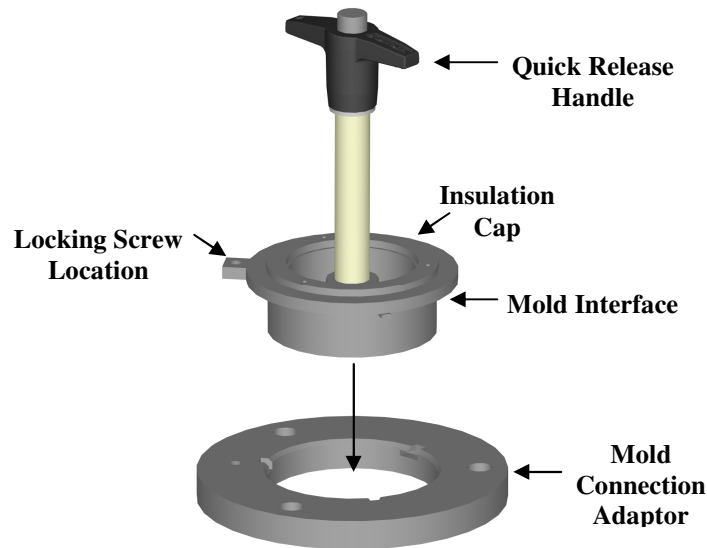


Figure 4.15: Insulated Mold Interface Assembly

The mold connection adaptor was secured to the mold to hold the mold interface in place during operation by utilizing a twist lock design. An additional screw secured from the interface to the adaptor prevented further unwanted movement of the mold interface during the bi-axial rotation of the mold. Within the mold interface, there existed a channel with a 2 mm outer wall thickness where the interface came in contact with the non-foamable skin. The purpose of this channel was to drastically reduce the heat transfer ability of the interface by filling it with a high temperature ceramic fiber insulation commercially known as Fiberfrax® 7000 Series Fiber (material data sheet located in Appendix B) that was contained by the insulation cap. During operation, once the non-foamable skin layer had been formed within the mold, this insulated interface was removed from the mold using a quick release T-handle bringing with it a section of the molten skin to remain on the bottom of the interface during foam filling. After filling was complete, the mold interface was reattached to the mold for the expanding foam to adhere to the semi-molten resin attached to the interface.

In order to properly perform successful experiments, however, new material formulations had to be determined as use of the new insulated mold interface assembly caused a change in total mold volume. The modified cylindrical and flat-plate mold volumes were 1469.51 cm^3 and 1447.05 cm^3 , respectively. The modified skin volumes were determined to be 228.97 cm^3 and 263.90 cm^3 for the cylindrical and flat-plate mold, respectively. Therefore, the new material formulations for both molds are listed in Appendix C (Tables C4-C5).

(2) Additional Mold Venting Modifications: As an attempt to eliminate continued clogging difficulties, larger diameter Teflon tubes with angled slits were created to allow trapped air to escape if the top of the tube were to get clogged with foam. Steel wool was also used in these tubes to allow air and gases to escape without letting foam or skin clog the tubes.

(3) New Nozzle Design: The continued existence of a non-uniform foam structure, potentially caused by continued overheating, resulted in the need to further simplify the extrusion process. To accomplish this, a new nozzle system was created that attached directly to the extruder requiring use of only one band heater that reduced the length of the nozzle system. It was the goal of this new system to reduce residence time of the foaming compound so it would not have to travel as far in a heated environment improving the resulting foam quality. Eliminating excess band heaters also reduced the amount of extruder parameters during experimentation. This nozzle system is presented in Figure 4.16.

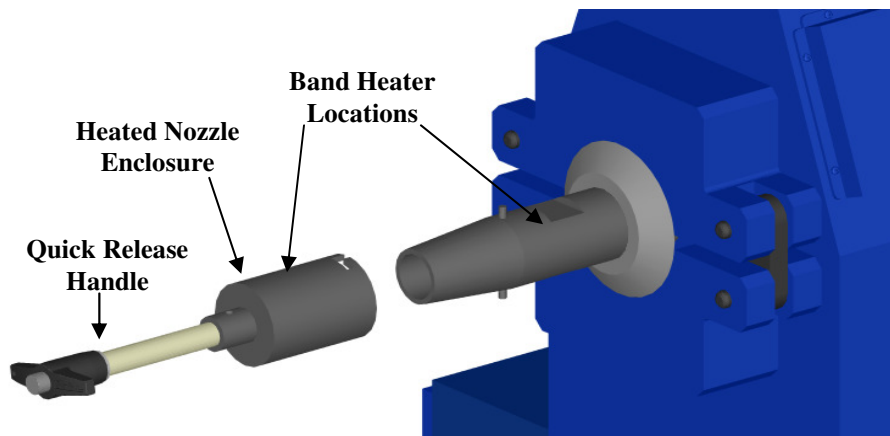


Figure 4.16: Second Extruder Nozzle Modification

Also pictured with the newly designed nozzle is a heated enclosure where when not in operation, the heated enclosure contained any gases released from the CBA before filling. Use of an additional band heater on the enclosure was to help maintain the elevated temperature of the nozzle before filling, but did not add to the extruder parameters. The enclosure was held on the nozzle with a simple twist lock system that was controlled by its accompanying quick release T-handle.

4.8 Process Modifications of RRFM

After performing experiments using the RRFM process with both molds, an even more significant improvement in foam quality was achieved with continued minor quality difficulties. This resulted in the final process modifications listed below:

(1) Interface System Redesign: To reduce the potential for foam intrusion so that an excellent quality mold interface area could always be achieved, the channel depth where the mold interface protrudes into the top of each molding was reduced by 2 mm. The outer profile of this channel was also modified to feature rounded edges to mimic how the skin layer adhered to the original mold interface.

(2) Venting System Redesign: A final attempt to solve the venting problem of the cylindrical mold involved using a very short Teflon tube at the bottom of the mold just past where the non-foamable skin layer would exist. This venting arrangement focused on only expelling air during filling, rather than expelling gases created during foam formation, to promote a better quality fully filled molding. For the flat-plate mold, despite the large trapped air pockets within its four corners, it appeared that the original venting tubes were not getting clogged as foam fully surrounded their locations. This required additional venting tubes and venting tube supports in the four corners of mold to be added to the mold bottom plate.

4.9 Final RRFM Experimental Setup

The final custom built lab-scale experimental setup used to assess the performance capabilities of RRFM consisted of the same lab-scale oven, uni- and bi-axially rotating mechanism integrated onto a translation apparatus, lab-scale extruder with the

accompanying final nozzle design, and the modified mold shape variations. The final versions of these mold designs are presented in Figure 4.17.

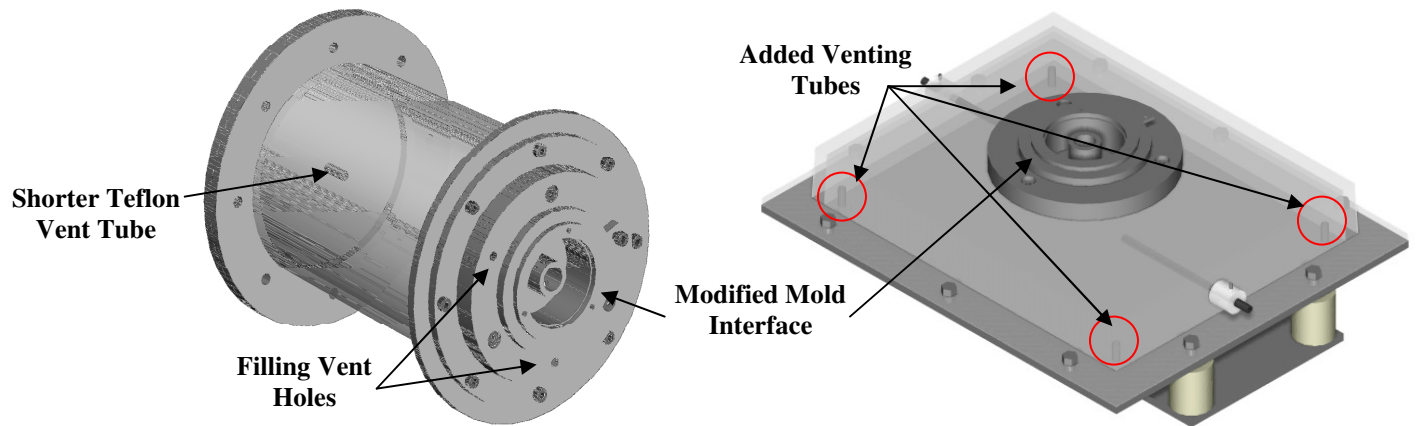


Figure 4.17: Final Cylindrical and Flat-Plate Mold Designs

While all other components remained the same, as they were previously described, an up-to date CAD representation of the entire experimental setup with use of the flat-plate mold is presented in Figure 4.18.

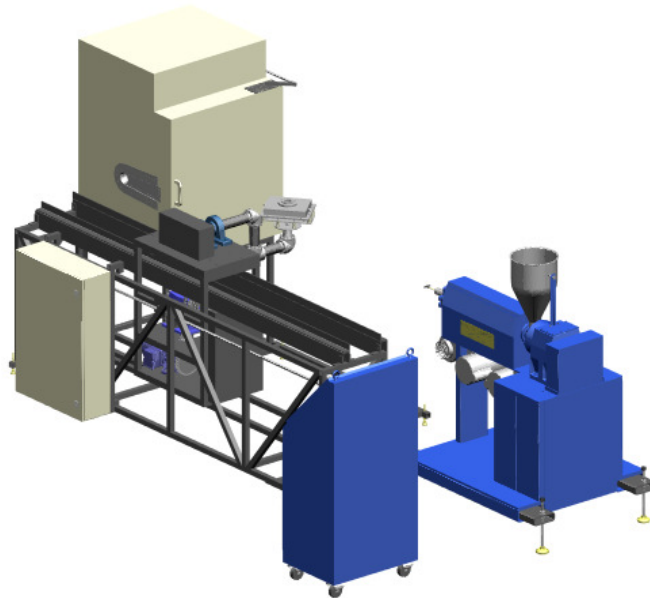


Figure 4.18: Final RRFM Experimental Setup

4.10 Final RRFM Processing Variables

As only few major modifications were made, most processing variables, as stated in Section 3.3, remained the same. However, the newest variables pertaining to mold filling and extrusion as a result of the modifications will now be discussed.

RRFM Mold Filling Variables: An important consideration with RRFM involves the foam pushing the molten or semi-molten skin layer. Since the extruder-foamed compound to be filled into the mold quickly adhered to the skin layer, any foam filled behind it had the potential to push the skin away causing thinning as found with experiments using the flat-plate mold. This could be directly related to the amount of CBA in the foaming compound, and the rate and orientation of filling as dictated by the extruder screw speed and extruder nozzle. Similarly, the temperature of the skin as it was removed from the oven, which should match the oven heating temperature during the rotational molding cycle, would have an effect on the skin uniformity. If this temperature was too high, or the MFR of the resin used was high, the resulting softer skin could be more susceptible to thinning from foam filling.

Once filling was complete, the amount of time the mold was left bi-axially rotating before cooling commences was important for foam formation. As found through previous experiments, especially for lower VER foam formulations, foam formation requires a wait time before cooling or an incomplete foam core would be produced. However, if left too long before cooling, the foam would begin to experience cell coalescence especially in the center of the molding as it would be remaining in a high temperature environment for a longer period of time. This would be due to the insulating ability of the foam where, even though the mold was made of a high heat transfer material, the foam within the center was shielded by itself containing the high temperatures produced by the extrusion process.

RRFM Extrusion Variables: To ensure an excellent foam structure could be achieved using extrusion, it was important to create a well dispersed foamable compound near the exit of the extruder. A well dispersed compound that had begun foaming had the potential to produce fine-celled foam if the amount of CBA gas lost was reduced before mold filling commenced. This was accomplished by optimizing the time between filling the hopper with the dry-blended foamable formulation and mold filling, and also with use

of the nozzle enclosure until the time filling commenced. Similar to the focus of the rotational molding heating cycle for foam formation in EARFM, the extruder parameters were utilized at the lowest achievable temperatures to ensure foaming can occur within the extruder and cause a fine-celled structure.

4.11 Final RRFM Material Preparation

As part of the process refinement, additional steps were added to the material preparation stage in order to improve the achieved foam quality. These steps will now be described:

Dry-Blending: The dry-blending process of preparing both the non-foamable and foamable formulations appeared to work effectively for previous experiments. However, due to the nature of the CBA powder it appeared difficult to break up all clumps in the foamable formulation. To improve CBA mixing during dry-blending, a sifting screen was used to break up any large clumps before the CBA was added to the resin powder.

Skin and Foamable Formulations: As dimensional modifications were performed on the mold interface, new skin and foamable formulations were created to make certain that correct formulations were used. Therefore, the final cylindrical and flat-plate mold volumes were 1467.54 cm³ and 1448.70 cm³, respectively. The modified skin volumes were determined to be 224.89 cm³ and 259.82 cm³ for the cylindrical and flat-plate mold, respectively, resulting in the final material formulations for both molds listed in Appendix C (Tables C6-C7).

4.12 Final RRFM Processing Steps

The required processing steps to create a PE integral-skin foam core molding with the final RRFM process are now presented:

Step 1: Charge the mold with the predetermined amount of suitable PE resin in powder form (designated for making the desired skin thickness) dry-blended with an appropriate amount of pigment.

Step 2: The oven was pre-heated to the desired processing temperature, at which time the mold was moved on the carriage system into the oven with the oven door closing

behind it with use of the pneumatic door control. Once in the oven, the bi-axial rotation of the mold was activated to evenly distribute the resin over the inner surface of the mold.

Step 3: The extruder was charged with a pre-dry blended foamable formulation in powder form (consisting of a non-foamable resin and a prescribed amount of CBA for achieving a desired VER). As a result, a foaming compound was produced. Melt compounding and initial skin formation within the mold still occurred simultaneously to reduce the heating segment of the traditional rotational foam molding cycle time.

Step 4: Once the non-foamable resin had a chance to melt and adhere to the walls of the mold, the oven door was opened and the mold was translated towards the extruder while only rotating uni-axially to be aligned with the extruder nozzle.

Step 5: The mold interface was removed and set aside while the extruder nozzle then entered the mold through the interface opening to fill the newly foaming compound completely inside the molten skin layer.

Step 6: After filling was complete, the mold interface was replaced onto the mold. The mold was then translated to its cooling location between the oven and extruder to allow for final foam shape formation.

Step 7: After a small wait time cooling commenced with an industrial sized fan with continued bi-axial rotation.

Step 8: The molding was then taken out of the mold once it has reached room temperature where plastic welding could be performed, if required. Then the cycle could be repeated, if required.

4.13 Introduction of Plastic Welding (Where Necessary)

As a back-up to ensure the foam core was fully encapsulated within the non-foamed skin layer, secondary processing in the form of plastic welding could be utilized. To test the capability of this, a plastic welding system known as “Injectiweld” from Drader Manufacturing was used to fill in the channel remaining from the mold interface with PE [63]. This system could also be used to fill in any holes remaining from vent tubes that would be important if these moldings were required to be air-tight.

CHAPTER 5

EXPERIMENTAL RESULTS AND DISCUSSION OF EARFM PROCESS AND RESULTING PROCESS ITERATIONS

5.1 Introduction

Experimental results to prove the feasibility of all process iterations described in Chapter 4 are presented and discussed within this chapter.

5.2 Experimental Results and Discussion of Extrusion-Assisted Rotational Foam Molding (EARFM)

Investigatory experiments were performed relating to various EARFM process steps using only LLDPE and the cylindrical mold to determine the feasibility of producing integral-skin foamed core moldings. These experiments were only performed using a 6 VER to ensure process feasibility before introducing new variables, such as use of the flat-plate mold and/or investigating different VER values.

5.2.1 Skin Formation

Initial rotational molding experiments were performed to ensure successful creation of a uniform skin hollow part with use of the “pizza valve”. The preliminary trials revealed that, apart from a very small amount of resin powder leaking at the beginning of the heating cycle, the “pizza valve” successfully contained the molten resin during bi-axial rotation of the mold, as presented in Figure 5.1.



Figure 5.1: Typical "Pizza Valve" Functionality Result

Further experimentation was conducted to determine, when the molten skin was punctured with the extruder nozzle, if the skin could successfully re-heal itself over the "pizza valve" upon further heating. After several trials, it was found the skin could re-heal itself over the "pizza valve", as presented in Figure 5.2.

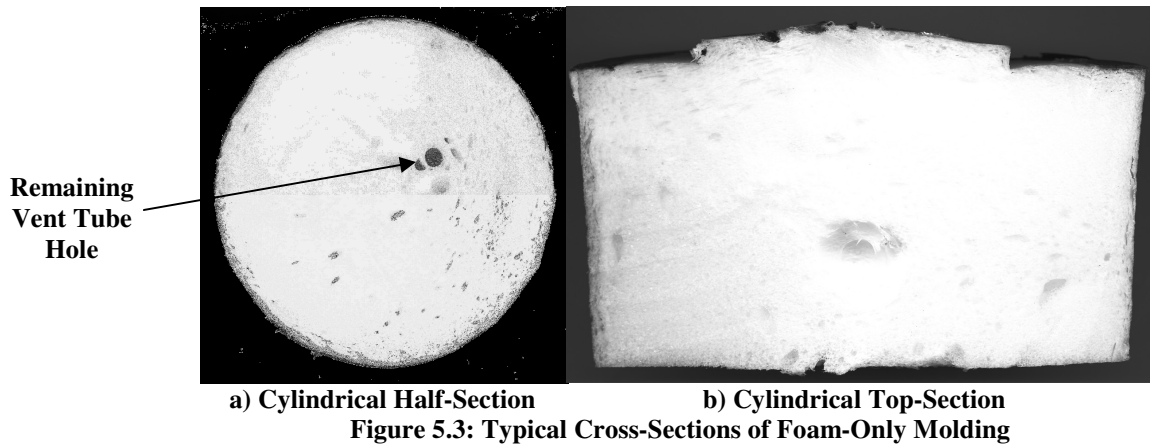


Figure 5.2: Typical "Pizza Valve" Puncture Test Result

5.2.2 Foam Formation

The next set of investigatory experiments involved determining the feasibility of creating fully filled foam-only moldings. From this, it was determined that successful creation of an un-foamed melt using the chosen extruder and accompanying equipment was not possible. This could have been caused by the lack of precise temperature control due to the extruder having only three temperature zones, compared to more complex extrusion systems. As a result, foaming occurred near the extruder exit causing severe clogging of the static melt blender, as shown in Figure 3.7, preventing further use of this component. After further attempts without the static melt blender, it was concluded that either an insufficiently mixed compound could be created at lower temperatures due to insufficient melting of the resin, or a new foaming compound at the extruder exit could be created. In

hopes to continue the foam-only experiments, trials were conducted using the latter foaming method with the typical achieved foam quality is presented in Figure 5.3.



Qualitative Molding Quality Analysis: The experimental results revealed a fully filled foam molding, as in the foam conformed to the dimensions of the mold, but featured a non-uniform cell structure, as presented by the above illustrations with the presence of large bubbles. In the radial direction, foam near the mold wall was overheated as a result of the thermal gradient created across the mold surface. As a result, it appeared that quite severe cell coalescence occurred. In the center of the molding, as presented in Figure 5.3 (b), the presence of the large bubble also indicated an insufficient dispersion of the CBA particles within the resin matrix.

To further investigate the achieved foam quality, SEM micrographs were taken of a typical foam sample, as pictured in Figure 5.4.

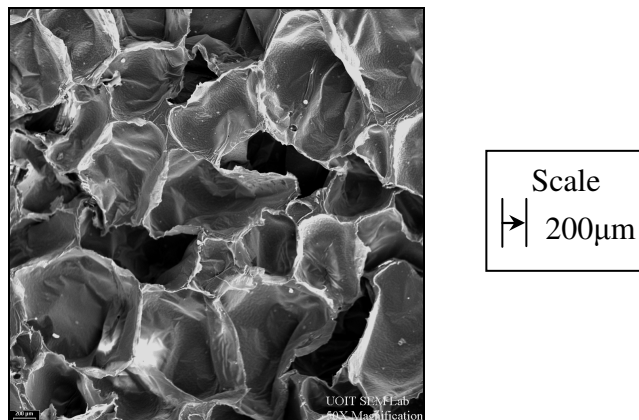


Figure 5.4: Micrograph of Typical EARFM Foam-Only Sample (50x Magnification)

This micrograph illustrates that the foam featured severely thinned cell walls, which was potential evidence that the foam was overheated. It can also be further concluded that due to this thinning there was a greater possibility that cell coalescence and cell coarsening occurred.

Quantitative Molding Quality Analysis: Average cell size and cell population density were used to quantitatively track process improvements from a single molding that was visually determined to be the most foam filled and featured the best foam quality. The values were determined for this process to be 353.58 μm and 2.18×10^5 cells/cm³, respectively. This indicated that it was potentially feasible to produce fine-celled foam with uniform cell-size distribution, but further refinement of the processing parameters would be necessary to achieve this.

5.2.3 Integral-Skin Foam Core Formation

Utilizing the results from the skin and foam formation experiments, further experiments were performed to produce integral-skin foamed core moldings with EARFM. It was the goal of these experiments to attempt to achieve at least five consecutive fully filled moldings, where experimentation ended only when it was concluded that this goal could not be accomplished. The results of these experiments proved to be quite different from previous experiments as integration of the skin and foam layer appeared to add complications to the process. The typical process parameters for these results are listed below in Tables 5.1-5.2.

Table 5.1: EARFM Skin Formation Parameters

Process Parameters	Typical Values
Oven Temperature ($^{\circ}\text{C}$)	220
Oven Heating Time (min)	40
Mold/Arm Rotation Ratio	3.94:1

Table 5.2: EARFM Foam Formation Parameters

Process Parameters	Typical Values
Barrel Zone 1 (°C)	122
Barrel Zone 2 (°C)	126
Barrel Zone 3 (°C)	132
Die Zone 1 (°C)	137
Die Zone 2 (°C)	137
Melt Temperature (°C)	121
Average Melt Pressure (PSI)	2300-0
Screw RPM	90
Oven Temperature (°C)	300
Oven Heating Time (min)	15

After performing approximately twenty experiments with this process, with no potential to achieve the required five consecutive acceptable moldings, the best molding, as illustrated in Figure 5.5, was used for further analysis.

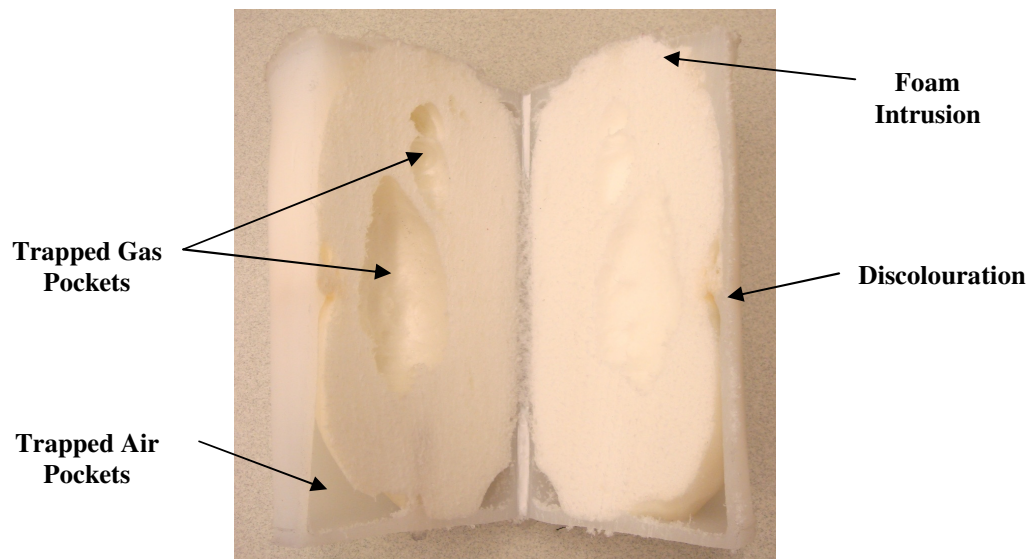


Figure 5.5: Typical Integral-Skin Foam Core Result of EARFM

Qualitative Molding Quality Analysis: Common to most of the achieved moldings were several problems including trapped air and gas pockets, foam discolouration, cell coalescence, and foam intrusion of the “pizza valve” skin layer. The trapped air pockets seen in the bottom and sometimes the top corners of the molding were potentially caused by insufficient venting during filling and foam formation. As the foaming compound was filled into the mold, it adhered to the molten skin and around the venting tube causing it to clog and prevent any air between the skin and foam from

exiting the mold. This clogging also caused a gas build-up generated in the center of the molding resulting in a large cavity that would greatly reduce the mechanical properties of this part. Discolouration occurred only in the outer layer of the foam that did not adhere to the skin potentially caused by overheating of the foam during foam formation. Cell coalescence was observed in the foam structure potentially caused by overheating. The amount observed, however, appeared to be reduced from what was observed in the foam-only moldings, potentially due to the presence of the skin layer. The foam compromised skin layer in the “pizza valve” area was evident in all achieved moldings as displayed in Figure 5.5. Although the “pizza valve” could successfully contain the skin during rotational molding, with the addition of foaming it was found that the “pizza valve” was not strong enough to contain the foam after filling and during foam formation.

To investigate the achieved foam and skin/foam interface quality, SEM micrographs were taken of typical samples, as pictured in Figure 5.6.

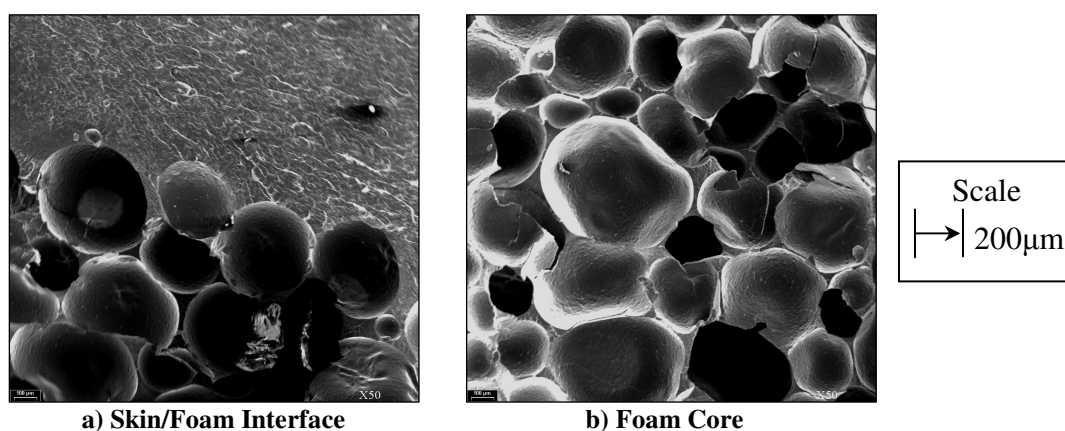


Figure 5.6: Micrographs of Typical EARFM Sample (50x Magnification)

As seen in Figure 5.6 (a), it was apparent where the skin layer and foam structure occur and that an excellent interface was achieved between them as the cells appear to protrude into the skin layer. This ultimately showed that filling the foaming material into the mold within the skin layer in a molten or semi-molten state allowed for a superior quality skin/foam interface to be produced. Looking at the typical foam structure achieved by these moldings, as pictured in Figure 5.6 (b), there was a significant improvement in the achieved cell structure compared to the previously obtained foam-only experiments. This

fact was apparent as the cell walls appeared to be thicker allowing the cell structure to maintain its shape, unlike the foam-only cell structure.

Quantitative Molding Quality Analysis: The determined results for average cell size and cell population density for the best molding of the EARFM process were 337.41 μm and 2.49×10^5 cells/cm³, respectively.

5.3 Experimental Results and Discussion of Extrusion-Assisted Direct Foaming Rotational Molding

Due to the modifications of the EARFM process, listed in Section 4.6, the Extrusion-Assisted Direct Foaming Rotational Molding (EADFRM) process was introduced. The typical process parameters for the experimental results of this new process are listed in Tables 5.3-5.4.

Table 5.3: EADFRM Skin Formation Parameters

Process Parameters	Typical Values
Oven Temperature (°C)	220
Oven Heating Time (min)	35
Mold/Arm Rotation Ratio	3.94:1

Table 5.4: EADFRM Foam Formation Parameters

Process Parameters	Typical Values
Barrel Zone 1 (°C)	120
Barrel Zone 2 (°C)	135
Barrel Zone 3 (°C)	150
Die Zone 1 (°C)	150
Die Zone 2 (°C)	150
Melt Temperature (°C)	140
Average Melt Pressure (PSI)	500-0
Screw RPM	90

After performing approximately twenty experiments with this process, again with no potential to achieve the required five consecutive acceptable moldings, the best molding, as illustrated in Figure 5.7, was used for further analysis.

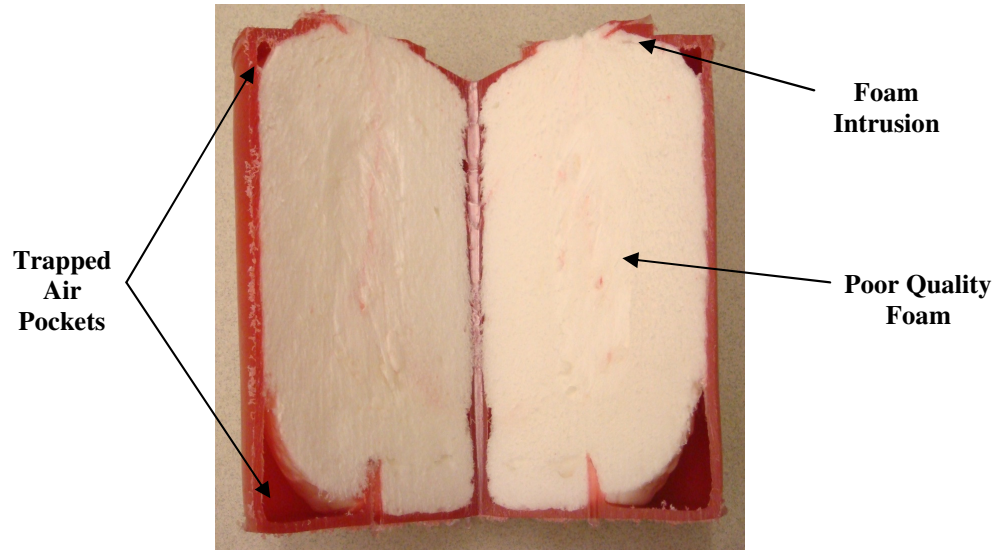


Figure 5.7: Typical Result of the EADFRM Process (VER = 6)

Qualitative Molding Quality Analysis: As seen in the previous illustration, the modified “pizza valve” was able to achieve a slightly improved interface quality as less foam intrusion was observed. The difficulties regarding clogging were reduced with use of the Teflon tubes, but a poor quality foam section replaced the inner cavity previously created. During filling, with the added venting tubes there was evidence of improved filling, but air was still getting trapped in various corners of the mold. In terms of foam quality, cell coalescence was still observed but to a lesser extent compared to EARFM results. The major observed improvement, however, was that there was no evidence of degradation in the foam of the achieved moldings. There also appeared to be little to no visual difference in quality of the moldings for each resin resulting in the need to quantify any differences on a cellular level.

Analyzing the moldings to determine modification effectiveness and use of different resins first involved examining SEM micrographs of typical LLDPE moldings for a 3 and 6 VER, as presented in Figure 5.8.

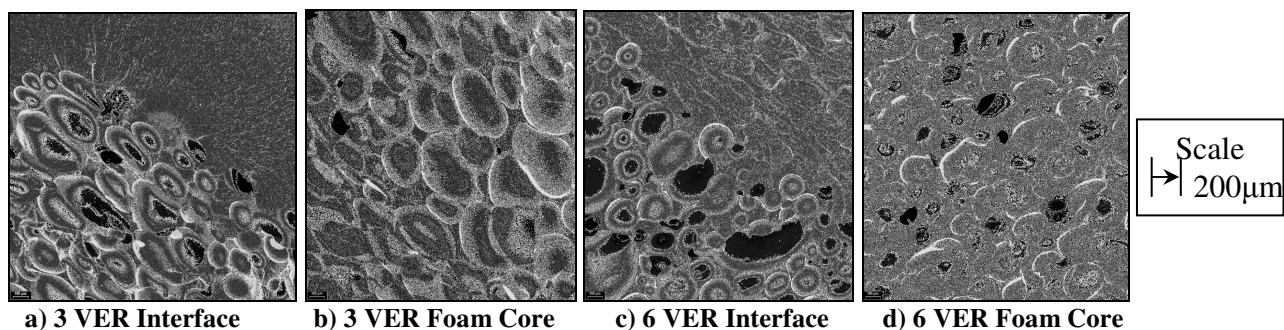


Figure 5.8: Micrographs of LLDPE EADFRM Sample (50x Magnification)

Micrographs were then taken of typical HDPE moldings for a 3 and 6 VER that are presented in Figure 5.9.

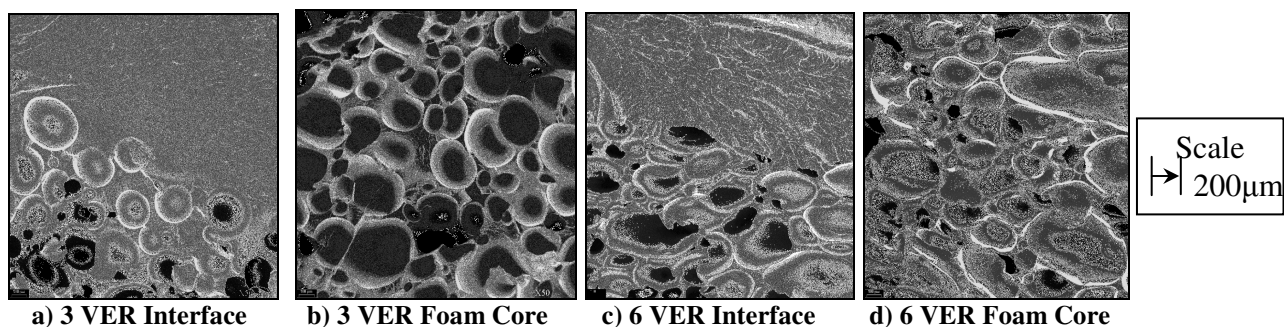


Figure 5.9: Micrographs of HDPE EADFRM Sample with (50x Magnification)

From these micrographs, it was apparent that the same level of interface quality obtained previously could be achieved for the different VER values and different resins with the only difference occurring in the cell structure. For the shape of the cells, there appeared to be mostly circular bubbles with evidence of oval shaped bubbles. These oval bubbles could have been created by a pulling or shearing of the cells caused by the foaming compound flowing along the molten/semi molten skin during mold filling.

Quantitative Molding Quality Analysis: Further comparison of the foam structures, in terms of average cell size and cell population density, between the varying resins and VER values is summarized in Table 5.5.

Table 5.5: EADFRM Cell Analysis Results

Material	LLDPE		HDPE	
	3	6	3	6
Average Cell Size (μm)	346.35	293.55	360.50	295.91
Cell Population Density (cells/cm^3)	0.92×10^5	3.77×10^5	0.81×10^5	3.68×10^5

From this table it is apparent that the cell population density values increased with increasing VER, and that for a 6 VER there was a significant decrease in cell size compared to a 3 VER. This result was most likely caused by the increased amount of CBA for a 6 VER that allowed for more cells to be nucleated within less amount of resin.

5.4 Experimental Results and Discussion of Rapid Rotational Foam Molding (RRFM)

In light of the modifications of the EADRFM process described in Section 4.7, this process was renamed to be finally known as Rapid Rotational Foam Molding (RRFM). The main focus of further experimentation involved improving moldings achieved using the cylindrical mold, and determining the feasibility of using the flat-plate mold with only LLDPE and a 6 VER.

The typical process parameters for these results, including those achieved for the flat-plate mold are listed in Tables 5.6-5.7.

Table 5.6: RRFM Skin Formation Parameters

Process Parameters	Typical Values
Oven Temperature (°C)	270
Oven Heating Time (min)	26
Mold/Arm Rotation Ratio	3.94:1

Table 5.7: RRFM Foam Formation Parameters

Process Parameters	Typical Values
Barrel Zone 1 (°C)	110
Barrel Zone 2 (°C)	125
Barrel Zone 3 (°C)	140
Die Zone 1 (°C)	140
Nozzle Hood (°C)	140
Melt Temperature (°C)	135
Average Melt Pressure (PSI)	800-0
Screw RPM	90

After performing approximately twenty experiments with this process, with improved potential but again failing to achieve the required five consecutive acceptable moldings, the best moldings from both molds, as illustrated in Figure 5.10 and Figure 5.11, were used for further analysis.

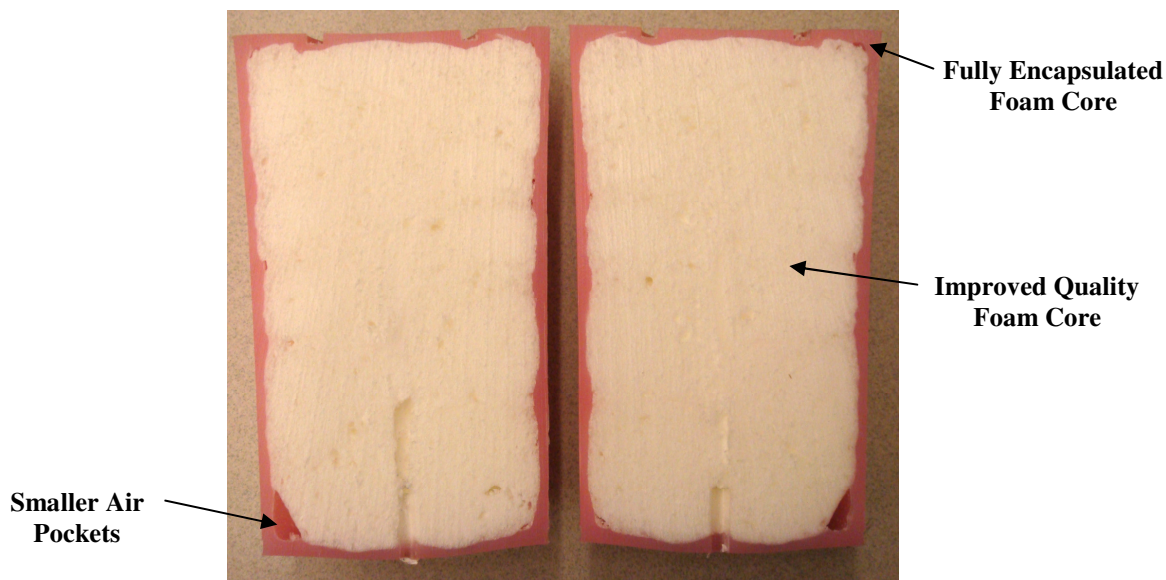


Figure 5.10: Typical Result of RRFM for the Cylindrical Mold

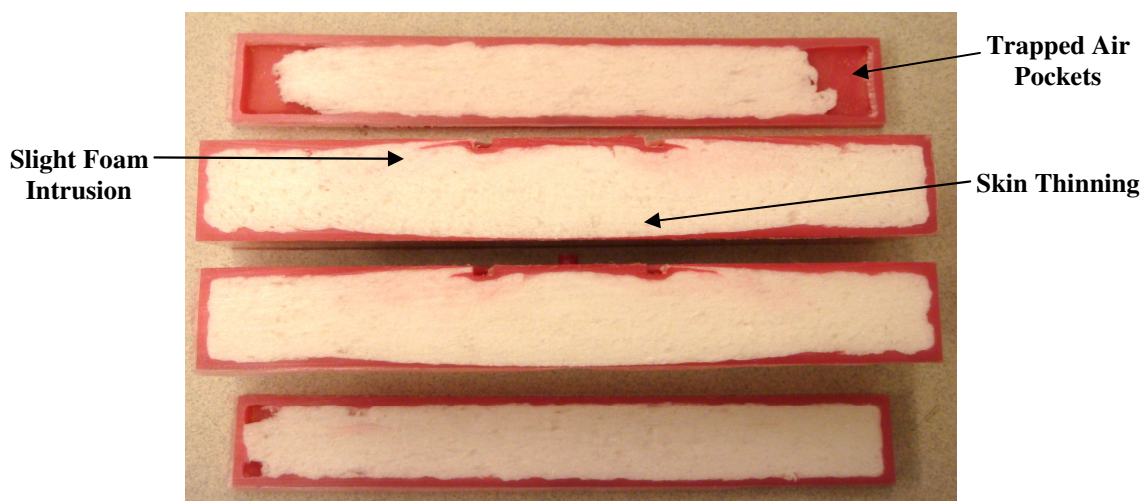


Figure 5.11: Typical Result of RRFM for the Flat-Plate Mold

Qualitative Molding Quality Analysis: Using the cylindrical mold, it was determined that the insulated mold interface allowed the skin to melt and adhere to it allowing this section of skin to be removed for foam filling. After filling when the interface was replaced, as seen from Figure 5.10, the detached skin layer successfully re-healed itself fully encapsulating the foam resulting in a more than adequate interface quality.

The venting modification of using larger Teflon tubes with slits and steel wool, dramatically improved foam filling, but achieving fully filled moldings was still difficult, as pictured in Figure 5.10 where smaller air bubbles still existed near the bottom of the

mold. The foam core quality, however, improved greatly with the venting modifications as a visually apparent uniform foam structure was observed at the center of the moldings.

For the flat-plate mold, the first significant difference between an achieved molding with this mold compared to the cylindrical mold was that no foam cavity was created in the center of the molding. This was potentially due to the reduced thickness of the flat-plate mold, and because of its two offset vent tubes increasing the venting capacity compared to the cylindrical mold.

Filling the flat-plate mold, however, appeared to cause similar problems as those experienced by the cylindrical mold where air pockets were trapped in the outer corners of this mold. Additionally unlike the cylindrical mold, skin thinning occurred along the bottom of these moldings where it was evident that the speed and orientation of filling was the direct cause.

The resulting interface quality of the flat-plate mold experiments was generally comparable to what was achieved for the cylindrical mold for most moldings. However, a potential quality issue arose regarding slight foam intrusion through the skin around the sides of the interface, as seen in Figure 5.11. Despite this intrusion, the level of quality of the mold interface had been greatly improved from previous attempts, and thus no further major modifications of this component were required.

One thing evident in the achieved foam structures of both molds was the continued existence of cell coalescence, resulting in the need to further investigate the affect of filling processing temperatures during foam creation.

To determine if there was a difference in achieved foam or skin/foam interface quality with use of the different mold shapes, SEM micrographs were taken of typical molding samples that are presented in Figure 5.12.

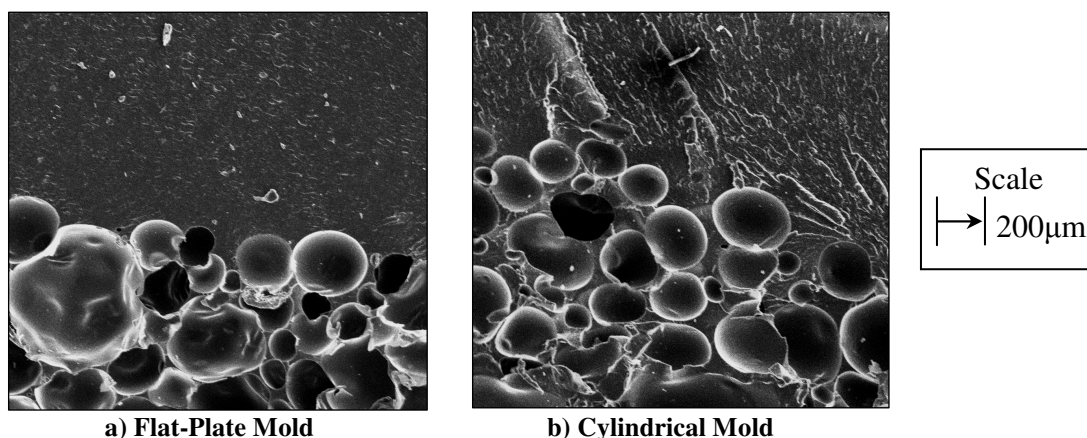


Figure 5.12: Micrographs of RRFM Skin/Foam Interface (50x Magnification)

It appeared from these micrographs that the same level of skin/foam interface quality could be achieved for the flat-plate mold, yet there does appear to be a slight difference in cell size.

Quantitative Molding Quality Analysis: Accordingly, cell analysis was performed to determine if an increase in foam quality was achieved with the most recent modifications, and with use of the flat-plate mold. The resulting average cell sizes for the cylindrical and flat-plate molds were determined to be 254.73 μm and 251.88 μm , respectively. The resulting cell population densities for both molds were also determined to be 5.78×10^5 cells/cm³ and 5.32×10^5 cells/cm³, respectively.

5.5 Quality Comparison of Process Iterations

To better illustrate the quality improvements achieved with each process iteration, a table summarizing the experimental results achieved with these processes is listed in Table 5.8.

Table 5.8: Summation of Experimental Results for all Process Iterations

Process Iteration	Mold	VER	Material	Average Cell Size (μm)	Cell Population Density (cells/cm ³)
EARFM	Cylindrical	6	LLDPE	337.41	2.49×10^5
EADFRM	Cylindrical	3	LLDPE	346.35	0.92×10^5
			HDPE	360.50	0.81×10^5
		6	LLDPE	293.55	3.77×10^5
			HDPE	295.91	3.68×10^5
RRFM	Cylindrical	6	LLDPE	254.73	5.78×10^5
	Flat-Plate			251.88	5.32×10^5

Clearly illustrated within this table is that there was a noteworthy decrease in average cell size and increase in cell population density when comparing like experiments. This change demonstrated an increase in foam quality that was further improved through the following optimization focused experimentation with the final RRFM process.

5.6 Experimental Optimization Results and Discussion of Rapid Rotational Foam Molding (RRFM)

Due to the final modifications of the RRFM process, described in Section 4.8, additional experimentation was required to determine if further quality improvements could be successful. Looking closely at the final process steps, it appeared that the main factor influencing the achieved foam structure was the extruder processing temperatures. Additional experiments were performed on both molds with all resins to determine how these temperatures dictate different quality levels, and at what temperature can an excellent quality foam be created using RRFM. Given results of previous processing parameters, the chosen melt temperatures for these experiments were 130 °C, 135 °C and 140 °C keeping all other process variables, such as material formulations, the same. The typical process parameters for these results are listed in Tables 5.9-5.10.

Table 5.9: Final RRFM Skin Formation Parameters

Process Parameters	Typical Values
Oven Temperature (°C)	270
Oven Heating Time (min)	26
Mold/Arm Rotation Ratio	3.94:1

Table 5.10: Final RRFM Foam Formation Parameters

Process Parameters	Typical Values		
Barrel Zone 1 (°C)	100	110	120
Barrel Zone 2 (°C)	115	125	135
Barrel Zone 3 (°C)	130	140	150
Die Zone 1 (°C)	130	140	150
Nozzle Hood (°C)	130	140	150
Melt Temperature (°C)	130	135	140
Average Melt Pressure (PSI)	1000-0	800-0	700-0
Screw RPM (Cylindrical/Flat-Plate)	90/70	90/70	90/70

Further experiments were not performed at lower melt temperatures as melting of the resin would not occur within the lab-scale extruder. Also, activation of the CBA that is not achieved at temperatures lower than 160 °C, was achieved through the high heating rate and resulting frictional heating of the screw rotations, that was not considered accurately in the melt temperature readings. Additional heating of the foaming compound was accomplished within the heated environment of the mold as it was heated to 270 °C in the oven during skin formation for every experiment.

5.6.1 Qualitative Quality Analysis

Effect of Processing Parameters on Molding Quality in RRFM: The resulting conventionally scanned and SEM micrograph illustrations for the LLDPE moldings using the cylindrical mold are presented in Figure 5.13.

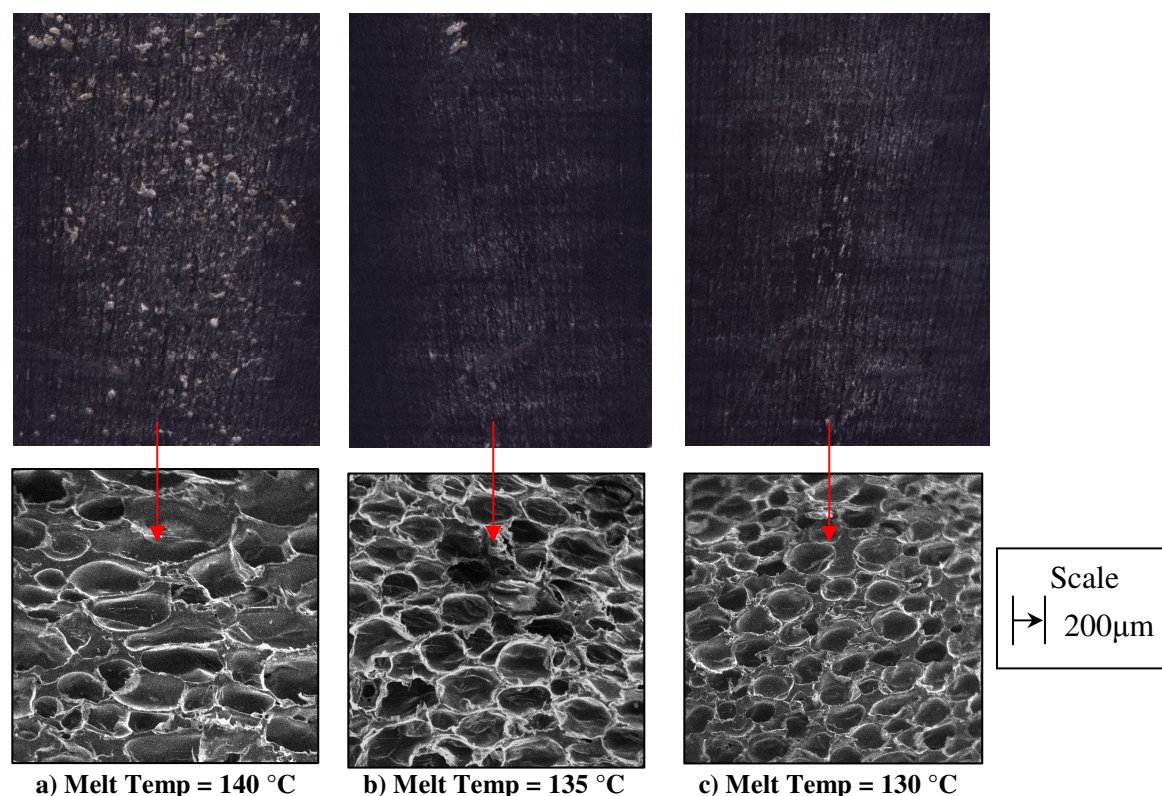


Figure 5.13: Scanned Foam and Micrograph (50x Magnification) Results of Varying Melt Temperature with LLDPE using the Cylindrical Mold

As well, the resulting conventionally scanned and SEM micrograph illustrations for HDPE using the cylindrical mold are presented in Figure 5.14.

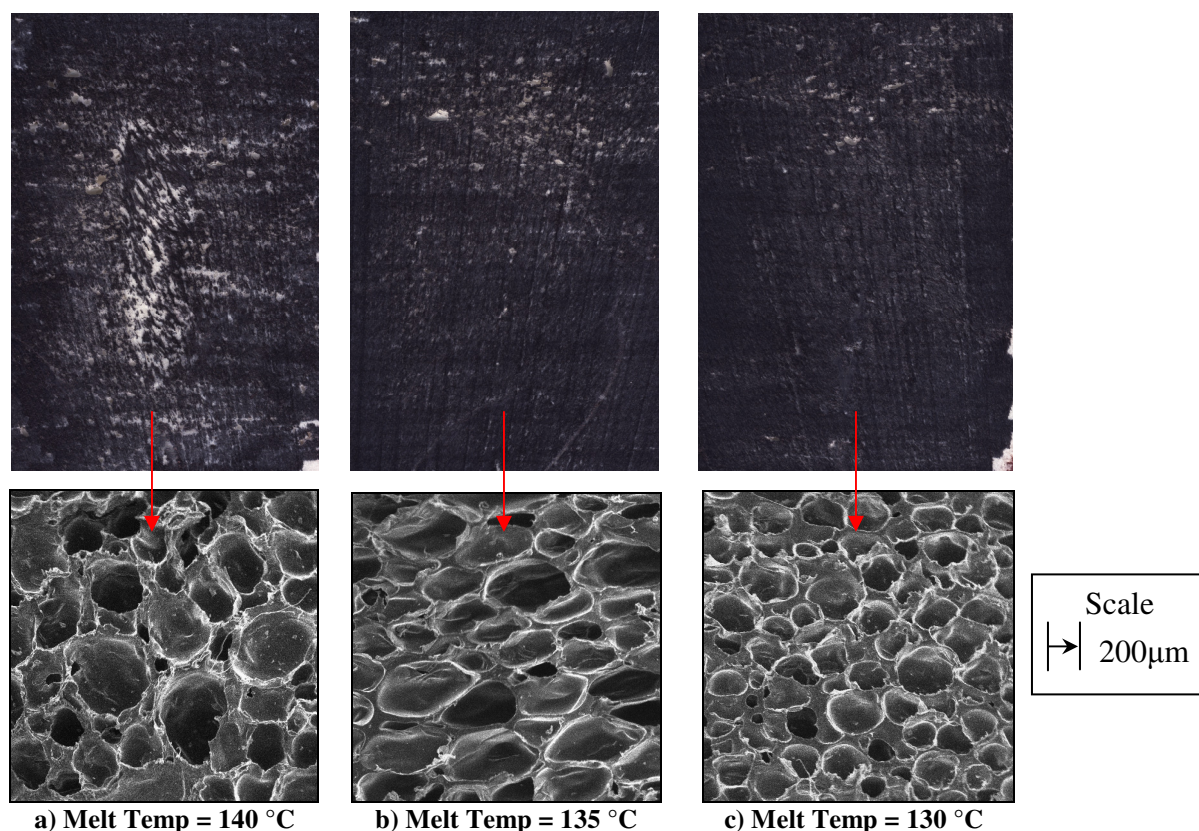


Figure 5.14: Scanned Foam and Micrograph (50x Magnification) Results of Varying Melt Temperature with HDPE using the Cylindrical Mold

Effect of Melt Temperature in RRFM: From the conventionally scanned illustrations it was apparent that the level of cell coalescence decreased with decreasing melt temperature for both materials. This fact was described throughout previously published research that states that increasing the melt strength by way of reducing processing temperatures reduces the potential for cell coalescence [43-44]. To further reduce the level of cell coalescence, as the extruder processing temperatures could not be reduced lower than 130 °C; the oven heating temperature to produce the molten skin layer could be reduced. However, in doing so the mold may have to remain in the oven longer increasing the total cycle time rather than reducing it. It may also be possible to start cooling the mold right after mold filling, yet this could risk insufficient filling if the foam has not fully expanded before cooling begins.

Analyzing the micrographs shows a distinct cell size reduction with decreasing melt temperature for both resins, thus illustrating that lower processing temperatures have the capability of producing better quality foams.

Effect of Resin Type in RRFM: Comparing the visible foam and cell structure obtained with both materials it appeared that they both exhibited a similar reduction in cell coalescence and cell size with decreased melt temperature. Although, there appeared to be an increase in the amount of cell coalescence observed in the HDPE moldings compared to the LLDPE moldings of the same melt temperature. This occurrence could be due to the difference in crystallization temperatures between the two materials, as LLDPE featured a lower crystallization temperature. Thus potentially showing what was previously hypothesized in Section 4.3, that a lower crystallization temperature have the ability to begin to solidify sooner given the same cooling rate, thus reducing the amount of cells that coalesce.

Visually comparing the observed cell sizes between the two materials at the same melting temperature, it also seemed that the average cell size of the LLDPE molding appeared to be smaller. This also could be contributed to the crystallization temperature where, with continued heating, the amount of CBA gas generated after cell nucleation ends continues to fill the already created cells increasing their size. Therefore utilizing a lower crystallization temperature resin, continued gas generation and cell growth would be stopped more rapidly causing smaller cells as the resin would solidify sooner retarding continued cell growth.

Effect of Mold Shape in RRFM: Comparing the same processing parameters by varying the extruder melt temperature using the flat mold, the resulting conventionally scanned and SEM micrograph illustrations for LLDPE are presented in Figure 5.15.

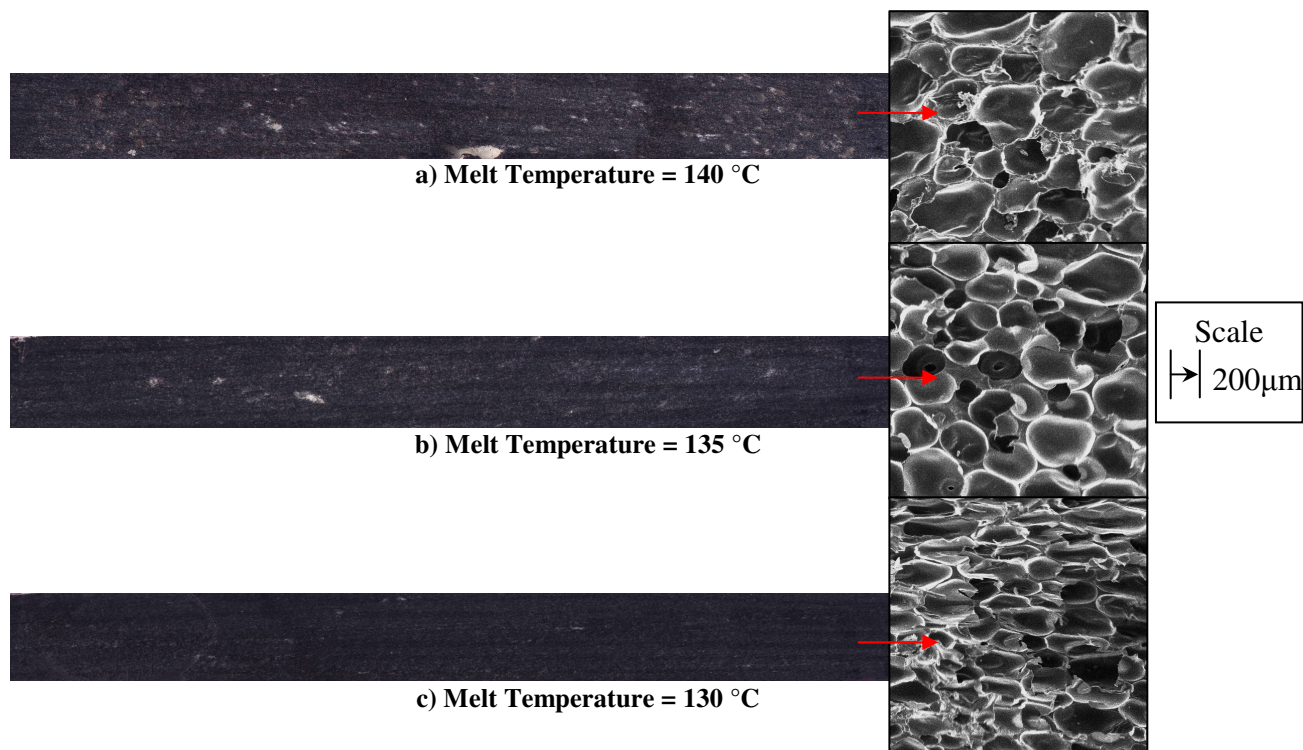


Figure 5.15: Scanned Foam and Micrograph (50x Magnification) Results of Varying Melt Temperature with LLDPE using the Flat-Plate Mold

Within these samples, in addition to featuring the same reduced level of cell coalescence at lower melt temperatures, a greatly reduced amount of cell coalescence was observed compared to use of the cylindrical mold with the same resin. This result could be due to the reduced volume of the mold, or more specifically how the mold volume is stretched over more of a surface area. It is believed that the larger surface area allowed more heat to escape the center of the mold even with the insulative capabilities of the produced foam. Conversely with the cylindrical mold, heat was trapped within the center of the mold as there was more foam separating it from the mold surface. This caused the insulative capabilities of the foam to be more apparent as the majority of cell coalescence observed in the moldings of both materials occurred in the centre of the cylindrical moldings.

The results obtained using HDPE with the flat-plate mold, as presented in Figure 5.16, will now be discussed to confirm the previously discussed mold comparative observations.

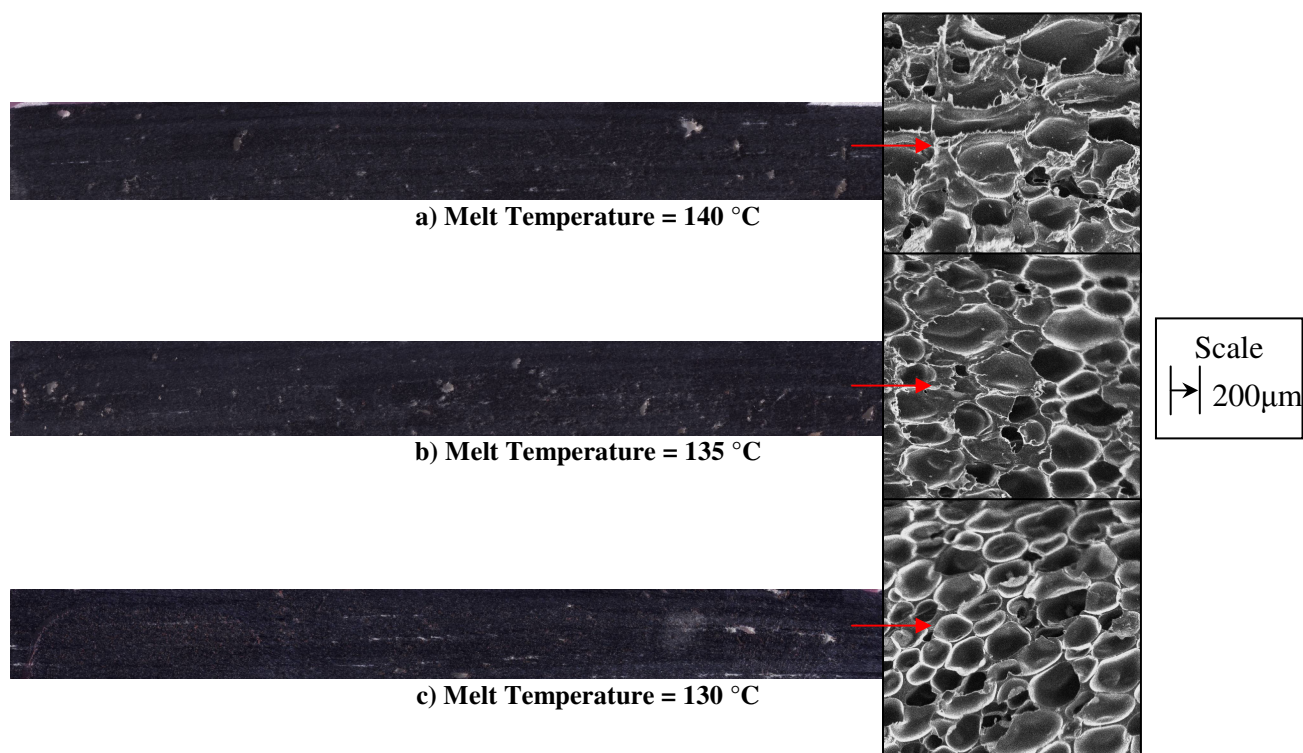


Figure 5.16: Scanned Foam and Micrograph (50x Magnification) Results of Varying Melt Temperature with HDPE using the Flat-Plate Mold

It appeared that using the flat-plate mold with HDPE featured the same pattern of cell coalescence reduction with decreased melt temperatures that was reduced from the level obtained with the cylindrical mold. Once more, the amount of cell coalescence observed with this resin was slightly increased compared to use of LLDPE with the flat-plate mold. Thus confirming that LLDPE was able to produce better quality foams using both mold shapes in RRFM, likely due to its lower crystallization temperature.

In terms of the observed cell size difference between both molds, there was a possibility that the flat-plate mold featured reduced cell sizes compared to the cylindrical mold. This fact was investigated further with quantitative cell analysis discussed later in this chapter.

It was also observed that with the flat-plate mold, the resulting cell structures appeared elongated rather than circular. This cell shape difference can be contributed to the foam quickly adhering to the molten outer skin when entering the mold, where subsequent foam pushes behind it creating a shearing or pushing effect. This was observed to occur more with the flat-plate mold as it featured an elongated and narrow

cavity compared to the cylindrical mold. In addition, in terms of the resin type, it was observed that LLDPE was more susceptible to this elongated cell structure within the flat-plate mold, potentially due to its higher melt flow rate or lower density.

Effect of Volume Expansion Ratio in RRFM: To ensure that the achieved foam quality had in fact been improved for both molds, experiments were performed with melt temperatures of 130 °C to produce moldings featuring a 3 VER, as previously obtained through investigation of EADFRM. These moldings were compared to ones achieved at the same melt temperature, but with a 6 VER. The resulting SEM micrographs of both resins are presented in Figure 5.17 for the cylindrical mold.

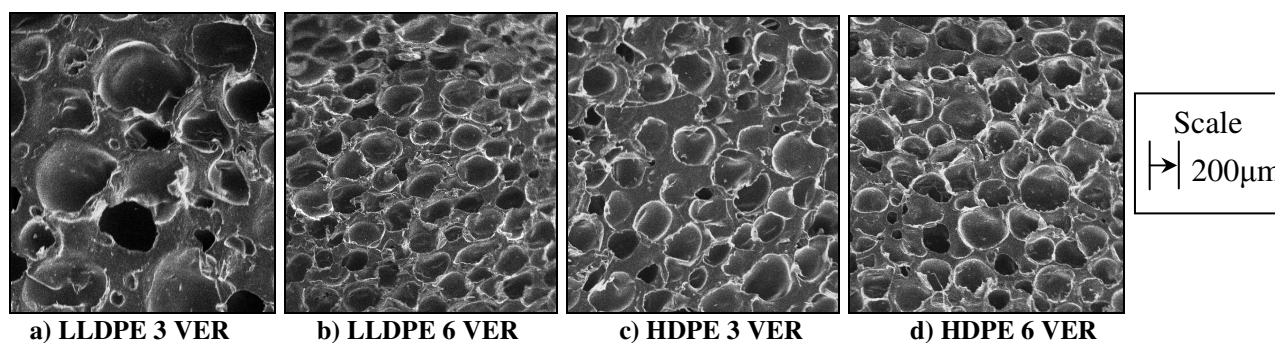


Figure 5.17: VER Comparison for Cylindrical Mold

What appeared clearer from the LLDPE molding with a 3 VER was that the average cell size seemed to be larger than for the molding with a 6 VER. However, visible in both moldings with a 3 VER was that there were larger gaps between cells, resulting in increased cell to cell distances that would increase the average cell size and reduce the cell population density. This could merely be caused by the reduction in the amount of CBA used in the foamable formulation. To ensure this potential cause was still valid, SEM micrographs of both resins at the varying VER values created with the flat-plate mold, as presented in Figure 5.18, were investigated.

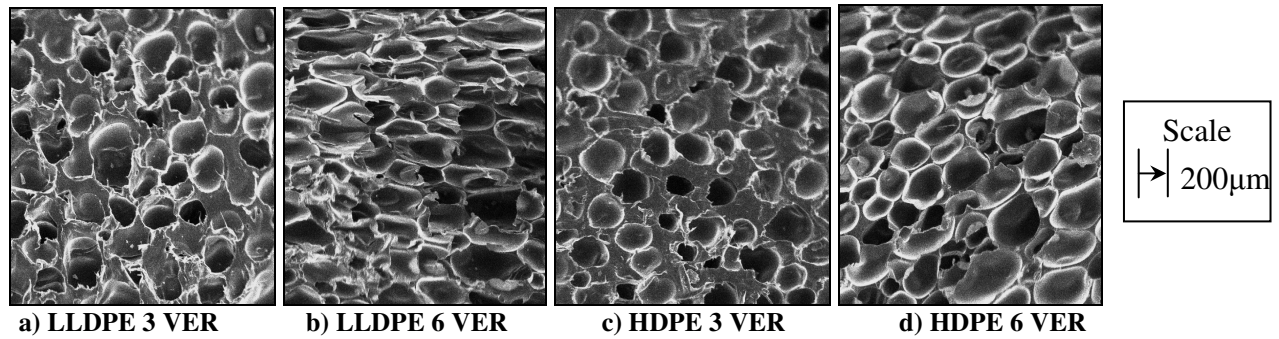


Figure 5.18: VER Comparison for Flat-Plate Mold

With use of this mold, increased cell to cell distances were again observed showing the potential for increased average cell sizes and reduced cell population densities for the moldings with a 3 VER.

Effect of Mold Shape on Mold Filling in RRFM: With final venting modifications in place, it was determined that fully filled foamed core moldings could be achieved with both molds. Yet the ability of obtaining a fully filled molding was found to be different between the mold shapes. To illustrate this, typical examples of filled moldings are presented in Figure 5.19.

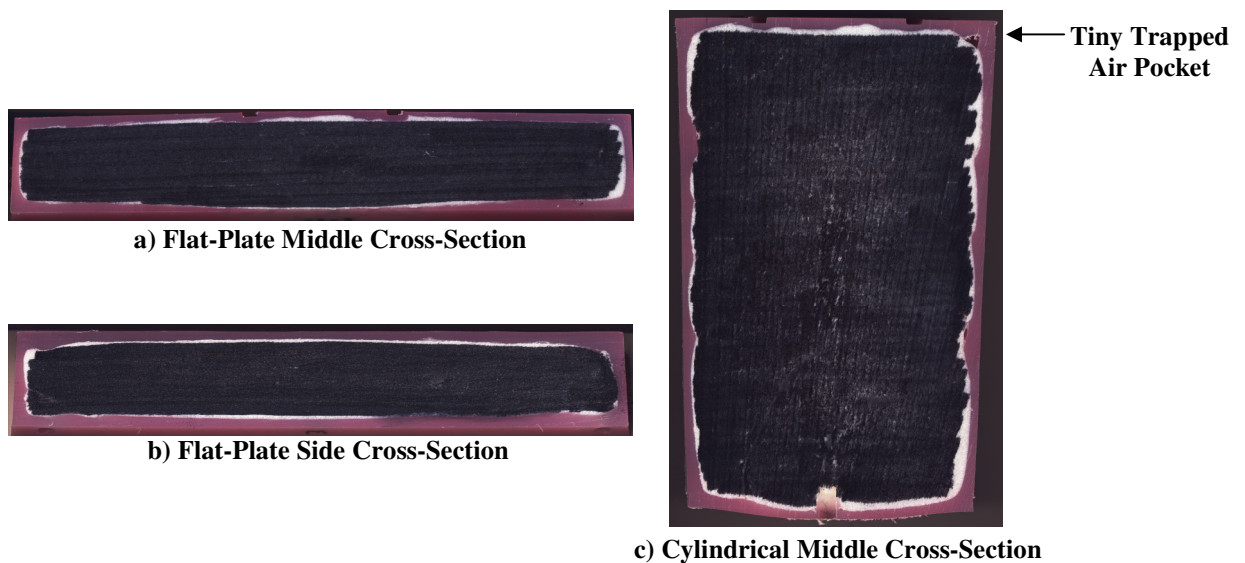


Figure 5.19: Typical Mold Filling Result of Both Molds

Even though fully filled moldings could be achieved for both molds, the cylindrical mold experienced more cases on average of having tiny trapped air pockets between the skin and foam as viewed in Figure 5.19 (c). It was believed that the cause of this was due to

sagging of the molten skin that appeared more predominant in the cylindrical molding potentially due to its longer required uni-axial filling time compared to the flat-plate mold. The sagging effect was also observed less at higher melt temperatures of the foaming compound. This could mean that when filling, the foam was indeed pushing the skin, where at higher melt temperatures the foaming compound would have a lower melt strength causing less disturbance of the skin. A potential solution to prevent this would be to increase the melt strength of the skin, by either heating it at lower temperatures, or to cool it before foam filling to increase its melt strength. This, however, could have an effect on the skin/foam adhesion quality if the skin cools too much before the foam can adhere to it.

The flat-plate mold, despite creating fully filled moldings with every experiment, did experience skin thinning at the bottom of the mold adjacent to the mold interface opening, as pictured in Figure 5.19 (a). This result was observed more as the melt temperature in creating the foam was reduced, as mentioned previously, where the resulting increased melt strength made it easier for the foam to push the skin aside during filling. The amount of thinning was reduced from moldings achieved using the previous RRFM experiments as the screw rotation speed was reduced slightly. A potential solution to prevent skin thinning altogether would be to further reduce filling screw speed, thus having to increase melt temperature to ensure activation of the CBA decomposition. This would, however, increase the time to fill the mold as well as the total cycle time.

In performing numerous experiments with RRFM using two different mold shapes it was apparent that the shape of the mold has a great deal of effect on the achievable molding quality in terms of filling and foam structure. With this information, future mold shapes can be designed with minimal modifications by utilizing the knowledge gained throughout these experiments.

Effect of Mold Interface and Secondary Processing in RRFM: Use of the slightly modified final insulated mold interface for both molds proved that a successful clean opening of the molten non-foamable skin layer could be achieved to allow for the newly foaming compound to be filled into the mold. It was also observed that during filling the molten skin remaining on the interface did not endure excessive cooling due to the relatively quick filling times associated with both molds. Upon completion of filling

and foam expansion, the skin on the mold interface appeared to successfully adhere to the newly created foam with little to no gaps between the skin and foam. This result is similar to the adhesion obtained with the previous mold interface, as presented in Figure 5.20.



Figure 5.20: Typical Mold Interface Result

If, however, the filling time was altered as part of a future solution to increase foam quality, as mentioned previously, additional heating while the interface was detached from the mold may be considered to prevent the possibility of further cooling.

Following the molding process, as previously described, plastic welding can be used to completely fill in the channel created by the mold interface, as depicted in Figure 5.21. This secondary processing can be desired to either eliminate the channel, or to ensure the foam is fully encapsulated if foam intrusion were observed due to a mishap in closing the mold after filling.



Figure 5.21: Sample PE Weld to Fill Mold Interface Channel

To determine if this welding process did in fact assist in creating a fully encapsulated integral-skin outer layer, a scanned micrograph was taken of a welded interface molding and is presented in Figure 5.22.

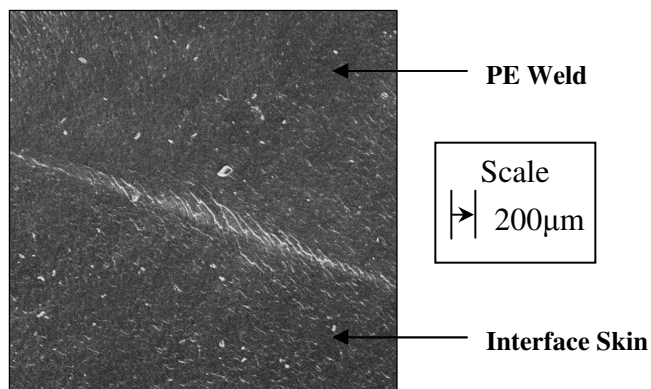


Figure 5.22: Scanned Picture of Sample PE Weld in Mold Interface Channel (50x Magnification)

The weld successfully adhered to the interface skin with the only evidence of its existence being a slight jagged line, as illustrated in Figure 5.22. Therefore, by utilizing this process to fill in the mold interface channel and any remaining vent holes could allow a molding of the RRFM process to be wholly encapsulated by a non-foamed PE skin layer.

5.6.2 Quantitative Quality Analysis

Further analysis was performed to determine the quality of the internal foam structures created by each resin and each mold by characterizing the foam in terms of foam density, average cell size and cell population density.

Foam Density in RRFM: Foam density was determined for all experimental results previously discussed in Section 5.61, with the results listed in Table 5.11.

Table 5.11: Foam Density Results for Final RRFM Experiments

Mold	Melt Temperature (°C)	VER	Material	Foam Density (g/cm ³)
Cylindrical	130	3	LLDPE	0.306
			HDPE	0.273
		6	LLDPE	0.150
			HDPE	0.175
	LLDPE		0.155	
	HDPE		0.162	
	135	6	LLDPE	0.142
			HDPE	0.184
140		6	LLDPE	0.142
			HDPE	0.184
Flat-Plate	130	3	LLDPE	0.244
			HDPE	0.297
		6	LLDPE	0.141
			HDPE	0.169
	LLDPE		0.146	
	HDPE		0.165	
	135	6	LLDPE	0.122
			HDPE	0.175
140		6	LLDPE	0.122
			HDPE	0.175

Foam densities were compared in Figure 5.23 for what appeared to be the best achieved samples for both molds that occurred at a melt temperature of 130 °C to determine the effect of mold shape.

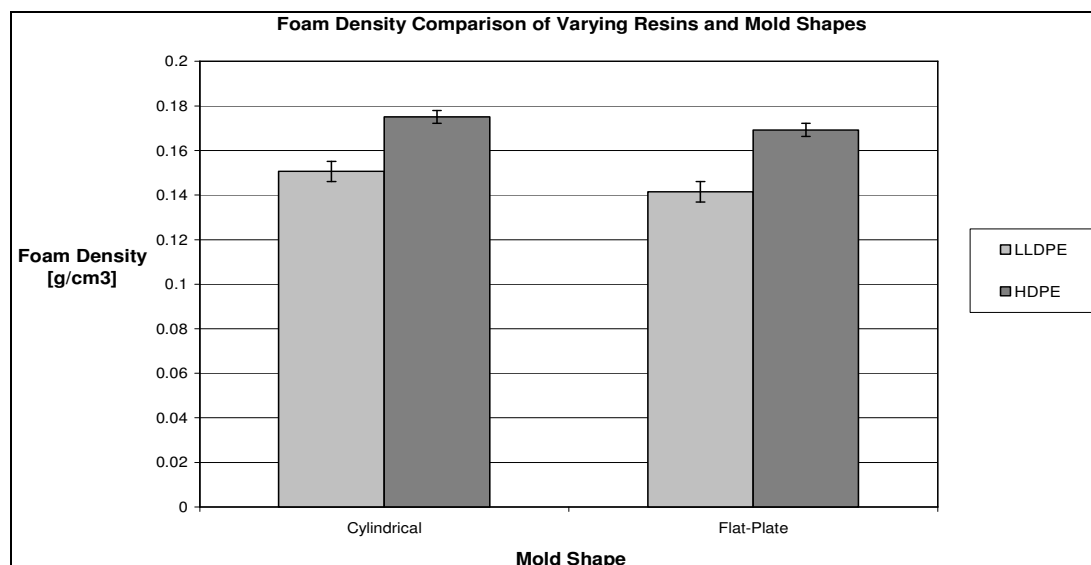


Figure 5.23: Foam Density Comparison Varying Resins and Mold Shapes @ 130°C

Comparing these results, the HDPE resin featured a higher foam density justified by the higher density of this resin compared to LLDPE. In terms of mold shape, there appeared to be no drastic difference in foam density apart from being lower for the flat-plate mold. This result could be due to the fact that more cells spaced closer together were observed in the micrographs of the flat-plate moldings compared to the cylindrical moldings.

Foam densities were also compared to determine the influence of VER of the moldings with both molds, the results of which are presented in Figure 5.24.

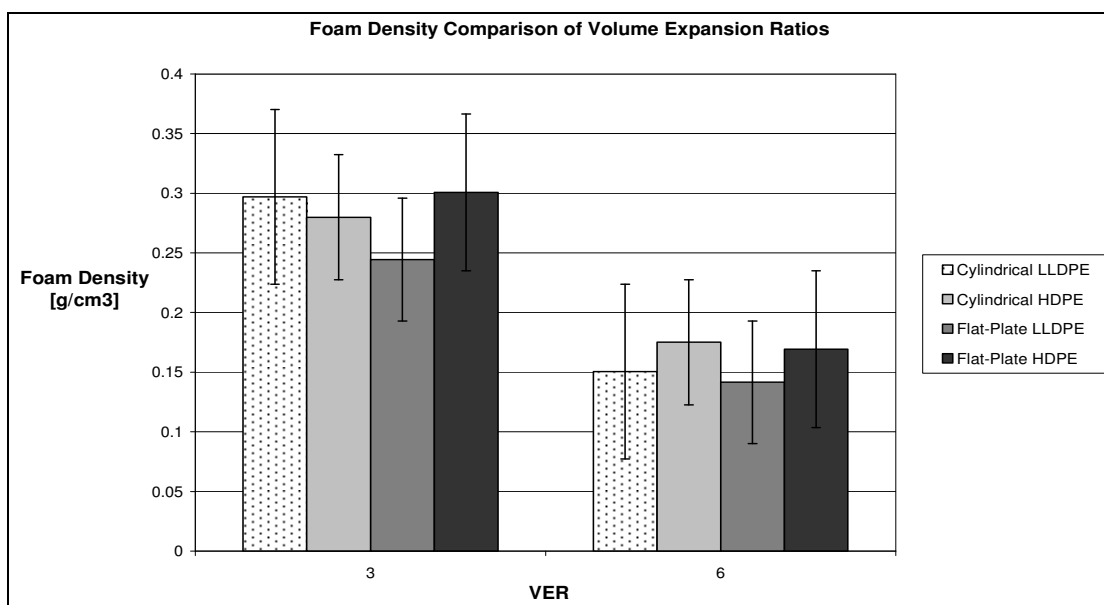


Figure 5.24: Foam Density Comparison Volume Expansion Ratios @ 130°C

Clearly illustrated above is that a higher foam density exists for the 3 VER. This can be contributed to the fact that less CBA and more resin were used, where fewer cells spaced further away result in the foam structure thus increasing the foam density.

Cell Size Analysis in RRFM: Using micrographs of moldings (Figures 5.13 to 5.18), average cell size and cell population density were determined to quantify the results determined from the visual quality analysis of the moldings in Section 5.61. The results of this analysis are listed in Table 5.12.

Table 5.12: Average Cell Size Results for Final RRFM Experiments

Mold	Melt Temperature (°C)	VER	Material	Average Cell Size (µm)
Cylindrical	130	3	LLDPE	279.24
			HDPE	266.25
		6	LLDPE	216.59
			HDPE	227.91
	135		LLDPE	255.75
			HDPE	279.20
	140	LLDPE	286.80	
		HDPE	284.98	
Flat-Plate	130	3	LLDPE	257.47
			HDPE	251.44
		6	LLDPE	212.70
			HDPE	226.31
	135		LLDPE	254.22
			HDPE	272.71
	140	LLDPE	282.42	
		HDPE	284.66	

From these results, it appeared that the average cell size decreased with decreasing melt temperature, thus resulting in the best moldings that occurred at a melt temperature of 130 °C being used for the comparative cell analysis. The resulting average cell size comparison to determine the effect of mold shape is presented in Figure 5.25.

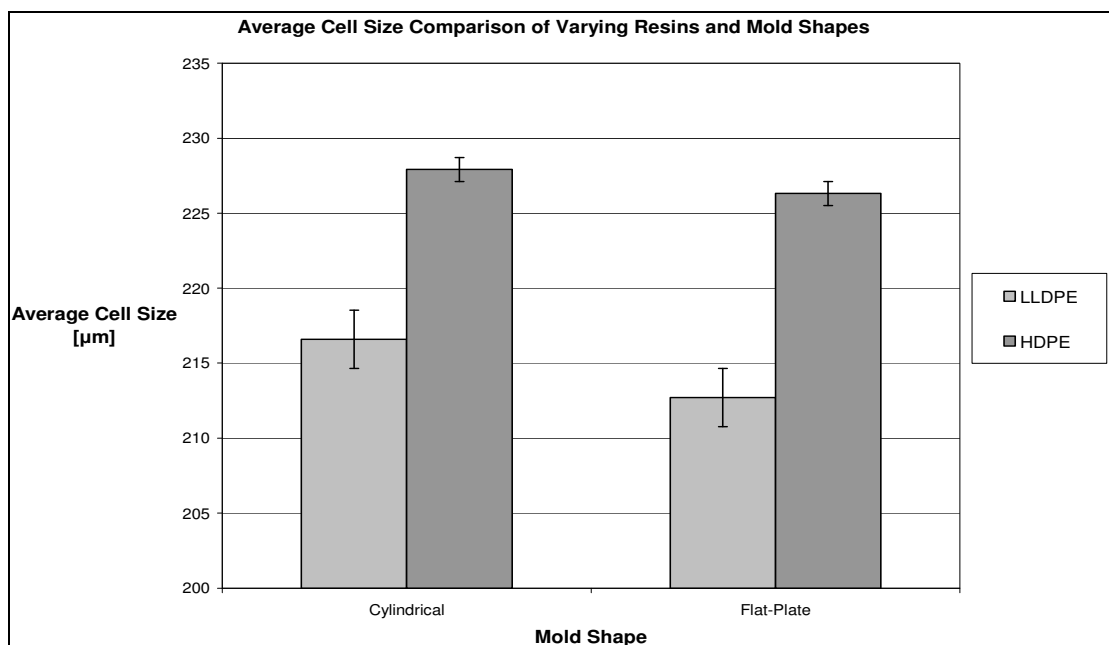


Figure 5.25: Average Cell Size Comparison Varying Resins and Mold Shapes @ 130°C

As expected, this graph shows that LLDPE was able to produce finer-celled foams for both molds. In addition, with the flat-plate mold both resins showed a superior average cell size compared to those created with the cylindrical mold.

The corresponding cell population density results are listed in Table 5.13.

Table 5.13: Cell Population Density Results of Final RRFM Experiments

Mold	Melt Temperature (°C)	VER	Material	Cell Population Density (μm)
Cylindrical	130	3	LLDPE	1.75E+05
			HDPE	2.02E+05
		6	LLDPE	9.44E+05
			HDPE	7.49E+05
	135	6	LLDPE	7.20E+05
			HDPE	4.43E+05
140	6	LLDPE	4.05E+05	
		HDPE	4.18E+05	
Flat-Plate	130	3	LLDPE	2.26E+05
			HDPE	2.40E+05
		6	LLDPE	9.92E+05
			HDPE	8.24E+05
	135	6	LLDPE	5.81E+05
			HDPE	4.71E+05
	140	6	LLDPE	4.42E+05
			HDPE	3.32E+05

Similarly, from these results it appeared that the cell population density increased with decreasing melt temperature, further illustrating that the best moldings occurred at a melt temperature of 130 °C. The resulting cell population density comparison to determine the effect of mold shape is presented in Figure 5.26.

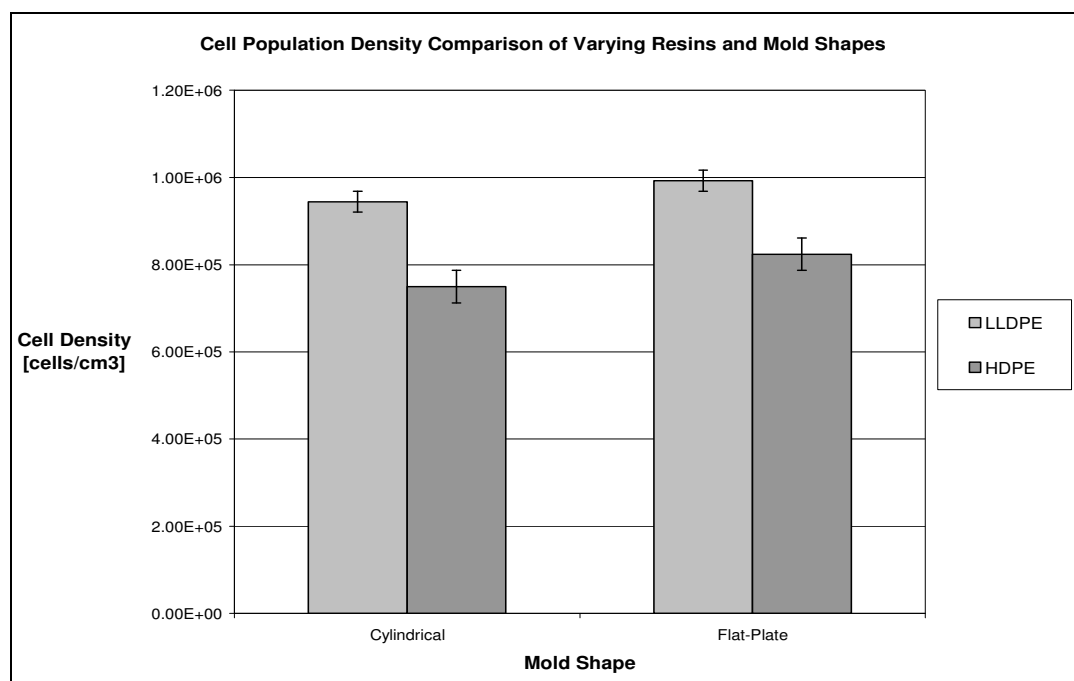


Figure 5.26: Cell Population Density Comparison Varying Resins and Mold Shapes @ 130°C

This graph further indicated the superiority of LLDPE and use of the flat-plate mold for producing higher quality foams as evidenced by the increased cell population densities.

Average cell size analysis was also performed to compare the influence of varying VER values, the results of which are presented in Figure 5.27.

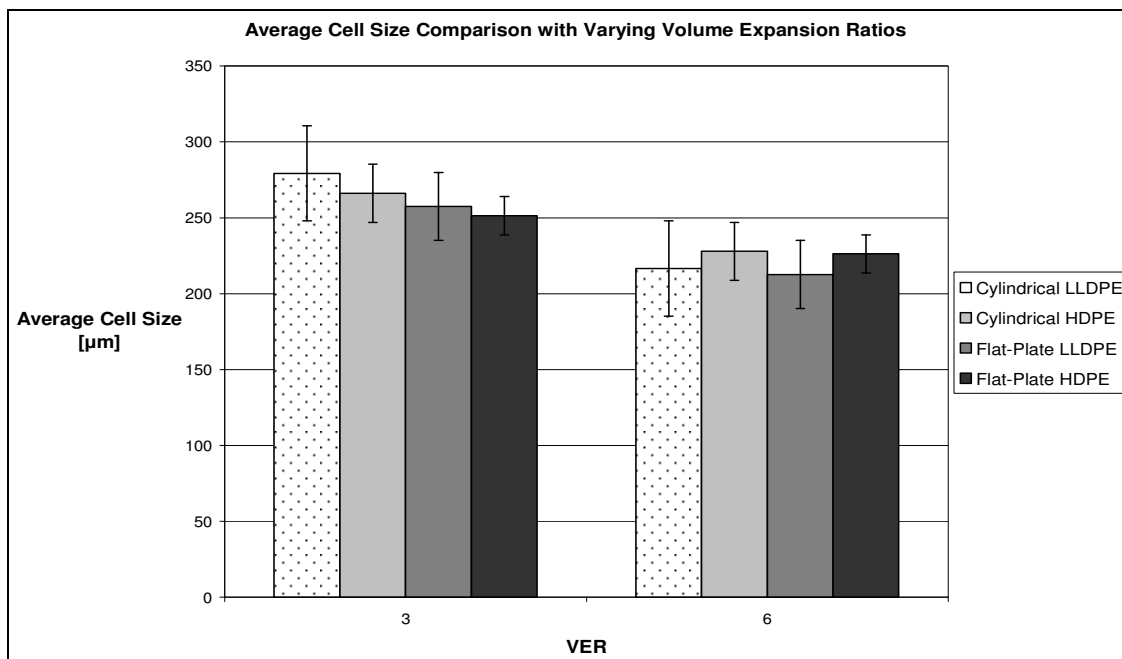


Figure 5.27: Average Cell Size Comparison Varying Volume Expansion Ratios @ 130°C

As expected, these results illustrated that increasing the VER decreased the average cell size of the foam. The accompanying cell population density results are presented in Figure 5.28.

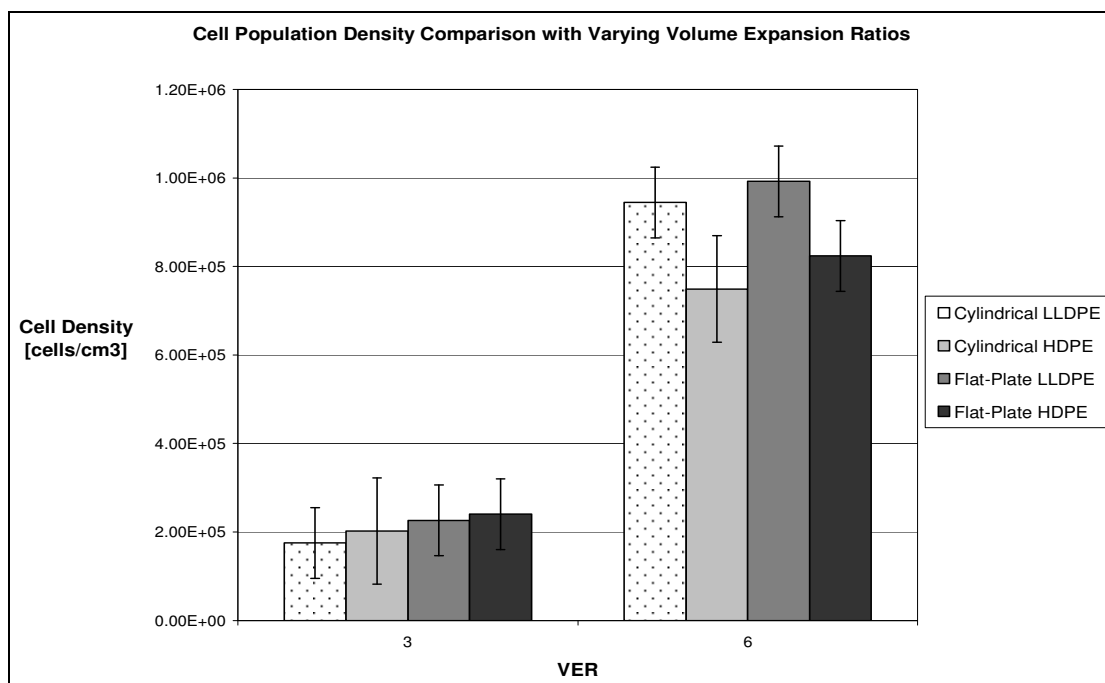


Figure 5.28: Cell Population Density Varying Volume Expansion Ratios @ 130°C

Similar to the previous graph, these results further indicated that better quality foams were achieved with increasing the VER evidenced by the increased cell population densities.

In summation, comparing these results with those formerly obtained using the experimental results of various design iterations in creating the final RRFM process it has now been shown that there was an even greater improvement in foam quality both visually and on a cellular level.

5.7 Final Process Comparison Analysis

The principal objective of the creation of this novel process was to reduce the overall heating cycle time, thus reducing the total cycle time, in creating PE integral-skin foam core moldings. Therefore, it was imperative at this stage that the total cycle time for all process iterations be compared to a current comparable process. The most relevant comparable process being conventional RFM where single-charge RFM is seen as the most effective means of producing integral-skin foamed core moldings compared to multi-charge RFM.

A representation of the approximate timelines of the process iterations created within this research, compared to single-charge RFM is presented in Figure 5.29.

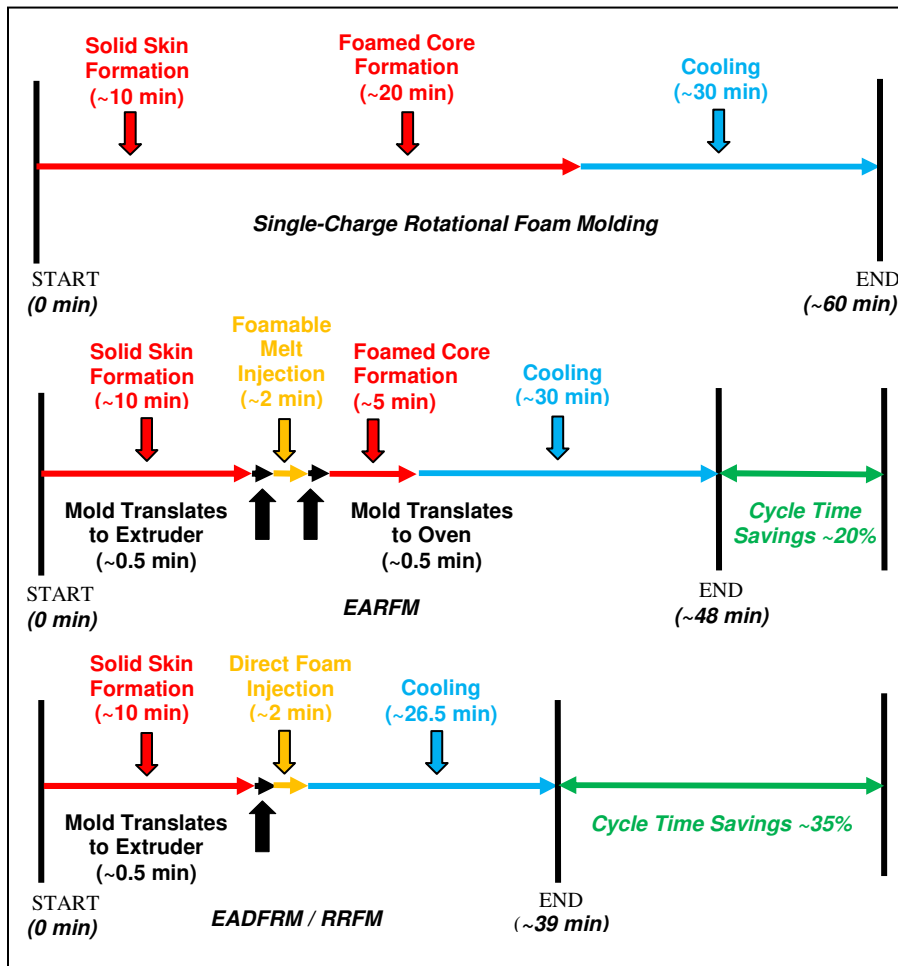


Figure 5.29: Processing Cycle Timeline Comparisons [64]

The Extrusion-Assisted Rotational Foam Molding (EARFM) process first offered a chance to reduce the lengthy heating cycle associated with single-charge RFM. This was accomplished by eliminating pelletizing when creating the foamable compound, and instead offering direct injection of the foamable melt into the mold. It is reasonable to say that the resulting total cycle time reduction of this process, compared to the single-charge method, was approximately 20%. In terms of part quality, EARFM offered a comparable skin/foam interface quality to single-charge moldings, despite the venting and filling problems that occurred. The labour and material set-up involved in this process, compared to the single-charge method, would be the same as essentially the same processing steps are occurring only at different stages during the two processes.

With the somewhat travel inefficiency of the mold and quality issues of EARFM, this gave way for further cycle time reductions through process improvements. The result

of this was the introduction of the Extrusion-Assisted Direct Foaming Rotational Molding (EADFRM) process. This second process iteration not only eliminated the need for the mold to be heated in the oven a second time, but also decreased the travel of the mold, further reducing the total cycle time. The resulting total cycle time reduction associated with this process was approximately 35%, compared to single-charge RFM [64]. The achieved part quality in terms of the skin/foam interface remained the same, but with improved foam morphologies that were not at the same level that could be achieved with single-charge moldings. The labour involved in this second process iteration, compared to the single-charge method, would be minutely increased with use of the mold interface, with material set-up remaining the same.

The final process iteration, Rapid Rotational Foam Molding (RRFM), shared the same processing steps as the previous process (EADFRM) resulting in the same total cycle time reduction, required labour and material set-up. This was due to the design of this process being focused on quality improvement through minor component modifications. The final part quality again featured a comparable skin/foam interface with greatly improved foam morphologies that could be on par with those achieved through the single-charge process.

If plastic welding is utilized within the RRFM process, depending on the way in which it is implemented i.e., manually or in an automated fashion, it would not require an excessive amount of time. For example during experimentation, plastic welding took less than a minute to completely fill in the mold interface channel. From this, it could be concluded that even with use of plastic welding, the final RRFM process offers an acceptable total cycle time reduction that could be translated into a noteworthy energy savings.

CHAPTER 6

CONCLUSIONS AND RECOMMENDATIONS FOR FUTURE WORK

6.1 Concluding Remarks

In light of current industry trends of implementing lower cost more efficient processes, Rapid Rotational Foam Molding (RRFM) was created for the specific purpose of reducing the heating cycle time and energy consumption for producing polyethylene (PE) integral-skin foam core moldings. The novel portion of this newly designed and patent pending process was that the actual creation of the foam was totally decoupled from the subsequent pellet shaping step, which resulted in dramatic improvements in terms of reducing the overall heating cycle and total energy consumption. Additionally, as seen throughout experimental analysis of this research the achieved moldings were shown to have the capability of producing an excellent skin/foam interface with a relatively high quality foam core using two different mold designs.

Higher quality foams were found to be achieved with the lowest possible extrusion temperatures of the chosen lab-scale extruder using linear low density PE (LLDPE), potentially due to its characteristic lower crystallization temperature compared to high density PE (HDPE). In terms of mold shape, it was determined that the flat-plate mold with its reduced cavity spread over a larger surface area was less influenced by the insulating capabilities of the created foam structure resulting in reduced cell coalescence and improved foam morphologies compared to the cylindrical mold.

All of these results were achieved through experiments performed on the custom-built lab-scale experimental setup that in addition to the abovementioned process advantages requires little to no maintenance that could make it attractive to industry molders potentially warranting a future industrial scale-up.

6.2 Summary of Contributions

By completing this research, a process named Extrusion-Assisted Rotational Foam Molding (EARFM) that was proposed to reduce the heating cycle of producing integral-skin foam core moldings was translated into a lab-scale experimental setup. The initial claims associated with EARFM were experimentally investigated warranting a great deal of process and component modifications that created several design iterations known as Extrusion-Assisted Direct Foaming Rotational Molding (EADFRM) and finally RRFM to ensure acceptable quality moldings could be achieved. The finally presented process was experimentally verified with two mold shapes to make certain that the process was capable of producing improved and acceptable quality moldings.

6.3 Recommendations for Future Work

In hopes that this process will one day be utilized for industrial purposes it is recommended that use of additional PE and other commercially common resins be investigated. Furthermore, introducing additional and potentially more complex mold shapes will further aid in increasing the flexibility of the process.

The process of foam filling may benefit from the investigation of an elongated nozzle that can reach the back of the mold and be retracted during filling. Other nozzle profiles can be investigated to aid in this process and potentially improve resulting foam quality, including one that fills perpendicular to the original flow of the extruder.

In terms of the extruder, utilizing a twin screw extruder would improve mixing and particle dispersion of the foamable formulations. This could greatly improve the resulting foam quality that could be achieved.

Increased temperature monitoring within the mold that is not affected by bi-axial rotation, and with the addition of more advanced venting technologies such as a mechanically or electrically operated venting system that is unable to clog would allow for further process optimization to be precisely controlled.

Given some of the minor quality issues in the achieved moldings of the final RRFM process there remains the potential for slight quality improvement. Whereas improved skin uniformity may be achieved with an investigation of different extruder

nozzle profiles for the flat-plate mold, and with further optimization of non-foamable skin heating and accompanying foaming compound temperatures in a way that does not adversely alter molding quality for the cylindrical mold.

REFERENCES

- [1] J.L. Thorne. *Thermoplastic Foams*. Sherwood Technologies, Inc., Hinkley, Ohio: Sherwood Publishers, 1996.
- [2] D. Klemptner and K.C. Frisch. *Handbook of Polymeric Foams and Foam Technology*. New York: Hanser Publishers Inc., 1991.
- [3] A.J. Peacock. *Handbook of Polyethylene: Structures, Properties, and Applications*. New York: Marcel Dekker, Inc., 2000.
- [4] A. Mariacher. "Downgauging Boosts Resin's Popularity." *Modern Plastics Worldwide: World Encyclopedia 2008*. pp. 72-73, 2008.
- [5] R.J. Crawford. *Rotational Moulding of Plastics*, Second Edition. Toronto: John Wiley & Sons Inc., 1996.
- [6] G.L. Beall. *Rotational Molding: Design, Materials, Tooling, and Processing*. Cincinnati: Henser/Gardner Publications, Inc., 1998.
- [7] P. Mapleston. "Rotational Moulding: Rotomoulders Take Control." *Plastics Engineering*, pp. 10-16, Nov. 2008.
- [8] R. Pop-Iliev and C.B. Park. "Rotofeasibility of Polyolefin Resins." *SPE ANTEC*, 2004, pp. 855-859.
- [9] M. Tolinski. "Foams Seek Sustainability." *Plastics Engineering*, pp. 6-8, Jan. 2009.
- [10] K. Christian and R. Pop-Iliev. "Extrusion-Assisted Rotational Molding of Fine-Celled Polyethylene Foams." *SPE FOAMS Conference Proceedings*, Sept. 2008.
- [11] Persico S.p.A, "Equipments and Services for Rotational Moulding Technology." Internet: <http://www.persico.com/INGLESE/ROTATIONAL.pdf>, [Jan. 26, 2009].
- [12] T. Deligio. "Rotomolding turns the tables." *Modern Plastics Worldwide*. pp. 21-22, Nov. 2008.
- [13] R.G. Griskey. *Polymer Process Engineering*. New York: Chapman & Hall, 1995.
- [14] R.J. Crawford. *Plastics Engineering*, Third Edition. Boston: Butterworth Heinmann, 1998.

- [15] R.J. Crawford. *Rotational Moulding of Plastics*, Second Edition. Toronto: John Wiley and Sons Inc., 1996.
- [16] T.A. Osswald and G. Menges. *Materials Science of Polymers for Engineers*, Second Edition. Cincinnati: Hanser/Gardner Publications, Inc., 2003.
- [17] R. Pop-Iliev, G. Rizvi, and C.B. Park, "The Importance of Timely Polymer Sintering while Processing Polypropylene Foams in Rotational Molding." *Polymer Science and Engineering*, Vol. 43, No. 1, pp. 40-54, 2003.
- [18] P. Hoppe, H-W. Paffrath, E. Weinbrenner, and K. Breer. "A Method of Centrifugally Molding Cellular Plastics." U.S. Patent 3,052,927, Sept. 1962.
- [19] F.J. Rielly, and H. Nungesser. "Rotationally Molding Method For Forming Multilayered Articles." U.S. Patent 3,542,912, Nov. 1970.
- [20] K. Hosoda, N. Shiina, Y. Kadowaki, M. Hashimoto, N. Suzuki, and T. Sugita. "Method for Producing a Composite Foamed Article." U.S. Patent 3,814,778, June 1974.
- [21] S.G. Lammers. "Method of Rotational Molding." U.S. Patent 3,984,511, Oct. 1976.
- [22] H. Mori, E. Adachi and Y. Noguchi. "Method of Producing Composite Foamed Shaped Articles from Thermoplastic Resins." U.S. Patent 3,962,390, June 1976.
- [23] C.B. Park, G. Liu, F. Liu, R. Pop-Iliev, S. D'Uva, and B. Zhang. "Production of Foamed Low-Density Polypropylene by Rotational Molding." U.S. Patent 6,103,153, Aug. 2000.
- [24] J. Slapnik. "Plastic Process." U.S. Patent 2,989,783, June 1961.
- [25] K. Duffy. "Method for Forming Expanded Foam Rotomolded Products." U.S. Patent 4,952,350, Aug. 1990.
- [26] G.E. Carrow and R.L. Rees. "Rotationally Molding a Multi-layered Article." U.S. Patent 3,976,821, Aug. 1976.
- [27] R. Pop-Iliev. "Processing of Fine-Cell Polypropylene Foams in Compounding-Based Rotational Foam Molding." M.A.Sc Thesis, University of Toronto, Canada, 1999.

- [28] R. Pop-Iliev, G. Liu, F. Liu, C.B. Park, A. D'Uva, and J.A. Lefas. "Comparison of Dry Blending-Based and Melt-Compounding-Based Rotomolding Techniques for LLDPE Foams." *SPE ANTEC*, 1999, pp. 1457-1467.
- [29] J. Vlacholoulos. *Chemical Engineering 4X03/6X03: Introduction to Plastics Processing*, Hamilton: McMaster University Custom Publishing Solutions, 2007.
- [30] M.E. Reedy. "Chemical Foaming Agents Improve Performance and Productivity." Internet: <http://www.caropresoassociates.com/paper2.html>, [Oct. 17, 2007].
- [31] A.B. Strong. *Plastics: Materials and Processing*, Third Edition. New Jersey: Pearson Education Inc., 2006.
- [32] S.J. Liu and C.H. Tsai. "An Experimental Study of Foamed Polyethylene in Rotational Molding." *SPE ANTEC*, 1998, pp. 1161-1165.
- [33] A. Kumar and R.K. Gupta. *Fundamentals of Polymer Engineering*, Second Editions Revised and Expanded. New York: Marcel Dekker, Inc., 2003.
- [34] C.A. Harper. *Handbook of Plastics Technologies: The Complete Guide to Properties and Performance*. Toronto: McGraw-Hill, 2006.
- [35] M.J. Schoning, M. Ali, B. Pahlavanpour, and M. Eklund. "Composition Measurement." Internet: <http://www.engnetbase.com>, 2000 [Oct. 17, 2007].
- [36] W.D. Callister Jr. *Materials Science and Engineering an Introduction*, Sixth Edition. Hoboken, NJ: John Wiley & Sons, Inc., 2003.
- [37] H. K. D. H. Bhadeshia. "Thermal Analysis Techniques." Internet: <http://www.msm.cam.ac.uk/phase-trans/2002/>, 2002 [Oct. 17, 2007].
- [38] R.L. Danley. "Heat Flux Differential Scanning Calorimeter Sensor." U.S. Patent 6,431,747, Aug, 2002.
- [39] Equistar Chemical Company. "Polyolefin Flow Characteristics: More than Just Melt Index or Melt Flow Rate." Internet: www.lyondellbasell.com/techlit/techlit/Tech%20Topics/General/Flow%20Characteristics.pdf, [Oct. 17, 2007].
- [40] R. Pop-Iliev, G. Rizvi, and C.B. Park. "Formulating Foamable Resins for Achieving a Given Volume Expansion Ratio in Rotational Foam Molding." *SPE ANTEC*, 2001, pp. 1598-1613.
- [41] N. Mills. *Polymer Foams Handbook: Engineering and Biomechanics Applications and Design Guide*. New York: Butterworth-Heinemann, 2007.

- [42] D. Xu, R. Pop-Iliev, C.B. Park, and R.G. Fenton. "Fundamental Study of CBA-blown Bubble Growth and Collapse Under Atmospheric Pressure." *Journal of Cellular Plastics*, Vol. 41, No. 6, pp. 519-538, 2005.
- [43] C.I. Chung and R.A. Barr. "Energy Efficient Extruder Screw." U.S. Patent 4,405,239, 1983.
- [44] S.K. Goyal. "Influence of Polymer Structure on Melt Strength Behavior of PE Resins." *Plastics Engineering*, Vol. 51, No. 2, 1995.
- [45] P.G. Ranky. *Concurrent/Simultaneous Engineering (Methods, Tools and Case Studies)*, Second Edition. Hoboken, NJ: John Wiley & Sons, Inc., 2004.
- [46] D.G. Ullman. *The Mechanical Design Process*, Third Edition. Toronto: McGraw-Hill, 2003.
- [47] *ASTM Standard D 1622-08*, West Conshohocken, PA: ASTM International, 2008.
- [48] R. Pop-Iliev, K-H Lee, and C.B. Park. "Manufacture of Integral Skin PP Foam Composites in Rotational Molding." *Journal of Cellular Plastics*, Vol. 42, No. 2, pp. 139-152, 2006.
- [49] R. Pop-Iliev. "Generating Alternative Time and Energy Saving Processing Concepts for Rotational Foam Molding." *SPE ANTEC*, 2007, pp. 2732-2736.
- [50] G. Gogos. "Bubble Removal in Rotational Molding." *Polymer Engineering and Science*, Vol. 44, No. 2, pp. 388-394, 2004.
- [51] G.W.G McDowell, M.C. Cramez, E.M.A Harkin-Jones, W. McMinn, and R.J. Crawford. "The Effect of Cooling Rate on Rotationally Molded Parts." *SPE ANTEC*, pp. 1226-1230, 2003.
- [52] Z. Dennis. "Bi-Axial Extrusion Assisted Rotational Foam Molding: Design And Development Of A Mold Interface Mechanism." Undergraduate Thesis, University of Ontario Institute of Technology, Canada, 2007.
- [53] B. Fagan. "Bi-Axial Extrusion-Assisted Rotational Foam Molding: Design and Development of a Mold and Oven." Undergraduate Thesis, University of Ontario Institute of Technology, Canada, 2007.
- [54] M. Macleod. "Design And Development Of A Selectable Uni/Bi-Axial Mold Rotating Device Which Permits Interface With An Extruder For Extrusion

- Assisted Rotational Foam Molding.” Undergraduate Thesis, University of Ontario Institute of Technology, Canada, 2007.
- [55] K. Lee, R. Pop-Iliev, and C.B. Park. “Manufacture of Integral Skin PP Foam Composites in Rotational Molding.” *Journal of Cellular Plastics*, Vol. 42, No. 2, pp. 139-152, 2006.
- [56] Equistar Chemicals. *Microthene® - MP643662 Data Sheet*. 2008.
- [57] Equistar Chemicals. *Microthene® - MP652762 Data Sheets*. 2008.
- [58] Compton Corporation. “Celogen® OT for Plastics.” Internet: http://www.cromptoncorp.com/servlet/ContentServer?pagename=Crompton/ck_prod/product&c=ck_prod&cid=1014147761353&countryid=990049202907&invoke_r=results&p=985964216258, [Oct. 6, 2008].
- [59] L.C. Thomas. *Characterization of Melting Phenomena in Linear Low Density Polyethylene by Modulated DSC™ (TA-227)*. New Castle, DE: TA Instruments, Inc., 2006.
- [60] R.L. Blaine. *Isothermal Crystallization of Polypropylene by Differential Scanning Calorimetry*. American Laboratory, 2002.
- [61] M. Kelsey, and J. Foreman. “Temperature Measurements in TGA, Limitations of Test Methods for Plastics.” *ASTM STP 1369*, J.S. Peraro, Ed., West Conshohocken, PA: American Society for Testing and Materials, 2000.
- [62] S. Hunt. “RE: Question Regarding TGA Q 50” Personal Email (Dec 14, 2007).
- [63] Drader Manufacturing. “Plastic Welding Equipment & Supplies: Drader Injectiweld.” Internet: <http://www.drader.com/drader/injectiweld/about.html>, [Mar. 5, 2009].
- [64] K. Christian, E. Abdalla, G. Eberle and R. Pop-Iliev. “Extrusion-Assisted Direct-Foaming Rotational Molding Process”, *SPE ANTEC*, 2009, pp. 1956-1960.

APPENDIX A

QFD HOUSE OF QUALITY

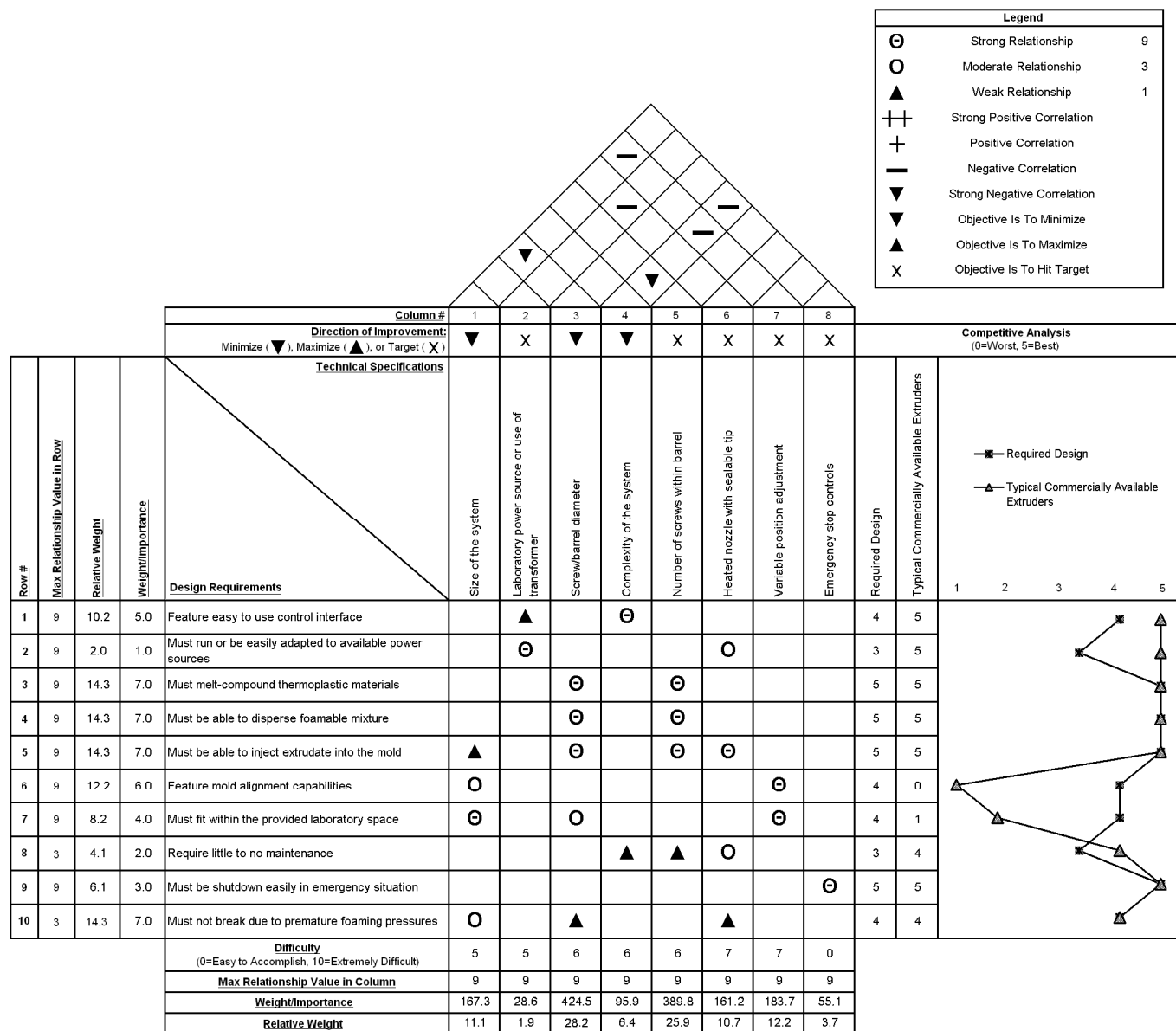


Figure A1: Extruder House of Quality

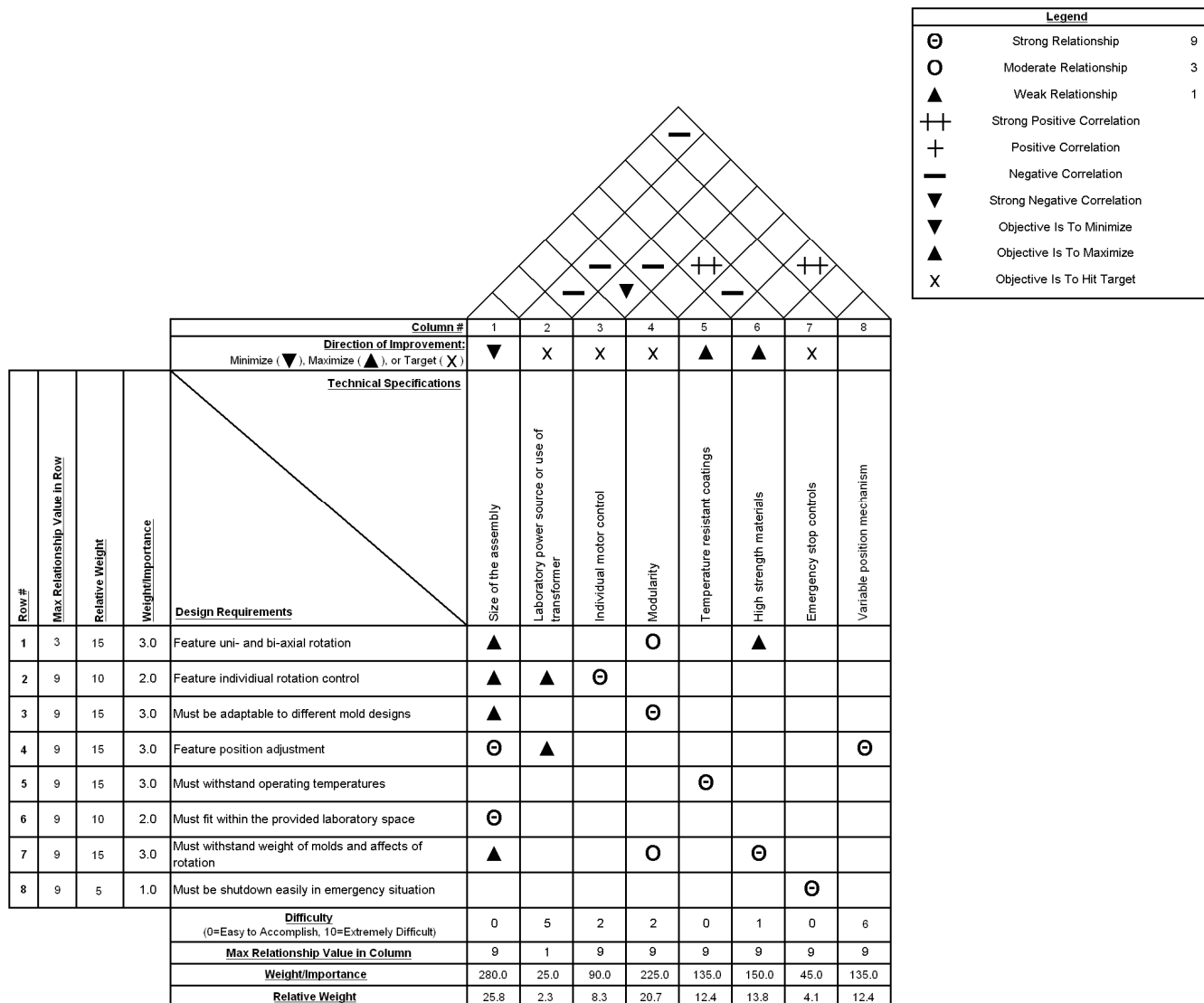


Figure A3: Mold Rotational Mechanism House of Quality

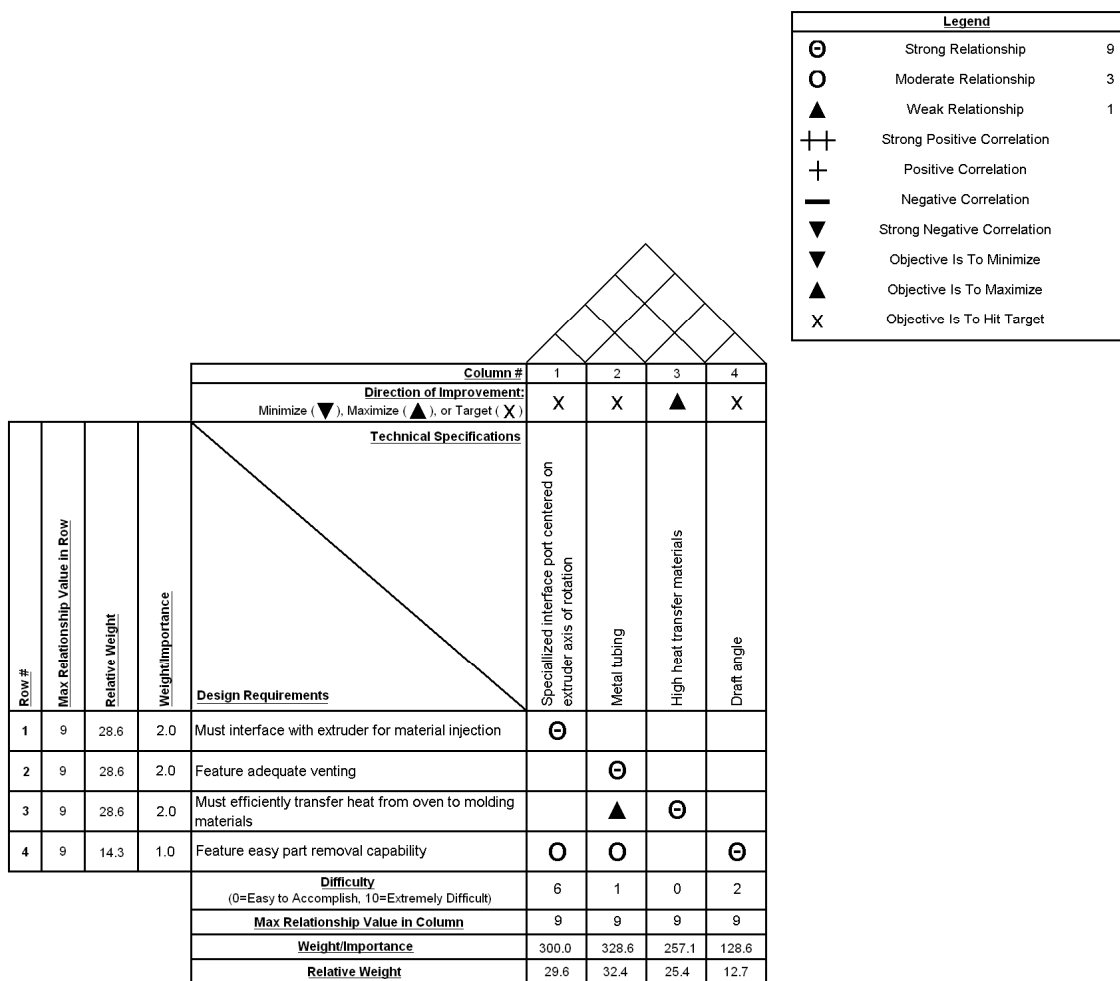


Figure A4: Mold House of Quality

APPENDIX B

MATERIAL DATA SHEETS

Microthene®

MP643662

Linear Low Density Polyethylene Powder

Rotational Molding Grade

Melt Index 3.6 Density 0.9395

Applications

MICROTHENE MP643662 is a linear medium density polyethylene powder for rotomolding a variety of objects, including drums, agricultural and chemical storage containers, playground equipment and municipal trash containers. MP643662 is a UV-stabilized, 35-mesh powder and is also available in pellet form as PETROTHENE® GA643662.

Regulatory Status

MP643662 meets the requirements of the Food and Drug Administration, 21CFR Section 177.1520. This regulation allows the use of this olefin polymer in "...articles or components of articles intended for use in contact with food..." Specific limitations or conditions of use may apply. Contact your Equistar sales representative for more information.

Processing Techniques

Specific recommendations for conditions under which MP643662 should be processed can be made only when the end use and type of processing equipment are known. For exact recommendations, please contact your Equistar sales representative.

Typical Properties

Property	Nominal Value	Units	ASTM Test Method	Sample
Melt Index	3.6	g/10 min.	ASTM D 1238	Pellets
Density	0.9395	g/cc	ASTM D 1505	Compression molded
ESCR, Cond. A, F ₅₀ , 100% Igepal®	<1,000	hrs	ASTM D 1693	Rotomolded*
10% Igepal®	480	hrs	ASTM D 1693	Rotomolded*
Flexural Modulus, 1 % Secant	110,000	psi	ASTM D 790	Rotomolded*
Tensile Strength @ Yield, 2"/min**	2,600	psi	ASTM D 638	Rotomolded*
Heat Distortion Temp. @ 66 psi	52	°C	ASTM D 648	Rotomolded
@ 264 psi*	40	°C	ASTM D 648	Rotomolded*
Low Temp. Impact, 1/8 " specimen	51	ft-lbs.	ARM STD	Rotomolded*
1/4 " specimen	140	ft-lbs.	{-40°F impact}	Rotomolded
Meets FDA Requirements	yes			
UV-stabilized	yes			

* Thickness of specimen 1/8".

** Type IV specimen.

® Igepal is a registered trademark of the Rhone-Poulenc Co., Inc.

The information on this document is, to our knowledge, true and accurate. However, since the particular uses and the actual conditions of use of our products are beyond our control, establishing satisfactory performance of our products for the intended application is the customer's sole responsibility. All uses of Equistar products and any written or oral information, suggestions or technical advice from Equistar are without warranty, express or implied, and are not an inducement to use any process or product in conflict with any patent.

Equistar materials are not designed or manufactured for use in implantation in the human body or in contact with internal body fluids or tissues. Equistar makes no representation, promise, express warranty or implied warranty concerning the suitability of these materials for use in implantation in the human body or in contact with internal body tissues or fluids.

More detailed safety and disposal information on our products is contained in the Material Safety Data Sheet (MSDS). All users of our products are urged to retain and use the MSDS. A MSDS is automatically distributed upon purchase/order execution. You may request an advance or replacement copy by calling our MSDS Hotline at 800.700.0946.

® Microthene and Petrothene are registered trademarks of Equistar Chemicals, LP.



Lyondell Chemical Company
1221 McKinney, Suite 700
P.O. Box 2583
Houston, Texas 77252-2583
800.615.8999
<http://www.lyondell.com>



Microthene®
MP652762
High Density Polyethylene Powder
Rotational Molding Grade
Melt Index 2.0 Density 0.942

Applications

MICROTHENE MP652762 is a hexene HDPE powder used mainly for rotationally molding large tank applications. MP652662 is a UV 8-stabilized, 35-mesh powder and is also available in pellet form as PETROTHENE® GA652762.

Regulatory Status

MP652762 meets the requirements of the Food and Drug Administration, 21CFR Section 177.1520. This regulation allows the use of this olefin polymer in "...articles or components of articles intended for use in contact with food..." Specific limitations or conditions of use may apply. Contact your Equistar sales representative for more information.

Processing Techniques

Specific recommendations for conditions under which MP652762 should be processed can be made only when the end use and type of processing equipment are known. For exact recommendations, please contact your Equistar sales representative.

Typical Properties

Property	Nominal Value	Units	ASTM Test Method	Sample
Melt Index (190/2.16)	2.0	g/10 min	D 1238	Pellets
Density	0.942	g/cc	D 1505	Compression molded
Melting Point	129	°C	D 3418	Rotomolded**
ESCR, Condition A, F ₅₀				
100% Igepal®, CO-630	720	hrs	D 1693	Rotomolded**
10% Igepal®, CO-630	48	hrs	D 1693	Rotomolded**
Flexural Modulus, 1% Secant	130,000	psi	D 790	Rotomolded**
Tensile Strength @ Yield, 2"/min*	3,220	psi	D 638	Rotomolded**
Tensile Elongation @ Yield	18	%	D 638	Rotomolded**
Heat Distortion Temperature @ 66 psi	67	°C	D 648	Rotomolded**
@ 264 psi	42	°C		
Low Temperature Impact			ARM STD	
1/8" specimen	80	ft-lbs	-40°F impact	Rotomolded**
1/4" specimen	190	ft-lbs	-40°F impact	Rotomolded
Meets FDA Requirements	yes			
UV 8-stabilized	yes			

* Thickness of specimen 1/8".

** Type IV specimen.

® Igepal is a registered trademark of the Rhone-Poulenc Co., Inc.

The information on this document is, to our knowledge, true and accurate. However, since the particular uses and the actual conditions of use of our products are beyond our control, establishing satisfactory performance of our products for the intended application is the customer's sole responsibility. All uses of Equistar products and any written or oral information, suggestions or technical advice from Equistar are without warranty, express or implied, and are not an inducement to use any process or product in conflict with any patent.

Equistar materials are not designed or manufactured for use in implantation in the human body or in contact with internal body fluids or tissues. Equistar makes no representation, promise, express warranty or implied warranty concerning the suitability of these materials for use in implantation in the human body or in contact with internal body tissues or fluids.

More detailed safety and disposal information on our products is contained in the Material Safety Data Sheet (MSDS). All users of our products are urged to retain and use the MSDS. A MSDS is automatically distributed upon purchase/order execution. You may request an advance or replacement copy by calling our MSDS Hotline at 800.700.0946.

® Microthene and Petrothene are registered trademarks of Equistar Chemicals, LP.



Lyondell Chemical Company
1221 McKinney, Suite 700
P.O. Box 2583
Houston, Texas 77252-2583
800.615.8999
<http://www.Lyondell.com>

PRODUCT

CELOGEN® OT for Plastics
Low-Temperature Chemical Foaming Agent

CELOGEN OT is a low-temperature foaming agent suitable for operating temperatures of 300-350°F (149-177°C). It is recommended for rubber, LDPE, EVA, and soft vinyl compounds. It generates a polymeric, non-polar residue that does not interfere with electrical properties in wire insulation applications. Process temperatures should not exceed 350°F (177°C) when using CELOGEN OT. Materials such as triethanolamine and urea are strong decomposition activators. Zinc oxide and similar materials provide moderate to weak activation. CELOGEN OT is oil-treated to reduce dustiness. It has three FDA sanctions for use in food-contact applications.

▪ **Product Description**

Chemical Composition:	p,p'-oxybis(benzenesulfonylhydrazide)
Appearance:	White to off-white powder
Decomposition Point:	320°F (160°C)
Gas Yield:	125 cc/g
Gas Composition:	Nitrogen, steam
Specific Gravity:	1.55
Bulk Density:	31 lbs./cu.ft. (496 kg/m ³)

▪ **Solubility**

Soluble with reaction in ketones; very soluble in DMSO and DMF; moderately soluble in ethanol and polyalkylene glycols; insoluble in benzene, ethylene dichloride and water.

▪ **Storage Stability**

Good under normal conditions.

▪ **Flammability**

This product will burn rapidly when ignited. It should be stored in a cool, dry place away from hot steam pipes, free flames, direct sunlight, and any source of static or spark.

Please consult the Celogen OT Material Safety Data Sheet for additional information.

Rev. 03/25/04

The information contained herein is correct to the best of our knowledge. Your attention is directed to the pertinent Material Safety Data Sheets for the products mentioned herein. All sales are subject to Crompton's standard terms and conditions of sale, copies of which are available upon request and which are part of Crompton's invoices and/or order acknowledgments. Except as expressly provided in Crompton's standard terms and conditions of sale, no warranty, express or implied, including warranty of merchantability or fitness for particular purpose, is made with respect to the products described herein. Nothing contained herein shall constitute permission or recommendation to practice any invention covered by a patent without a license from the owner of the patent.



Pigments & Additives Division

Product Data Sheet - Organic Pigments for Plastics

Graphtol Red 2BN

Edition 04/02/2008

Pigment Red 262

Chem. Group: Disazo Condensation
Product No.: 111429

C.I.-No: -

CAS No.: 79665-24-0

Application Profile

PO	PC	Fibers
●	●	
PVC ●	POM -	> PP ●
Rubber ●	PA -	> PET -
PS ●	PBT ○	> PA -
ABS ●	PUR ●	> PAN -

● recommended ○ limited suitability - not recommended

Physical & Chemical Properties

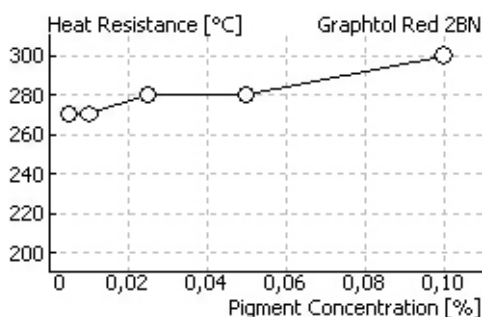
Density [g/cm ³]	1.42
Bulk Density [l/kg]	3.0
Average Particle Size [nm]	171
Alkali Resistance	5
Acid Resistance	5
Specific Surface [m ² /g]	60

Commentary

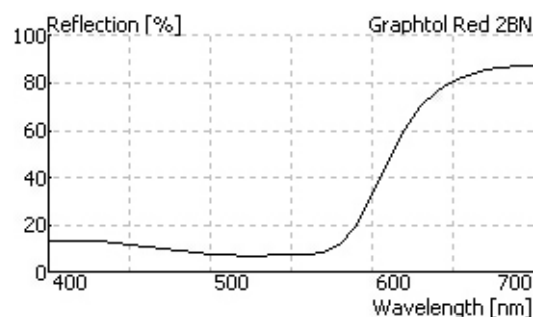
A bluish red pigment exhibiting high color strength and heat resistance. An economical pigment suitable for film, injection and blow moulding applications and fibres.

	PE	PP	PVC	PS	ABS	PC
SD 1/3 [g/kg]	1.2	1.2	4.0	1.2	1.2	1.3
Hue Angle [°]	3.1	5.7	5.4	4.5	4.4	9.8
Chroma	47.8	49.1	54.8	51.1	52.5	52.6
Lightfastness (Pure Shade)	7-8	7-8	7-8	6	6	7-8
Lightfastness (Reduction)	7	7-8	7-8	5-6	6	7
Heat Resistance [°C]	300	300	-	300	290	300
Weathering Fastness	3	-	-	-	-	-

Limiting Concentration in HDPE



Reflectance



Additional Technical Properties

Suitability for Low Warping Applications	-
Cable Sheathing	-
Fastness to Bleeding in PVC-P	4

Other Applications

For all specifications, deliveries and services following
DISCLAIMER applies: [Disclaimer_E](#)

Explanation of data and values: [Organic Pigments for Plastics](#)

Clariant - www.clariant.com - Pigments & Additives Division -
www.pa.clariant.com

Contact: pa.plastics@clariant.com

Fiberfrax® Ceramic Fiber

Introduction

Fiberfrax® ceramic fibers are a family of high-temperature fibers designed to be used in a variety of industrial and commercial applications. Manufactured from alumina-silica materials, Fiberfrax fibers are chemically inert. Some of the unique properties these fibers offer are:

- High-temperature stability
- Low thermal conductivity
- Low heat storage
- Excellent thermal shock resistance
- Lightweight

Fiberfrax fibers are available in a variety of chemistries and diameters which can service a wide variety of applications. In addition, these fibers can be further modified by chopping or by removal of the unfiberized particles (called shot). Lubricants can also be added to the fiber to enhance fiber properties.

Fiberfrax fibers exhibit excellent chemical stability and resistance to attack from most corrosive agents. Exceptions include hydrofluoric acid, phosphoric acid and strong alkalis. Fiberfrax fibers also effectively resist oxidation and reduction. If wet by water or steam, thermal and physical properties are restored upon drying. Fiberfrax fibers contain no water of hydration.

Fiberfrax Bulk Fibers

Fiberfrax Bulk Fibers are manufactured to be used as feedstock in manufacturing processes or other applications where product consistency is critical. Manufactured on large, computer-controlled furnaces, these products provide customers with consistent material properties. Fiberfrax Bulk Fibers are typically used in the manufacture of other ceramic fiber based product forms such as:

- High-temperature boards, felts, and papers
- Combustion chambers for commercial and residential boilers
- Riser sleeves for molten metal casting
- Fireplace logs and panels for gas fireplaces
- Tap out cones for molten metal applications
- Specialized vacuum-formed shapes

These bulk fibers can also be directly used as high-temperature fill and packing material in a variety of high-temperature applications, such as:

- Expansion joints
- Furnace base seals
- Tube seals
- Burner tile packing
- Chimney insulation



Fiberfrax 7000 Series Fiber

Fiberfrax 7000 Series fibers are manufactured from high-purity alumina-silica materials for use in applications up to 2300°F (1260°C). These products are manufactured on computer-controlled, state-of-the-art furnaces to provide customers with consistent fiber properties. Fiberfrax 7000 Series fibers can also be chopped into several grades (coarse, medium, and fine) to provide customers with a fiber ideally suited for their application. Benefits of Fiberfrax 7000 Series fibers include:

- Low thermal shrinkage at high temperatures
- Consistent fiber properties
- Several chopped grades

Fiberfrax 6000 Series

Fiberfrax 6000 Series fibers have many of the same properties as the 7000 Series fibers. The main difference is that 6000 Series fibers are manufactured from kaolin clay rather than high-purity alumina-silica raw materials. Since kaolin is a mined material, it may contain impurities such as Fe_2O_3 , TiO_2 , and Na_2O as listed in the chemical composition chart on page 2. Even with these impurities, Fiberfrax 6000 Series fibers can provide an effective solution in many vacuum-forming and related applications.

Refer to the product Material Safety Data Sheet (MSDS) for recommended work practices and other product safety information.

APPENDIX C

MATERIAL FORMULATIONS

EARFM Skin Formulations:

Table C1: 3mm Skin Formulations for Both Molds with “Pizza Valve”

Material	LLDPE	HDPE
ρ_{PE} (g/cm ³)	0.9395	0.942
Cylindrical Mold		
m_{SKIN} (g)	207.75	208.30
Flat-Plate Mold		
m_{SKIN} (g)	240.57	241.21

*EARFM Foam Formulations:*Table C2: Foam Formulations ($\varphi_{Corrected}$ = 163.23 cc/g) for Both Molds with “Pizza Valve”

Material	LLDPE	HDPE
Cylindrical Mold		
V_{FOAM} (cm ³)	1275.95	1275.40
VER		3
V_i (cm ³)	425.32	425.13
m_{FOAM} (g)	399.58	400.47
m_{CBA} (g)	5.21	5.21
%CBA (%wt)	1.29	1.28
VER		6
V_i (cm ³)	212.66	212.57
m_{FOAM} (g)	199.79	200.24
m_{CBA} (g)	6.51	6.59
%CBA (%wt)	3.16	3.18
Flat-Plate Mold		
V_{FOAM} (cm ³)	1219.83	1219.19
VER		3
V_i (cm ³)	406.61	406.40
m_{FOAM} (g)	382.01	382.83
m_{CBA} (g)	4.99	4.98
%CBA (%wt)	1.29	1.28
VER		6
V_i (cm ³)	203.31	203.20
m_{FOAM} (g)	191.01	191.41
m_{CBA} (g)	6.23	6.30
%CBA (%wt)	3.16	3.18

EADFRM Skin Formulations:**SEE TABLE C1****EADFRM Foam Formulations:****Table C3: Foam Formulations ($\phi_{STD} = 125$ cc/g) for Both Molds with “Pizza Valve”**

Material	LLDPE	HDPE
Cylindrical Mold		
V_{FOAM} (cm ³)	1275.95	1275.40
VER		3
V_i (cm ³)	425.32	425.13
m_{FOAM} (g)	399.58	400.47
m_{CBA} (g)	6.81	6.80
%CBA (%wt)	1.67	1.67
VER		6
V_i (cm ³)	212.66	212.57
m_{FOAM} (g)	199.79	200.24
m_{CBA} (g)	8.51	8.60
%CBA (%wt)	4.08	4.12
Flat-Plate Mold		
V_{FOAM} (cm ³)	1219.83	1219.19
VER		3
V_i (cm ³)	406.61	406.40
m_{FOAM} (g)	382.01	382.83
m_{CBA} (g)	6.51	6.50
%CBA (%wt)	1.67	1.67
VER		6
V_i (cm ³)	203.31	203.20
m_{FOAM} (g)	191.01	191.41
m_{CBA} (g)	8.13	8.22
%CBA (%wt)	4.08	4.12

RRFM Skin Formulations:**Table C4: 3mm Skin Formulations for Both Molds with Mold Interface**

Material	LLDPE	HDPE
ρ_{PE} (g/cm ³)	0.9395	0.942
Cylindrical Mold		
m_{SKIN} (g)	215.11	215.69
Flat-Plate Mold		
m_{SKIN} (g)	247.93	248.59

RRFM Foam Formulations:**Table C5: Foam Formulations (ϕ_{STD} =125 cc/g) for Both Molds with Mold Interface**

Material	LLDPE	HDPE
Cylindrical Mold		
V_{FOAM} (cm ³)	1252.43	1251.85
VER		3
V_i (cm ³)	417.48	417.28
m_{FOAM} (g)	392.22	393.08
m_{CBA} (g)	6.68	6.68
%CBA (%wt)	1.67	1.67
VER		6
V_i (cm ³)	208.74	208.64
m_{FOAM} (g)	196.11	196.54
m_{CBA} (g)	8.35	8.44
%CBA (%wt)	4.08	4.12
Flat-Plate Mold		
V_{FOAM} (cm ³)	1199.13	1198.47
VER		3
V_i (cm ³)	399.71	399.49
m_{FOAM} (g)	375.53	376.32
m_{CBA} (g)	6.40	6.39
%CBA (%wt)	1.67	1.67
VER		6
V_i (cm ³)	199.85	199.75
m_{FOAM} (g)	187.76	188.16
m_{CBA} (g)	7.99	8.08
%CBA (%wt)	4.08	4.12

Final RRFM Skin Formulations:**Table C6: 3mm Skin Formulations for Both Molds with Modified Mold Interface**

Material	LLDPE	HDPE
ρ_{PE} (g/cm ³)	0.9395	0.942
Cylindrical Mold		
m_{SKIN} (g)	211.28	211.85
Flat-Plate Mold		
m_{SKIN} (g)	244.10	244.75

Final RRFM Foam Formulations:**Table C7: Foam Formulations ($\varphi_{STD} = 125$ [cc/g]) for Both Molds with Modified Mold Interface**

Material	LLDPE	HDPE
Cylindrical Mold		
V_{FOAM} [cm ³]	1258.23	1257.66
VER		3
V_i [cm ³]	419.41	419.22
m_{FOAM} [g]	394.03	394.91
m_{CBA} [g]	6.71	6.71
%CBA [%wt]	1.67	1.67
VER		6
V_i [cm ³]	209.70	209.61
m_{FOAM} [g]	197.02	197.45
m_{CBA} [g]	8.39	8.48
%CBA [%wt]	4.08	4.12
Flat-Plate Mold		
V_{FOAM} [cm ³]	1204.60	1203.95
VER		3
V_i [cm ³]	401.53	401.32
m_{FOAM} [g]	377.24	378.04
m_{CBA} [g]	6.42	6.42
%CBA [%wt]	1.67	1.67
VER		6
V_i [cm ³]	200.77	200.66
m_{FOAM} [g]	188.62	189.02
m_{CBA} [g]	8.03	8.12
%CBA [%wt]	4.08	4.12